PB82-229360

Determination of Effects of Ambient Conditions on Aircraft Engine Emissions Data Analysis and Correction Factor Generation

Calspan Corp.
Buffalo, NY

Prepared for

Environmental Protection Agency
Ann Arbor, MI

Sep 77

U.S. Department of Commerce
National Technical Information Service
NTIS

TECHNICAL REPORT DATA

(Please read Instructions on the reverse before completing)

1. REPORT NO.
EPA-460/3-77-019

2.

3. RECIPIENT'S ACCESSION NO.
PB82 229360

4. TITLE AND SUBTITLE
DETERMINATION OF EFFECTS OF AMBIENT CONDITIONS ON AIRCRAFT ENGINE EMISSIONS: Data Analysis and Correction Factor Generation

5. REPORT DATE
September 1977

6. PERFORMING ORGANIZATION CODE

7. AUTHOR(S)
Paul J. Donovan, William R. Fairchild, and Kenneth W. Graves

8. PERFORMING ORGANIZATION REPORT NO.

9. PERFORMING ORGANIZATION NAME AND ADDRESS
Calspan Corporation
P.O. Box 235
Buffalo, N.Y. 14221

10. PROGRAM ELEMENT NO.

11. CONTRACT/GRANT NO.
No. 68-03-2159

12. SPONSORING AGENCY NAME AND ADDRESS
Environmental Protection Agency
Office of Air and Waste Management
Office of Mobile Source Air Pollution Control
Emission Control Technology Division
Ann Arbor, Michigan 48105

13. TYPE OF REPORT AND PERIOD COVERED

14. SPONSORING AGENCY CODE

15. SUPPLEMENTARY NOTES

16. ABSTRACT

This report presents a set of correction factors for variations in turbine aircraft HC, CO, NOX and smoke emissions due to non-standard day ambient temperature, pressure and humidity developed for the United States Environmental Protection Agency, Ann Arbor, Michigan. These correction factors are based on data from three EPA-sponsored full-scale engine tests, two EPA-sponsored combustor rig tests, and additional data solicited from industry sources. Key correlating parameters in this analysis were combustor inlet temperature, combustor inlet pressure, and ambient humidity. The correction factors have been developed using a multiple least squares regression analysis approach using functional emisssions models based upon theoretical considerations and an extensive review of current ambient effects literature. Emphasis has been placed upon relating correction factor coefficients within a general engine class to various operating characteristics of each individual engine. Tables and figures.

17. KEY WORDS AND DOCUMENT ANALYSIS

a. DESCRIPTORS	b. IDENTIFIERS/OPEN ENDED TERMS	c. COSATI Field/Group
Air Pollution turbine aircraft emissions Ambient Conditions		EPA 68A

18. DISTRIBUTION STATEMENT

19. SECURITY CLASS *(This Report)*

20. SECURITY CLASS *(This page)*

21. NO. OF PAGES

22. PRICE

EPA Form 2220-1 (Rev. 4-77) PREVIOUS EDITION IS OBSOLETE

PB82-229360

EPA-460/3-77-019
September 1977

DETERMINATION OF EFFECTS OF AMBIENT CONDITIONS ON AIRCRAFT ENGINE EMISSIONS

DATA ANALYSIS AND CORRECTION FACTOR GENERATION

U.S. ENVIRONMENTAL PROTECTION AGENCY
Office of Air and Waste Management
Office of Mobile Source Air Pollution Control
Emission Control Technology Division
Ann Arbor, Michigan 48105

REPRODUCED BY
NATIONAL TECHNICAL
INFORMATION SERVICE
U.S. DEPARTMENT OF COMMERCE
SPRINGFIELD, VA 22161

EPA-460/3-77-019

DETERMINATION OF EFFECTS OF AMBIENT CONDITIONS ON AIRCRAFT ENGINE EMISSIONS

DATA ANALYSIS AND CORRECTION FACTOR GENERATION

by

Paul J. Donovan, William R. Fairchild, and Kenneth W. Graves

Calspan Corporation
P.O. Box 235
Buffalo, N.Y. 14221

Contract No. 68-03-2159

EPA Project Officer: Thomas Cackette

Prepared for

ENVIRONMENTAL PROTECTION AGENCY
Office of Air and Waste Management
Office of Mobile Source Air Pollution Control
Emission Control Technology Division
Ann Arbor, Michigan 48105

September 1977

This report is issued by the Environmental Protection Agency to report technical data of interest to a limited number of readers. Copies are available free of charge to Federal employees, current contractors and grantees, and nonprofit organizations - in limited quantities - from the Library Services Office (MD-35), Research Triangle Park, North Carolina 27711; or, for a fee, from the National Technical Information Service, 5285 Port Royal Road, Springfield, Virginia 22161.

This report was furnished to the Environmental Protection Agency by the Calspan Corporation, P.O. Box 235, Buffalo, N.Y., in fulfillment of Contract No. 68-03-2159. The contents of this report are reproduced herein as received from Calspan Corporation. The opinions, findings, and conclusions expressed are those of the author and not necessarily those of the Environmental Protection Agency. Mention of company or product names is not to be considered as an endorsement by the Environmental Protection Agency.

Publication No. EPA-460/3-77-019

ABSTRACT

This report presents a set of correction factors for variations in turbine aircraft HC, CO, NOX and smoke emissions due to non-standard day ambient temperature, pressure and humidity developed for the United States Environmental Protection Agency, Ann Arbor, Michigan, under EPA Contract No. 68-03-2159. These correction factors are based on data from three EPA-sponsored full-scale engine tests, two EPA-sponsored combustor rig tests, and additional data solicited from industry sources. Key correlating parameters in this analysis were combustor inlet temperature, combustor inlet pressure, and ambient humidity. The correction factors have been developed using a multiple least squares regression analysis approach using functional emissions models based upon theoretical considerations and an extensive review of current ambient effects literature. Emphasis has been placed upon relating correction factor coefficients within a general engine class to various operating characteristics of each individual engine.

TABLE OF CONTENTS

Section — Title — Page No.

ABSTRACT . . . iii
LIST OF TABLES . . . vii
LIST OF FIGURES . . . ix
LIST OF APPENDICES . . . xiii

1 SUMMARY AND CONCLUSIONS . . . 1-1

2 INTRODUCTION . . . 2-1
  2.1 EPA-Sponsored Data . . . 2-2
  2.2 Contributed Data . . . 2-3
  2.3 Engine and Test Descriptions . . . 2-4
    2.3.1 TPE331-5-251 . . . 2-5
    2.3.2 GTCP85-98CK APU . . . 2-6
    2.3.3 ALF502 Full Scale Engine . . . 2-7
    2.3.4 ALF502 Combustor Rig . . . 2-7
    2.3.5 CFM56 Combustor Rig . . . 2-8

3 DEFINITIONS . . . 3-1

4 SUMMARY OF AMBIENT EFFECTS LITERATURE . . . 4-1
  4.1 Oxides of Nitrogen . . . 4-2
  4.2 Hydrocarbons . . . 4-5
  4.3 Carbon Monoxide . . . 4-7
  4.4 Smoke Number . . . 4-8

5 CORRECTION FACTOR APPROACH . . . 5-1
  5.1 Theoretical versus Empirical Emissions Models . . . 5-1
  5.2 Correlating Parameters - Ambient versus Combustor Inlet . . . 5-1
  5.3 Simple versus Complex Emissions Models . . . 5-4
  5.4 Data Variability . . . 5-7
    5.4.1 Test-to-Test Variability . . . 5-8
    5.4.2 Engine-to-Engine Variability . . . 5-9
  5.5 Regression Models and Correction Factors . . . 5-9

6 INDIVIDUAL ENGINE EMISSION MODELS . . . 6-1

Preceding page blank

TABLE OF CONTENTS (Cont.)

Section	Title	Page No.
	6.1 CFM56 Combustor Rig - Raw Data Plots	6-1
	6.2 CFM56 Combustor Rig - Summary Statistics by Mode	6-2
	6.3 CFM56 Combustor Rig - Regression Summary	6-2
7	GENERALIZED CORRECTION FACTORS	7-1
	7.1 Oxides of Nitrogen	7-4
	7.1.1 Temperature Correction Factor	7-4
	7.1.2 Humidity Correction Factor	7-8
	7.2 Hydrocarbons	7-9
	7.3 Carbon Monoxide	7-11
	7.4 Smoke Number	7-12
	7.5 Correction Factor Sensitivity Analysis	7-14
	7.6 Correction Factor Performance Analysis	7-17
8	REFERENCES	8-1
9	TABLES	9-1
10	FIGURES	10-1

LIST OF TABLES

Table No.	Title	Page No.
1	Engine/Combustor Rig Summary - EPA-Sponsored Data	9-3
2	Industry Contributed Data - Selected Experimental Design Features	9-4
3	Ambient Test Conditions - TPE331-5-251 and GTCP85-98CK APU.	9-5
4	TPE331-5-251 Engine Load Conditions	9-6
5	GTCP85-98CK APU Engine Load Conditions	9-7
6	Ambient Test Conditions - ALF502 Full Scale Engine	9-8
7	Ambient Test Conditions - ALF502 Combustor Rig	9-9
8	Ambient Test Conditions - CFM56 Combustor Rig	9-10
9	CFM56 Combustor Rig Replicate Analysis	9-11
10	TPE331-5-251 Full Scale Engine Replicate Analysis	9-12
11	Test-to-Test Variability - Mean Idle Coefficient of Variation by Engine	9-13
12	CFM56 Combustor Rig - Summary Statistics by Mode	9-14
13	CFM56 Combustor Rig - HC Regression Summary	9-15
14	CFM56 Combustor Rig - CO Regression Summary	9-16
15	CFM56 Combustor Rig - NOX Regression Summary	9-17
16	CFM56 Combustor Rig - Smoke Regression Summary	9-18
17	NOX Correction Factor Coefficients - Tabular Summary	9-19
18	NOX Correction Factor Coefficients - Summary Statistics	9-20
19	HC Correction Factor Coefficients - Tabular Summary	9-21
20	HC Correction Factor Coefficients - Summary Statistics	9-22
21	CO Correction Factor Coefficients - Tabular Summary	9-23

LIST OF TABLES (cont.)

Table No.	Title	Page No.
22	CO Correction Factor Coefficients - Summary Statistics .	9-24
23	Smoke Number Correction Factor Coefficients - Tabular Summary	9-25
24	Smoke Number Correction Factor Coefficients - Summary Statistics	9-26
C1	NOX Regression Coefficients vs. Model Formulation - GE CFM56 Combustor Rig, Idle to Takeoff	C-7
C2	NOX Regression Coefficients vs. Model Formulation - Pratt & Whitney JT9D-7A Pilot Lot Data, Idle to Takeoff .	C-8
D1	ALF502 Rig-Engine Correlation Analysis - Regression Summary	D-6
D2	ALF502 Rig-Engine Correlation Analysis - Coefficient Confidence Bound Summary	D-7

LIST OF FIGURES

Figure No.	Title	Page No.
1	Variation of Oxides of Nitrogen (NOX) EI with Ambient Temperature - ALF502 Combustor Rig, Approach Mode	10-3
2	Data Overview - EPA Aircraft Emissions Ambient Effects Program	10-4
3	Burner Inlet Temperature versus Ambient Humidity - TPE331-5-251	10-5
4	Effect of Engine Pressure Ratio and Equivalence Ratio on NOX Temperature and Humidity Correction Factors (from Blazowski)	10-6
5	Analytically Predicted Ambient Temperature Correction Factors for Hydrocarbons (from Blazowski and Marzewski) . .	10-7
6	HC EI versus CO EI - CFM56 Combustor Rig @ Idle and 1.5 Idle	10-8
7	Natural Log of HC EI versus Natural Log of CO EI - CFM56 Combustor Rig @ Idle and 1.5 Idle	10-9
8	General Correction Factor Development Overview	10-10
9	Combustor Inlet Temperature versus Ambient Temperature - CFM56 Combustor Rig at Idle	10-11
10	Natural Log of HC EI versus Combustor Inlet Temperature - CFM56 Combustor Rig at Idle (Pressure and Humidity Fixed) .	10-12
11	Natural Log of CO EI versus Combustor Inlet Temperature - CFM56 Combustor Rig at Idle (Pressure and Humidity Fixed) .	10-13
12	Natural Log of NOX EI versus Combustor Inlet Temperature - CFM56 Combustor Rig at Climb (Pressure and Humidity Fixed).	10-14
13	Natural Log of NOX EI versus Ambient Humidity - CFM56 Combustor Rig at Climb (Pressure and Temperature Fixed)	10-15
14	Ambient Effects Program - Regression Model Summary	10-16
15	Replicate Analysis - Coefficient of Variation for CFM56 Combustor Rig HC Idle Data	10-17

LIST OF FIGURES (cont.)

Figure No. | Title | Page No.

16 Correction Factor Structure 10-18

17 HC EI versus Combustor Inlet Temperature - CFM56 Combustor Rig, Idle to Takeoff 10-19

18 Natural Log HC EI versus Combustor Inlet Temperature - CFM56 Combustor Rig, Idle to Takeoff 10-20

19 CO EI versus Combustor Inlet Temperature - CFM56 Combustor Rig, Idle to Takeoff 10-21

20 Natural Log CO EI versus Combustor Inlet Temperature - CFM56 Combustor Rig, Idle to Takeoff 10-22

21 NOX EI versus Combustor Inlet Temperature - CFM56 Combustor Rig, Idle to Takeoff 10-23

22 Natural Log of NOX EI versus Combustor Inlet Temperature - CFM56 Combustor Rig, Idle to Takeoff 10-24

23 NOX EI versus Ambient Humidity - CFM56 Combustor Rig, Idle to Takeoff 10-25

24 Natural Log of NOX EI versus Ambient Humidity - CFM56 Combustor Rig, Idle to Takeoff 10-26

25 Smoke Number versus Combustor Inlet Pressure - CFM56 Combustor Rig, Idle to Takeoff 10-27

26 Natural Log of Smoke Number versus Combustor Inlet Pressure - CFM56 Combustor Rig, Idle to Takeoff 10-28

27 Regression Coefficient Summary - CFM56 Combustor Rig . . . 10-29

28 Correction Factor Coefficient versus Engine Operating Parameter - Development Approach 10-30

29 Correction Factor Nomenclature 10-31

30 T3MEAN versus Rated Pressure Ratio PR - Ambient Effects Data Base 10-32

31 NOX Combustor Inlet Temperature Coefficient T3COEF versus Combustor Inlet Pressure P3MEAN 10-33

LIST OF FIGURES (cont.)

Figure No.	Title	Page No.
32	NOX Emissions Index as a Function of Compressor Discharge Temperature - Production Engines (Reference 13)	10-34
33	NOX Temperature Coefficient versus Combustor Inlet Pressure P3MEAN - Confidence Bounds	10-35
34	NOX Combustor Inlet Temperature Coefficient T3COEF versus Rated Engine Pressure Ratio PR	10-36
35	NOX Combustor Inlet Temperature Coefficient T3COEF versus Mean NOX Emission Index NOXMEAN	10-37
36	Mean NOX Combustor Inlet Temperature T3MEAN versus Mean NOX Emission Index NOXMEAN	10-38
37	NOX Emission Index versus Combustor Inlet Temperature - Uncontrolled and Controlled Engines	10-39
38	HC Combustor Inlet Temperature Coefficient T3COEF versus Engine Idle Pressure Ratio IPR	10-40
39	CO Combustor Inlet Temperature Coefficient T3COEF versus Engine Idle Pressure Ratio IPR	10-41
40	Smoke Number Combustor Inlet Pressure Coefficient P3COEF versus Rated Engine Pressure Ratio	10-42
41	Smoke Number Combustor Inlet Pressure Coefficient P3COEF versus Mean Smoke Number SMKMEAN	10-43
42	NOX Temperature Correction Factors	10-44
43	NOX Humidity Correction Factors	10-45
44	HC Temperature Correction Factors	10-46
45	CO Temperature Correction Factors	10-47
46	Smoke Pressure Correction Factors	10-48
47	Correction Factor Sensitivity Analysis - NOX Temperature Correction	10-49
48	Correction Factor Sensitivity Analysis - NOX Humidity Correction	10-50

LIST OF FIGURES (cont.)

Figure No.	Title	Page No.
49	Correction Factor Sensitivity Analysis - HC Temperature Correction	10-51
50	Correction Factor Sensitivity Analysis - CO Temperature Correction	10-52
51	Correction Factor Sensitivity Analysis - Smoke Pressure Correction	10-53
52	NOX Ambient Effects Correction Summary	10-54
53	HC Ambient Effects Correction Summary	10-55
54	CO Ambient Effects Correction Summary	10-56
55	Smoke Ambient Effects Correction Summary	10-57
56	Hypothetical Emission Index Correction	10-58
C1	CFM56 Variance Map - Equation: LNNOX=f(T3)	C-9
C2	CFM56 Variance Map - Equation: LNNOX=f(T3, HAMB)	C-10
D1	Graphical Interpretation of ALF502 Rig-Engine Correlation	D-8
F1	Uncorrected HC Emissions Index versus Combustor Inlet Temperature - CFM56 Combustor Rig, Idle	F-3
F2	Corrected HC Emissions Index versus Combustor Inlet Temperature - CFM56 Combustor Rig, Idle	F-4
F3	Uncorrected CO Emissions Index versus Combustor Inlet Temperature - CFM56 Combustor Rig, Idle and 1.5 Idle	F-5
F4	Corrected CO Emissions Index versus Combustor Inlet Temperature - CFM56 Combustor Rig, Idle and 1.5 Idle	F-6
F5	Uncorrected NOX Emissions Index versus Combustor Inlet Temperature - CFM56 Combustor Rig, Idle to Takeoff	F-7
F6	Corrected NOX Emissions Index versus Combustor Inlet Temperature - CFM56 Combustor Rig, Idle to Takeoff	F-8
G1	Measured Fuel Flow versus Ambient Pressure - CFM56 Combustor Rig, Idle to Takeoff	G-3
G2	Corrected Fuel Flow versus Ambient Pressure - CFM56 Combustor Rig, Idle to Takeoff	G-4

LIST OF APPENDICES

Appendix No.	Title	Page No.
A	DATA BASE SUMMARY	A-1
B	COMBUSTOR INLET CONDITIONS RELATED TO AMBIENT CONDITIONS	B-1
C	MULTICOLLINEARITY AND AIRCRAFT EMISSIONS DATA . . .	C-1
D	COMBUSTOR RIG - FULL-SCALE ENGINE CORRELATION . . .	D-1
E	COMPARISON OF TWO LINEAR BIVARIATE REGRESSION LINES	E-1
F	SAMPLE EMISSION INDEX CORRECTION	F-1
G	COMPUTATION OF EPA EMISSION PARAMETER (EPAP) FROM EMISSION INDEX AND SPECIFIC FUEL CONSUMPTION .	G-1

1. SUMMARY AND CONCLUSIONS

1) The effect of variations in ambient temperature, pressure and humidity on hydrocarbon (HC), carbon monoxide (CO) and oxides of nitrogen (NOX) emission indices as well as on EPA smoke number (SMOKE) have been investigated and a set of general purpose correction factors developed.

2) The key correlating parameters in this analysis were combustor inlet temperature, combustor inlet pressure, and ambient specific humidity.

3) A regression analysis approach guided by a review of current ambient effects literature and theory indicates that the following emissions models can be used to predict the variation in aircraft emissions due to non-standard day ambient conditions:

Natural Log HC EI = f(Combustor Inlet Temperature)

Natural Log CO EI = f(Combustor Inlet Temperature)

Natural Log NOX EI = f(Combustor Inlet Temperature, Ambient Humidity)

Natural Log Smoke Number = f(Natural Log Combustor Inlet Pressure)

4) While various alternative correlating variables could have been chosen, it was felt that the above variables adequately describe the major portion of aircraft emissions variation due to ambient conditions required by a general correction factor system.

5) The functional forms of the proposed emission index correction factors are:

$$HC_{CORRECTED} = HC_{MEASURED} \cdot e^{T3COEF_{HC} \cdot (T3_{REF} - T3_{MEAS})}$$

$$CO_{CORRECTED} = CO_{MEASURED} \cdot e^{T3COEF_{CO} \cdot (T3_{REF} - T3_{MEAS})}$$

$$NOX_{CORRECTED} = NOX_{MEASURED} \cdot e^{T3\,COEF_{NOX} \cdot (T3_{REF} - T3_{MEAS})} \cdot e^{HAMBCOEF_{NOX} \cdot (HAMB_{REF} - HAMB_{MEAS})}$$

$$SMOKE_{CORRECTED} = SMOKE_{MEASURED} \cdot \left(\frac{P3_{REF}}{P3_{MEAS}}\right)^{P3COEF_{SMOKE}}$$

where T3 = Combustor Inlet Temperature

P3 = Combustor Inlet Pressure

T3COEF = Combustor Inlet Temperature Coefficient

HAMBCOEF = Ambient Specific Humidity Coefficient

P3COEF = Combustor Inlet Pressure Coefficient

Ref = Reference Value

Meas = Measured Value

6) The temperature, pressure and humidity correction coefficients for a particular engine are determined using the rated (PR) and idle (IPR) pressure ratios:

			Applicable Modes
$T3COEF_{HC}$	=	f(IPR)	IDLE
$T3COEF_{CO}$	=	f(IPR)	IDLE
$T3COEF_{NOX}$	=	f(PR)	IDLE TO TAKEOFF
$HAMBCOEF_{NOX}$	=	CONSTANT = -19.0	IDLE TO TAKEOFF
$P3COEF_{SMOKE}$	=	CONSTANT = -1.0	IDLE TO TAKEOFF

7) The correction coefficients for newer technology low emissions designs frequently vary from older design engines. In general, newer design engines exhibit decreased NOX temperature sensitivity (see Section 4 for discussion of "sensitivity") and increased HC and CO temperature sensitivity when compared to older technology engines of similar idle and rated pressure ratios.

8) The NOX combustor inlet temperature coefficient ($T3COEF_{NOX}$) was found to increase approximately linearly with rated engine pressure ratio.

9) The HC and CO combustor inlet temperature coefficients ($T3COEF_{HC}$ and $T3COEF_{CO}$) were found to increase in a negative direction with idle pressure ratio.

10) The high variability in measured smoke data makes the application of a general purpose smoke correction factor tenuous. While reasonably consistent trends were found between the pressure correction coefficients for various engines, only a small reduction in variability was observed when measured smoke data were corrected to standard day conditions.

11) A comparison of uncorrected and corrected emissions data indicates the proposed correction factor approach should provide the following expected reduction in emission index variability:

Pollutant	Expected Reduction Emission Index Variability Percent
NOX EI	70
HC EI	58
CO EI	63
SMOKE NUMBER	37

2. INTRODUCTION

The Clean Air Act Amendments of 1970 specified that the Federal Aviation Administration (FAA) promulgate regulations enforcing aircraft engine standards established by the Environmental Protection Agency (EPA). During the period since the enactment of this legislation, EPA has established standards for hydrocarbons (HC), carbon monoxide (CO), oxides of nitrogen (NOX), and smoke number applicable to variety of both new and in-use aircraft engines. A description of these standards and required test procedures is provided in Reference 1 and subsequent amendments.

In recognition of the influence of ambient conditions on aircraft engine emissions, EPA has conducted a program aimed at evaluating these effects and at formulating correction factors for adjusting measured emissions to standard[*] day conditions (ambient temperature = 59°F, ambient pressure = 29.92 in Hg, and specific ambient humidity = 0.00634 lb H_2O/lb dry air). The need for suitable ambient effects correction factors is demonstrated by Figure 1 which presents the variation of oxides of nitrogen (NOX) emission index for the ALF502 combustor rig operating at approach power versus ambient temperature at a fixed ambient pressure of 29.92 in Hg and a fixed specific ambient humidity of .0037 lb H_2O/lb dry air. As seen in this figure, NOX emissions increase from 4.9 lb NOX/1000 lb fuel at an ambient temperature of 19 °F to 6.1 lb NOX/1000 lb fuel at an ambient temperature of 85 °F. This 25% variation difference in NOX emission index, due solely to ambient temperature, clearly points out the desirability of developing ambient effects correction factors so that engine certification tests can be performed under a variety of nonstandard day conditions and the results compared to EPA emissions standards based on engine performance under standard day ambient conditions. This report summarizes the development of such a set of ambient effects correction factors.

---

[*] In this report, "standard" and "reference" day conditions are used interchangeably to indicate ambient temperature = 59°F, ambient pressure = 29.92 in Hg, and specific ambient humidity = 0.00634 lb H_2O/lb dry air.

2.1 EPA Sponsored Data

The ambient effects program was divided into two main tasks -- data collection and data analysis. Figure 2 presents an overview of these two tasks. The data collection task of the program can be subdivided into four phases:

- Full Scale Engine Tests -- Controlled Ambient Conditions
- Full Scale Engine Tests -- Uncontrolled Ambient Conditions
- Combustor Rig Tests -- Controlled Ambient Conditions
- Contributed Test Data from Industry

The first phase involved the testing of two small aircraft engines operating under controlled ambient conditions. These engines, tested by AiResearch in Phoenix, Arizona, under contract to EPA, were the P2 class TPE331-5-251 turboprop and the APU class GTCP85-98CK. A complete description of this portion of the test program can be found in the test contractor's final reports, References 2 and 3. By testing these engines under controlled ambient conditions, it is possible to explore the effects of a wide range of ambient conditions not practically available by relying solely on naturally occurring ambient variation.

The second phase of the data collection process, on the other hand, involved testing the T1 class ALF502 full scale engine under uncontrolled ambient conditions. These tests, also sponsored by EPA, were performed by AVCO Lycoming Division in Stratford, Connecticut. When testing under uncontrolled ambient conditions, ambient effects are deduced from emission response to naturally occurring changes in ambient conditions over a period of time. The results of limited CFM56 full scale engine testing by General Electric, scheduled as part of this phase of the test program, were not available for inclusion in the analysis encompassed by this report due to test scheduling difficulties. The omission of this small quantity of data is not expected to alter the findings of this report. Instead, it was intended to (1) supplement the limited smoke data currently available, (2) provide an additional source of data to validate combustor rig/engine correlations, and (3) provide additional large jet engine emissions data.

The third phase of the data collection process was performed in conjunction with phase two outlined above. During these test programs, the T1 class ALF502 and T2 class CFM56 combustor rigs (the ALF502 was previously tested as a full scale engine in Phase 2) were tested under a wide range of controlled ambient conditions. The main objectives of this portion of the program were (1) to provide a data source useful in establishing rig/engine correlating factors, and (2) to provide an extensive ambient effects data base on small (ALF502) and large (CFM56) gas turbine engines. The ALF502 combustor rig tests were performed by AVCO Lycoming and the CFM56 combustor rig tests were performed by General Electric in Cincinnati, Ohio. Both these test programs were performed under contract to EPA. Final contractors' reports have not been issued as of the publication date of this report.

Table 1 summarizes the EPA sponsored test programs. As shown in this table, the EPA sponsored data base represents over 900 tests on (1) a turboprop, (2) an auxiliary power unit, (3) a small jet engine, and (4) a large jet engine. These engines are representative of many engines currently in use in general and commercial aviation today. Also presented in this table is a comparison of emission levels of engines in the EPA sponsored test program with 1979 emissions standards. As demonstrated by this portion of Table 1, the test engines are representative of designs which are below, or relatively close, to 1979 emissions standards.

2.2 CONTRIBUTED DATA

In order to further generalize the data base used to develop ambient effects correction factors, EPA solicited test data from a variety of engine manufacturers and government agencies. The purpose of this contributed data was to supplement the EPA sponsored data base in order to provide wider input into the correction factor development process. Appendix A briefly summarizes the complete ambient effects program data base. Shown in this appendix are the engine, EPA class, number of tests, data source, availability of smoke data, power modes, and general comments. Approximately 2000 emissions tests on 30 engines were received during the data solicitation phase of the program. For the most part, the contributed data consists of emissions tests on several different full scale engines of the same model type operating under uncontrolled ambient conditions.

The Pratt & Whitney JT8D and JT9D pilot lot emissions tests are representative of this type of data. In addition, uncontrolled ambient conditions were used to extensively examine the ambient response over a period of several months of an individual engine such as the TF30. Finally, the contributed data includes parametric tests on combustor rigs where temperature, pressure or humidity are varied independently in a controlled fashion in order to investigate the independent effects of each ambient variable. Frequently, parametric test points do not correspond to a normal engine operating mode, such as idle or takeoff. As a result, care must be exercised when comparing the results of analyses using parametric experiments with data gathered while an engine is functioning in a normal operating mode. Parametric rig data, however, is particularly useful in evaluating the impact of changing engine operating parameters (e.g., idle pressure ratio) on correction factor coefficients. For instance, the T56 combustor rig was operated in a controlled environment at four simulated idle pressure ratios (IPR = 2, 3, 4, 5). An examination of the HC, CO and NOX correction factor coefficients determined at each idle pressure ratio provides valuable information in assessing the impact of this particular engine operating parameter on the magnitude of these correction factor coefficients. Table 2 briefly summarizes the salient features of the three basic experimental designs included in the contributed data base.

2.3 ENGINE AND TEST DESCRIPTIONS

In this section, a general description of the test matrix for each engine in the EPA sponsored data base will be provided. In addition, any deviation from normal engine operation resulting from either test facility limitations (e.g., maximum airflow), test engine limitations (e.g., maximum turbine temperature), or test procedures (e.g., incorrect parameter adjustment) will be noted where these deviations could be expected to influence the determination of ambient effects. The test description data for each engine will include four basic types of information:

- Engine Description
- Ambient Test Conditions
- Engine Power Conditions
- Data Anomalies

2.3.1 TPE331-5-251

The TPE331 series turboprop is a single-shaft gas turbine engine that operates at essentially constant rotor speed over a range of flight power settings. At ground idle and taxi, however, operation is reduced to 65 percent of rated engine speed to minimize noise and fuel consumption. Taxi-idle power is 5 percent of the takeoff rating. Accordingly, for purposes of this emission measurement program, the idle, 1.5 times idle, and 2 times idle, test conditions were performed at 65 percent rated engine rpm. All other power settings were operated at 100 percent rated speed. In conformance with EPA emission standards for P2 Class (turboprop) aircraft engines, the power settings for approach, climbout, and takeoff, are at 30, 90 and 100 percent of rated shaft horsepower. The turboprop engine cruise condition is limited by exhaust gas temperature and varies as a function of altitude, ambient temperature, and flight speed. As related to static test conditions, cruise power would be 85 percent of the takeoff-power rating. An intermediate power setting of approximately 70 percent of rated takeoff-power was selected to represent the cruise operating condition. The normal cruise setting is only 5 percent less power than climbout and the intermediate power setting provided a more favorable test point distribution for data interpolation. The TPE331 is the prime propulsion engine for business aircraft such as the Turbo Commander 690, and Swearingen Metro Liner. The turboprop combustor system, commonly used for engines in the 500 to 1000 eshp range, is a reverse-flow annular configuration. The fuel injection system is composed of 5 radial start and 10 axial main simplex fuel injectors staged through a single flow divider.

The engine inlet ambient conditions for the TPE331 are shown in Table 3. This table also represents the ambient test matrix for the GTCP85-98 APU. Turboprop engine emissions, for each engine inlet ambient condition, were measured for gaseous and smoke emissions at each power setting described in Table 4. Two replicates or a total of three data points were provided at each power/ambient test condition.

TA

Several comments should be made concerning the humidity control system used to simulate the varying ambient humidities required by the test matrix. The humidification technique employed used the injection of fine water droplets immediately upstream of the engine inlet. While this approach assured an accurate measurement of water introduced into the engine, it was not a true simulation of humidity since the liquid water had to absorb heat from the engine to reach a vapor state. This process lowered the compressor discharge temperature as "humidity" increased. In addition, total flow through the engine was slightly increased and the air specific heat changed to a small extent. The decrease in compressor discharge temperature (also referred to as burner inlet temperature) with increasing humidity is illustrated for the seven TPE331 test modes in Figure 3. The magnitude of this temperature change (approximately 5-10 percent over the range of simulated humidities), however, does not substantially alter either the nature of the functional relationships between the TPE331-5-251 emission indices and the correction factor correlating parameters (Section 5), or the magnitude of these relationships (Section 7). In addition, the NOX temperature and humidity coefficients for the TPE331-5-251 (Table 17) are consistent with the general coefficient trends observed for other engines in the test program.

2.3.2 GTCP85-98CK APU

The GTCP83 series pneumatic and shaft power gas turbine engine is designed for ground and on-board aircraft auxiliary power. The single-shaft engine provides mechanical shaft power driving aircraft accessories such as an alternator when airborne, provides pneumatic bleed-air power for starting main aircraft engines and for aircraft cabin air-conditioning when on the ground, and provides cooling air for engine lubricating oil and for the engine enclosure at all times. Typical aircraft applications for the 85 Series APUs include the Boeing 727 and 737 and the Douglas DC-9 commercial jetliners. The APU combustion system consists of a single-can combustor with a dual orifice fuel injector, oriented tangentially relative to the engine axis. This is a typical combustor configuration for the 200-350 eshp size APU.

The ambient conditions at which the engine was tested were identical to those presented in Table 3 for the TPE331-5-251. APU engine emissions, for each engine inlet ambient condition, were measured for gaseous and smoke emissions at each power setting described in Table 5. Two replicates or a total of three data points were provided at each power/ambient test condition. The same humidity control limitations encountered during the testing of the TPE331-5-251 are also applicable to the APU test program.

2.3.3 ALF502 Full Scale Engine

The ALF502 is a two-shaft, high bypass ratio, geared turbofan engine in the 6500 lb thrust class. This engine is aimed primarily at the commercial light transport and executive market. The combustor is a folded annular atomizing burner with the turbine parts packaged concentrically within it. This arrangement provides a shorter, compact engine design and permits reduced casing temperatures.

Limited emissions tests were performed on an ALF502 full scale engine. These tests were performed under uncontrolled ambient conditions at seven different thrust levels and seven ambient test conditions. Table 6 summarizes the ambient test matrix. As shown in this table, only a limited range of ambient conditions are present in this data source.

2.3.4 ALF502 Combustor Rig

In addition to the full scale ALF502 engine tests discussed in Section 2.3.3, tests were performed under controlled ambient conditions on an ALF502 combustor rig. Table 7 summarizes the ambient test matrix and power levels run during this phase of testing. Only the three low power levels (idle, 1.5 idle, and approach) were used during these tests. Certain anomalies exist in the test data on the ALF502 combustor rig which have a bearing on how ambient effects were deduced from this data. These anomalies are manifested in part by higher observed HC and CO emission indices at 1.5 idle than at idle. These findings were traced by AVCO to an eleven percent difference in airflow at idle and 1.5 times idle between the engine and rig tests. Although AVCO could not determine conclusively the reason for this variation, it is probable that an error in calculating the rig points was the cause. The likely error involved a subtraction of twice the proper amount of cooling air from the total core flow at idle and the lack of subtraction of any cooling air from the 1.5 times idle point. As a result of this discrepancy, the ALF502 combustor rig idle and 1.5 idle data sets were generally analyzed separately. Airflow levels at approach power agreed with those used during the full scale engine testing.

2.3.5 CFM56 Combustor Rig

The CFM56 is a two-shaft turbofan, high bypass ratio (6:1), high pressure ratio (25) engine in the 22,000 lb thrust class. Although this engine has not yet been certified for use, the proposed applications include the BAC-111, DC-9, 727, 7N7, 7X7, 707 and DC-8. The combustor type is a straight flow annular design.

Extensive tests under controlled ambient conditions were performed by General Electric in Cincinnati on a single CFM56 combustor rig. Table 8 presents a summary of the ambient effects test matrix which included 22 ambient conditions at each of 5 power settings. Of these 110 different test conditions, three could not be reached due to limitations on the air heater temperature. These were at simulated take-off conditions at 105 °F ambient temperature and 175 grains per pound humidity, and were well outside the operating limits of the CFM56 engine. Thus, instead of the planned 220 readings (2 replications each of 110 test conditions), there were 214 readings for which data were obtained. In addition, the highest power conditions, climbout and takeoff, were run at reduced pressure due to facility limitations.

3. DEFINITIONS

A list of abbreviations used throughout this report is presented below:

Abbreviation	Meaning	Units
TAMB	Ambient Temperature	Deg F
PAMB	Ambient Pressure	IN HG
HAMB	Ambient Specific Humidity	lb H_2O/lb Dry Air
P3	Combustor Inlet Pressure	PSIA
T3	Combustor Inlet Temperature	Deg F
HC	HC Emission Index	lb HC/1000 lb Fuel
CO	CO Emission Index	lb CO/1000 lb Fuel
NOX	NOX Emission Index	lb NOX/1000 lb Fuel
SMOKE	EPA Smoke Number	
LN	Natural Logarithm (Prefix) e.g. LNHC = NATURAL LOG HC EI	
T3COEF	T3 Temperature Coefficient	
P3COEF	P3 Pressure Coefficient	
HAMBCOEF	Ambient Humidity Coefficient	
PTHRUST	Percent Rated Thrust	
FA	Fuel Air Ratio (overall)	

4. SUMMARY OF AMBIENT EFFECTS LITERATURE

Emissions from aircraft turbine engines are affected by the ambient levels of pressure, temperature, and humidity. Consequently, certification of such engines for compliance with established standards, if it is to be meaningful, must properly account for the effects of local test conditions on measured emissions. The obvious approach would be to determine correction factors which could be applied to the measured data to reduce it to an agreed upon set of standard conditions. This section of the report summarizes selected correction factor techniques representative of those found in the ambient effects literature.

The purpose of including these summaries, which are not intended to fully cover all the research performed to date, is twofold. First, they provide examples of parameters which other researchers have found useful in correlating emission variation with changes in ambient conditions. Second, they provide guidance (theoretical in most cases) on how correction factors change with macroscopic engine operating variables such as pressure ratio. For instance, theoretical analysis proves useful in addressing questions such as:

- Should the HC, CO or NOX emission index temperature sensitivity change with rated or idle engine pressure ratio?
- Should the NOX emission index humidity sensitivity change with rated engine pressure ratio?

An important distinction should be made concerning the use of the word "sensitivity." In the above context, sensitivity refers not to the magnitude of a particular emission index but, rather, to how the rate of change of that emission index changes with respect to a given correlating parameter. Thus, while it is well known that the magnitude of NOX emission levels increase with increasing combustor inlet temperature (T3), sensitivity analysis asks the question "How does the rate of change of NOX emission levels change with temperature?" It is this concept of rate of change which is important in analyzing the changes in emission levels induced by variation in ambient conditions.

From a historical viewpoint, a considerable body of data was collected on aircraft turbine engine exhaust emissions in engine test cells under uncontrolled ambient conditions during the early 1970's. Because of the narrow range of variability in local pressure, temperature and humidity during these tests and the large variability in the test data, the effects of ambient conditions on emissions could not be quantitatively determined (Reference 4). More recently, emissions test data have been collected under controlled conditions where pressures, temperatures and humidities can be regulated over a broad range. Such tests have been conducted using complete turbine engines as well as turbine combustor rigs. The latter configuration utilizes only the combustor (or a single combustor can) and offers many practical advantages (e.g., cost, simplicity, ease of parameter variation) over the use of a complete turbine engine. It is necessary, however, to verify the representativeness of combustor rig data and the ability to translate the data to the case of a complete engine. In the following, summaries of selected research on each regulated pollutant, NOX, HC, CO and Smoke are presented.

4.1 Oxides of Nitrogen

The response of oxides of nitrogen (NOX) emission levels to changing ambient conditions is unquestionably the best understood of the four regulated pollutants. Numerous NOX correction factor techniques appear in the ambient effects literature. Several representative approaches are outlined below. A key consideration in selecting the techniques presented in this report is their usefulness in predicting (1) how correction factor sensitivity changes with engine operating variables and (2) the functional relationships between NOX emission levels and engine operating parameters.

The relationship between NOX correction factors and engine operating parameters has been investigated by Blazowski and his co-workers at AFAPL (Reference 5). This analytical work on NOX emissions is based principally on the now well known fact (originally documented by Lipfert using plotted data, Reference 6) that these emissions correlate well with combustor inlet temperature. Blazowski therefore proceeds to determine how combustor inlet temperature is influenced by ambient factors (temperature, pressure and humidity) and engine operating parameters (pressure ratio, compressor efficiency, combustor residency time, equivalence ratio, etc.).

Assuming ambient air temperature and pressure conditions at the compressor inlet (dry air), together with a range of compressor pressure ratios and compressor efficiencies, a set of corresponding combustor inlet temperatures (T3) and pressures (P3) were obtained (a methodology for performing this calculation is given in Appendix B). From these inputs, the adiabatic flame temperature was calculated and this, in turn, permitted computation of the equilibrium concentrations of the significant combustion products. Using the equilibrium concentrations of O, N and N_2, the concentration of NO was computed from a relation based on the Zeldovich mechanism. This relation involves reaction rate constants dependent on temperature. NO concentrations were also dependent on the time the gas remained in the combustor.

Using empirical data on a T56 combustor rig, Blazowski solved his relations for residency time and found it to be substantially constant at a value of 0.6 msec. In addition, he found his assumed equivalence ratio, $\phi = 0.9$, in the NO formation zone to be valid. Using this mathematical model, NOX emission indexes were calculated for a wide range of combustor inlet temperatures. These results were in general agreement with published test data. Blazowski postulated, however, that a consideration of combustion efficiency variations may be required to achieve better prediction of idle NOX variation.

Figure 4a illustrates Blazowski's NOX temperature correction factors as a function of engine pressure ratio (PR) and equivalence ratio (ϕ). A key finding illustrated by this figure is that for a constant equivalence ratio. NOX temperature sensitivity increases with increasing pressure ratio. This increased temperature is manifested by an increase in the temperature correction factor (C_T) slope as pressure ratio increases.

Humidity correction factors, C_H, were also computed and graphically depicted in Figure 4b. This figure shows the strong dependence of NOX emissions on specific humidity. Presence of water vapor changes the specific heat of air in such a way that reduced flame temperatures result and, hence, reduced emissions. Higher pressure ratios result in higher combustor inlet temperatures (other factors being equal) and, therefore, higher emissions. An equivalence ratio of 0.9 is considered representative of current day engines, and corresponds to a favorable combination of temperature and available oxygen radicals for the formation of NO (future designs of engines are expected to operate at $\emptyset = 0.6$). A noteworthy feature of Figure 4b is the theoretically predicted variation in the NOX humidity correction factor with pressure ratio. As pressure ratio increases, an increased NOX humidity sensitivity is predicted. Blazowski hypothesized that a potential cause for this changing NOX sensitivity is that low pressure ratios have less NOX suppression with humidity because of the large portion of the emission which is prompt NO. This contribution is less sensitive to temperature changes than kinetically formed NO. Prompt NO is produced primarily in the initial stages of combustion and represents an empirically derived contribution to total NOX formation which attempts to account for the difference between NOX levels predicted by kinetic equilibrium analysis and those actually observed.

An alternative NOX emissions model has been developed at Pratt & Whitney by Sarli et al (Reference 7). This model is based on plug flow kinetic analysis and is summarized below:

$$\text{NOX EI}_{\text{corrected}} = \text{NOX EI}_{\text{measured}} * \text{CF}$$

where:

$$\text{CF} = \left(\frac{\text{P3}_{\text{ref}}}{\text{P3}_{\text{meas}}}\right)^{1/2} e^{0.00313\ (\text{T3}_{\text{ref}} - \text{T3}_{\text{meas}})}\ e^{19\ (\text{HAMB}_{\text{meas}} - 0.00634)}.$$

Verification of this equation was performed using JT9D production engine data (the JT9D pilot lot data used as part of the present analysis and outlined in Appendix A) as well as JT9D altitude data. An important feature of this model is the use of combustor inlet temperature and pressure (as opposed to ambient temperature and pressure) as the NOX correlating parameters. In addition, the Sarli analysis predicts the following functional dependence between NOX emissions and combustor inlet parameters.

$\text{NOX EI} \propto \text{P3}$ or $\text{LN(NOX EI)} \propto \text{LN(P3)}$

$\text{NOX EI} \propto e^{\text{T3}}$ or $\text{LN(NOX EI)} \propto \text{T3}$

$\text{NOX EI} \propto e^{\text{HAMB}}$ or $\text{LN(NOX EI)} \propto \text{HAMB}$

where LN( ) indicates the natural logarithm.

These theoretically predicted NOX models were extensively investigated using empirical data during the development of the correction factor system proposed in this report. Sections 5, 6 and 7 summarize and discuss this analysis.

4.2 HYDROCARBONS

Considerably less research than on NOX has been performed on analyzing the formation of hydrocarbon emissions in aircraft turbine engines. Three factors however (Reference 8) are generally agreed to have major influence on the formation of unburnt hydrocarbons from idling aircraft engines. First, low combustor inlet air temperatures cause quenching to occur thus terminating combustion before its completion. Second, low fuel air ratios (fuel lean combustion) results in low equivalence ratios in the primary zone of the combustor thus reducing burning intensity. Finally, low fuel and air flows at low power idle operation result in poor fuel atomization and distribution. An increasing amount of research is being reported in the literature which explores both the influence of engine operating parameters and the comparative significance of ambient temperature, pressure, and humidity on HC emissions. The results of two representative approaches are outlined below.

Blazowski and Marzewski (Reference 9) have studied the influence of ambient conditions on idle HC emissions using a T56 single combustor rig. With the aid of an analytical global reaction model of hydrocarbon consumption, they developed HC correction factors which compared favorably with their T56 model validation test data. Figure 5 illustrates the correction factors developed with this analytical model for engine idle pressure ratios in the range 2 to 5. A significant feature of this figure is the predicted increase in hydrocarbon temperature sensitivity as engine idle pressure ratio increases. This increased sensitivity is manifested by an increase in the slope of the correction factor curve. Lastly, a small ambient pressure correction was predicted.

An alternative approach to HC emission correction is typified by the results presented by Sarli, et (Reference 7) where an empirical correction of the form

$$\text{HC EI}_{\text{corrected}} = \text{HC EI}_{\text{measured}} * \frac{P3_{\text{meas}}}{P3_{\text{ref}}}$$

was proposed. Two features of this approach are noteworthy. First, HC emissions are correlated with combustor inlet rather than ambient test conditions. Second, is the basic simplicity of the technique. This use of a simplified HC correction factor is predicated less on the grounds that it fully explains all the variation in HC emissions but, rather, as other researchers have found, that it represents a reasonable approach to explaining a significant portion of the variation in highly variable hydrocarbon emissions.

A basic HC model of similar structure but with combustor inlet temperature as the independent variable served as a guideline in the development of the correction factors proposed in this report.

4.3 CARBON MONOXIDE

The behavior of carbon monoxide emissions is closely related in many aspects to that of unburnt hydrocarbons discussed in Section 4.2. In particular, the influence of engine idle pressure ratio is especially significant because combustion at higher pressures enhances the $CO \rightarrow CO_2$ reaction rate. In addition, the higher combustor inlet temperatures associated with this higher pressure increase the fuel droplet evaporation rate, thereby enhancing hydrocarbon reactions. Finally, the higher pressure into the combustor permits a greater pressure drop across the fuel injectors which can be used to shatter fuel drops. As a result, carbon monoxide emissions have been found to sharply decrease with increasing combustor inlet temperatures and pressures. The ratio of CO to HC emissions,on the other hand, tends to increase as the efficiency level increases (e.g., as higher power levels are approached). This finding is consistent with the chemical kinetics of combustion reactions which predict that HC compounds should be consumed faster than CO with the result that as gas turbine efficiency is increased, any remaining equilibrium products of combustion tend to exist mainly as CO. This phenomenon is demonstrated in Figure 6 where the HC emission indexes for CFM56 combustor rig idle and 1.5 idle data are plotted versus the corresponding CO emission indices. Figure 7 presents the same data in logarithmic form and suggests a linear relationship between LN(CO) and LN(HC) or, alternatively, that the HC emission index is proportional to the CO emission index raised to a power.

This interrelationship between HC and CO suggests the possibility of a parallel correction factor structure for HC and CO. An empirical correction factor used by Pratt & Whitney and discussed in Reference 7 demonstrates the use of such an approach. This reference postulates a CO correction factor of the form:

$$\text{CO EI}_{\text{corrected}} = \text{CO EI}_{\text{measured}} * \frac{\text{P3}_{\text{meas}}}{\text{P3}_{\text{ref}}}$$

This model, analogous to the HC model presented in Section 4.2, reemphasizes the basic tradeoff between complex emissions models which are typically optimized for a particular engine design configuration and simpler models which attempt only to explain the major portion of emission variation.

4.4 SMOKE NUMBER

Smoke emissions represent the visible segment of particulate emissions from gas turbines which result when particles of carbonaceous material formed during the combustion process agglomerate to sizes that are in the range of the wavelength of visible light (0.45 to 0.65 micrometers). These carbonaceous particles are caused by the incomplete combustion of hydrocarbon fuels and the thermal cracking of fuel in hot regions of the combustor with locally insufficient oxygen. One of the major influences on smoke emissions has been found to be fuel selection (Reference 10).

Only a limited body of data (mostly empirical) currently exists on the response of visible smoke emissions to ambient conditions. The results of several test programs are summarized below.

As part of their pilot lot test program, Pratt & Whitney analyzed the smoke emissions from 18 JT3D engines tested in 1973 and 1974. A moderate temperature effect was found with EPA smoke number decreasing as ambient temperature increased. A similar analysis on nine JT8D pilot lot engines tested from 1973 to 1976 revealed a similar temperature sensitivity with the JT8D EPA smoke number decreasing from approximately 27 at 35 Deg. F to around 18 at 85 Deg. F. The data scatter (±5 SN) exhibited by these data, however, makes the determination of a strong temperature effect difficult. Similar pilot lot JT9D test data did not reveal significant ambient effects.

An alternative approach to the assessment of smoke emissions is reflected in rig/engine correlation factors used by General Electric, where:

$$\text{Smoke Number}_{\text{corrected}} = \text{Smoke Number}_{\text{measured}} * \left(\frac{P3_{\text{engine}}}{P3_{\text{rig}}}\right)^{1.5}$$

In this model formulation, smoke number is assumed to increase as combustor inlet pressure increases. Considering the high positive correlation between combustor inlet temperatures and pressures, the Pratt & Whitney and General Electric findings appear contradictory if one assumes that combustor inlet temperatures and pressures are the only determinant of smoke production. The small magnitude of the corrections predicted by both manufacturers' approaches and the high degree of variability present in smoke emissions however suggests that the choice of an ambient effects smoke model of broad applicability is open to debate and that the major sources of smoke variability rest in other areas.

5. CORRECTION FACTOR APPROACH

This section of the report outlines the general approach used to develop the correction factors for aircraft engine emissions variations due to non-standard day temperature, pressure and humidity proposed in this report. Three major considerations were addressed before the design of this correction factor system was undertaken. These considerations were:

- Use of Theoretically vs. Empirically Derived Correction Factors
- Choice of Correlating Variables - Ambient vs. Combustor Inlet
- Model Structure - Simple vs. Complex

A brief discussion of each of these topics is presented below.

5.1 THEORETICAL VS. EMPIRICAL EMISSIONS MODELS

The first question addressed in selecting a correction factor development approach was whether a theoretical or an empirical approach should be used. Ambient effects literature as outlined in Section 4 provides reasonably successful examples of both theoretical and empirical correction factors. In general, for a single engine the performance of both approaches is comparable, with NOX correction factors reasonably well defined, HC and CO corrections considerably less refined, and Smoke Number corrections relatively unknown. An empirical approach using regression models based on current theoretical literature was selected for the study described in this report. Figure 8 outlines the general steps used to develop this general correction factor approach.

5.2 CORRELATING PARAMETERS - AMBIENT VS. COMBUSTOR INLET

In the review of current literature outlined in Section 4, two sets of variables were commonly used to correlate emission response to varying temperature, pressure, and humidity. These two sets of variables are:

- Ambient Conditions
    - ambient temperature (TAMB)
    - ambient pressure (PAMB)
    - ambient humidity (HAMB)
- Combustor Inlet Conditions
    - combustor inlet temperature (T3)
    - combustor inlet pressure (P3)
    - combustor inlet humidity
      (assumed equal to ambient humidity)

Combustor inlet parameters were chosen as the correlating parameters for this study. The reasons for this choice are summarized below.

The major objective of a correction factor system is the ability to relate emissions levels measured under non-standard ambient temperature, pressure and humidity to those which would have been measured under standard day conditions. Combustor inlet temperature and pressure can be directly related to ambient temperature and pressure. This relationship is presented in Appendix B. For a given engine, ambient conditions, engine pressure ratio and compressor efficiency determine the corresponding combustor inlet conditions. This direct relationship between ambient and combustor inlet conditions is also illustrated in Figure 9 where combustor inlet temperature is plotted versus ambient temperature for a subset of CFM56 combustor rig data. The data presented in this figure were taken at idle power and at a constant ambient pressure of 29.31 in Hg.

In addition, combustor inlet pressure, temperature, and humidity adequately predict emission levels. This observation has been clearly demonstrated in the ambient effects literature (References 5, 6, 7, and others). This correlation is further demonstrated in Figures 10 to 12 where the natural logarithms of CFM56 combustor rig HC, CO, and NOX emission indices (1b pollutant/1000 1b fuel) are plotted versus combustor inlet temperature. The HC and CO data in these figures were taken at idle power while the NOX emission data corresponds to climb power. Ambient humidity and pressure were held constant during this phase of testing. Figure 13 presents NOX climb data versus ambient humidity for fixed ambient (also combustor inlet) temperature and pressure. For the purposes of this report, ambient and combustor inlet specific humidity are assumed equal. The natural logarithm of the emission indices was selected as a correlating parameter over the emission indices themselves because of the linear relationship which exists between the emission index logarithm and combustor inlet temperature, and because of the theoretical dependence discussed in Section 4.1.

In the above, the relationship between ambient and combustor inlet conditions has been summarized and the ability to correlate aircraft emission levels with these combustor inlet parameters has also been demonstrated for a sample data set. Neither of these observations alone, however, provides a sufficient rationale for selecting combustor inlet over ambient parameters as the basis for a general correction factor system. The primary reason for this choice is that the use of combustor inlet parameters opens the possibility for a more direct comparison of correction factors developed for engines of differing pressure ratios, compressor efficiencies, classes, etc. Since combustor inlet conditions are the primary determinant of ultimate emission levels, their use as the correlating parameter avoids confounding effects due to compressor differences between engines and permits data from combustor rigs to be directly incorporated into the search for a generalized correction factor system. It should be noted, however, that the use of combustor inlet parameters as the only determinant of emission levels does not directly admit the possibility that changes within the combustor itself (changes which do not affect combustor inlet pressure and temperature) can effect emission levels. These internal combustor modifications are encorporated into the correction factor system through the use of a "technology"parameter which permits engines of more advanced designs to use different correction factor coefficients. This variation in correction factor is discussed fully in Section 7.

5.3 SIMPLE VS. COMPLEX EMISSIONS MODELS

Figure 14 presents the emissions models selected as the basis for the general correction factor system proposed in this report. These models are reformulated in terms of the emission indices themselves and summarized below:

AMBIENT EFFECTS PROGRAM REGRESSION MODEL SUMMARY

$$\text{HC EI} = a_0 * e^{a_1 * T3}$$

$$\text{CO EI} = b_0 * e^{b_1 * T3}$$

$$\text{NOX EI} = c_o * e^{c_1 * T3} * e^{c_2 * HAMB}$$

$$\text{SMOKE NUMBER} = d_0 * P3^{d_1}$$

where a_0, a_1, b_0, b_1, c_0, c_1, c_2, d_0, d_1 are coefficients determined from regression analysis.

T3 = Combustor Inlet Temperature (Deg. F)
P3 = Combustor Inlet Pressure (Psia)
HAMB = Ambient Specific Humidity (lb H_2O/lb Air)

The models were selected after an extensive examination of a variety of regression models which were applied to both the five EPA sponsored test engines and the approximately 30 engines in the industry contributed data base. A variety of reasons led to the final selection of these models; several of the more important are summarized below.

An examination of Figure 14 reveals that in each proposed emissions model, either the combustor inlet temperature (T3) or the natural logarithm of combustor inlet pressure (LNP3), but never both, appear in the regression model. The primary reason for this aspect of model formulation rests in the high degree of interdependence between combustor inlet temperature and pressure. The correlation coefficient between T3 and P3 provides a useful measure of this interdependence. The range of the correlation coefficient ρ is $(-1 \leq \rho \leq +1)$. A value of $\rho = 0$ indicates that T3 and P3 are not linearly related. A value of ρ that approaches (-1) reflects a very close inverse linear relationship. As ρ approaches (+1), a positive linear relationship between T3 and P3 is indicated. For the test data encompassed by this study, the correlation between combustor inlet temperature and combustor inlet pressure was typically in the range between 0.95 and 0.98. As a result, a knowledge of either T3 or P3 permitted the other to be determined. Similarly, a knowledge of emission variation with respect to either T3 or P3 alone was sufficient to determine the major influence of ambient variations. In fact, the inclusion of both T3 and P3 in a regression analysis can lead to a variety of analytical problems commonly referred to as multicollinearity. These problems make the determination of reliable and stable correction factor coefficients impossible. A basic description of multicollinearity and illustrations of this problem in aircraft emissions data is presented in Appendix C. Combustor inlet temperature was selected as the primary correlating variable for the HC, CO and NOX models since it provided a slightly better fit to the observed data. On the other hand, combustor inlet pressure represented the best predictor of visible smoke emissions.

Further examination of Figure 14 emphasizes the relative simplicity of the basic models selected. While more complicated emissions models involving multiple independent variables (e.g., inclusion of fuel air ratio for HC and CO, ambient humidity for CO, etc.) were found to give a small improvement in the ability to explain emissions variations for selected engines, neither the magnitude of this improvement nor its general applicability warranted the use of more terms in the regression models selected. Instead, it was felt that the development of a general empirical correction factor scheme required the least complicated emissions models in order to gain correction coefficient stability and to demonstrate general trends.

The overall performance of the emissions models selected is remarkably good considering the number and diversity of engines in the test data analyzed. A common statistic used to evaluate regression models is the coefficient of determination or R^2. This statistic expresses the fraction of the variation in a given set of test data explained by the regression model chosen. An R^2 value of 0, for instance, would indicate that 0 percent of the variation in emission levels was explained by the emission model selected. A value of 1 on the other hand, says that 100% of the variation in emission levels was explained by the regression model. The average R^2 values for the approximately 30 regressions examined for each pollutant are summarized below.

AMBIENT EFFECTS REGRESSION MODELS
MEAN COEFFICIENT OF DETERMINATION (R^2)
(Sample Size ≈ 30 Regressions/Pollutant)

Model	Mean R^2
LNHC = f(T3)	0.82
LNCO = f(T3)	0.86
LNNOX = f(T3,HAMB)	0.91
LNSMK = f(LNP3)	0.60

These performance figures should be judged in light of the inherent variability in the test data. This comparison is presented in Section 5.4.

The minimal increase in model performance which typically can be achieved by including additional terms in the regression model selected is demonstrated by the TF30 carbon monoxide regression statistics below. Shown in this summary is the increase in the coefficient of determination (R^2) which is achieved by adding new terms to the CO regression model.

TF30 CO REGRESSION MODEL SUMMARY

LNCO=f( )

Variables in Model	R^2	Increase in R^2
T3	.9820	-
+ LNP3	.9896	.0076
+ HAMB	.9911	.0015
+ P3	.9937	.0026
+ FA	.9938	.0001

5.4 DATA VARIABILITY

An important consideration in assessing the performance of the ambient effects emissions models proposed in the preceding section is the variability observed in aircraft emissions data. A typical question which might be asked is: How does the variability in measured emissions data compare to the magnitude of a correction factor for a particular pollutant? For instance, the application of a 5 percent correction factor to data with an observed variability of 20 percent is of dubious value.

Variability can be usefully divided into two components:

- Test-to-Test Variability
- Engine-to-Engine Variability

Test-to-test variability is manifested by the fact that replicate tests on a particular engine ostensibly operating under identical test conditions do not give the same results. This aspect of emissions variability is due in part to such factors as instrumentation errors, slight variation in engine power setting, test site, test sequence, etc. An extensive discussion of many of the causes of test-to-test variability in aircraft engine emission measurements is provided in References 11 and 12. Engine-to-engine variability on the other hand provides an additional source of variation in emission data. This phenomenon occurs when several engines of a particular model are tested. A discussion of each source of variability is given in the remainder of this section.

5.4.1 Test-to-Test Variability

Three test programs were used to assess test-to-test variability. First, each of the 112 test points for the TPE331-5-251 was repeated twice for a total of 3 measurements/test point. Second, each of the 107 test points for the CFM56 combustor rig was repeated once for a total of 2 measurements/test point. Finally, each of the 7 idle tests for the ALF502 full scale engine was repeated once for a total of 2 measurements/idle test point.

A measure of repeatability can be obtained as follows: Consider a particular engine tested in a given mode and compute the mean $\bar{X}_k$ $(k = 1,\ldots,N)$ of the replicate measurements. Then compute the variance of the replicates as follows:

$$\hat{\sigma}_k^{\,2} = \sum_{i=1}^{N} \frac{(X_{ik} - \bar{X}_k)^2}{N - 1}$$

where X_{ik} is the i^{th} replicate measurement for the k^{th} test point and N is the number of replicate measurements (2 for CFM56, 3 for TPE331-5-251, 2 for ALF502 engine).

The coefficient of variation or $\hat{\sigma}_k/\bar{X}_k$ represents a useful measure of the relative repeatability of the emissions measurements.

If the coefficients of variation for each test point in a given mode are computed and averaged, a measure of the average repeatability of emissions measurements for a given pollutant and mode can be obtained. Figure 15 illustrates this process for the 22 CFM56 combustor rig idle HC test points where a mean coefficient of variation of .2232 was determined. This parameter indicates that for HC CFM56 rig measurements the test-to-test variability $\hat{\sigma}_k$ is approximately 22% of the mean HC idle emission index. Tables 9 and 10 summarize the mode-by-mode coefficient of variation analysis for the CFM56 and TPE331-5-251 engines. In both these tables, high thrust HC and CO values were omitted because of the very low emission levels at these thrust levels. Of particular note is the high degree of repeatability (approximately 3-4%) obtained for NOX emission levels. Conversely, the repeatability for CFM56 smoke measurements was found to be around 40%. It should be noted that the above analysis does not include the engine-to-engine variability which can only be estimated by measurements on multiple engines.

A similar analysis was undertaken on the AVCO ALF502 full scale engine data using the two idle measurements presented for each test. These two idle settings represent the same nominal thrust level except that the first was taken just after start-up (TAXI-OUT) and the second after descending from full power (TAXI-IN). As such, this ALF502 data provides a measure of the test-to-test variability in this data. Table 11 presents a summary of the mean IDLE coefficient of variation for each of the four pollutants. Similar data presented in Tables 9 and 10 for the CFM56 and TPE331-5-251 is repeated for comparison.

5.4.2 Engine-to-Engine Variability

An evaluation of engine-to-engine emissions variability requires that different engines of the same model be tested under identical test conditions. Unfortunately, insufficient data was available in the ambient effects data base to adequately evaluate this aspect of emissions variability. In most instances, the test data consisted of multiple tests on a single engine or combustor rig. In those cases such as the Pratt & Whitney JT8D and JT9D pilot lot data where multiple engines were tested, varying ambient conditions for each engine limited the ability to segregate the effects of engine-to-engine variability. Some guidance in this area is provided by Reference 4 which concluded that engine-to-engine variability is on the same order of magnitude as test-to-test variability.

5.5 REGRESSION MODELS AND CORRECTION FACTORS

Figure 14 summarized the general regression models used to assess emission response to ambient effects. From these equations, correction factors can be derived as shown in Figure 16. The specific equation presented in this example has been derived from the CFM56 combustor rig NOX emissions data discussed fully in Section 6. The correction factor (CF) is defined as:

$$\text{CF} = \frac{\text{EMISSIONS AT STANDARD DAY CONDITIONS}}{\text{MEASURED EMISSIONS}}$$

The corrected emissions indices at standard day conditions are then given as:

$$\text{EMISSIONS}_{\text{(corrected)}} = \text{EMISSIONS}_{\text{(measured)}} * \text{CF}$$

6. INDIVIDUAL ENGINE CORRECTION FACTORS

This section presents a comprehensive example which illustrates the methodology used to develop correction factors for a single engine. The CFM56 Rig data was chosen for this example because it was sampled under controlled ambient conditions and it adequately represents the problems encountered in analyzing aircraft engine emissions data.

6.1 CFM56 Combustor Rig - Raw Data Plots

Figures 17 through 26 present CFM56 combustor rig data plots for the four pollutants and selected explanatory variables. Each pollutant and the natural log of that pollutant are presented to demonstrate the general pattern of the data and the effect of the log transformation upon the data. Figures 18 (LN(HC) vs T3), 20 (LN(CO) vs T3), and 22 (LN(NOX) vs T3) are of particular interest. The purpose of the log transformation is to make the data amenable to linear regression techniques. Ideally, the proper transformation would orient the data in a straight line when the dependent variable (say LN(NOX)) is plotted against the appropriate explanatory variable. In Figure 22, it is evident that the log transformation on the dependent variable works quite well. The remaining nonlinearities in this data plot are due primarily to humidity variation. A comparison of this plot with those for HC and CO (Figures 18 and 20) reveals a linearization of the data in only the portion of the curve where T3 is less than 500°. This portion of the curve represents the data for the idle and 1.5 idle modes and is the data used in developing the HC and CO correction factors. The other data points where T3 is greater than 500° were not used in developing the correction factors because the levels of HC and CO in this range were considered to be an insignificant contribution to the LTO cycle. Thus the HC and CO correction factors developed in this report are only applicable to the idle modes. No HC or CO correction is applied to the higher powered modes. Figures 23 and 24 show the decrease in the NOX levels as the ambient humidity increases. The data for all five test modes are presented in this plot. Figures 25 and 26 show a relatively large data scatter in the Smoke vs P3 data with perhaps a slight increase in smoke levels as P3 increases. The low smoke numbers for the CFM56 rig data are partially the result of facility limitations which necessitated running the rig tests at reduced P3 levels. As a result of these limitations, conditions favorable to high smoke production were not included in the test matrix.

6.2 CFM56 COMBUSTOR RIG - SUMMARY STATISTICS BY MODE

Summary statistics by mode for the CFM56 combustor rig data are given in Table 12 . This table demonstrates the response of the dependent and independent variables to changes in thrust. The constant values for HC in CLIMB and TAKEOFF modes are the result of nominally setting the HC values to .01 for small values of HC. Of particular interest in this table is the coefficient of variation (C.V.) or the ratio of one standard deviation in the data to the mean value of a particular data set. This statistic provides a measure of the relative scatter in a given set of data. Since the percent rated thrust (PTHRUST) is essentially constant in these mode-by-mode statistics, the coefficient of variation provides a good measure of the relative variation in the emissions data which is primarily due to ambient variation. Several of the more important modal coefficients of variation are summarized below.

CFM56 EMISSION INDEX MODAL COEFFICIENT OF VARIATION (C.V.)

Pollutant	Mode	C.V. %
HC EI	IDLE	98
CO EI	IDLE	25
NOX EI	TAKEOFF	19
SMOKE	TAKEOFF	31

6.3 CMF56 COMBUSTOR RIG - REGRESSION SUMMARY

Section 5 discussed the rationale for selecting the general form of the regression equations. Figure 27 summarizes the equations derived for the CFM56 Combustor Rig data. Tables 13 through 16 present selected regression statistics for these equations. It is useful here to explain some of the statistics presented in the regression summary.

We can begin by identifying the specific equation or model used in the least squares regression approach. (The reader is reminded that because the natural logs of the emissions are used instead of emissions themselves, only the log data will have the least squares properties such as the sum of the residuals equal to zero.) For example, the form of the equation chosen for the NOX model is given as:

$$LN(NOX) = a_0 + a_1 \, T3 + a_2 \, HAMB$$

where a_0, a_1, a_2 are the least squares parameter estimates, T3 is the combustor inlet temperature in degrees F, and HAMB is the specific humidity in lb H_2O/lb dry air. Thus in Table 15 we find under the heading "ESTIMATE" the values 0.46742286, 0.00250325 and -20.70200748 for a_0, a_1 and a_2, respectively. It is possible to perform a statistical test to determine if the parameter estimates are significantly different from zero. Obviously, if we cannot say that the parameter estimates for the T3 and HAMB coefficients are different from zero, we have been unable to establish a statistically valid model for the relationship we assumed between LN(NOX) and the explanatory variables T3 and HAMB. The statistical test on the parameter estimates is carried out as follows:

i) Select a significance level (typically .05 or .01), that is, the probability of rejecting the hypothesis that the parameter equals zero when in fact it actually is zero.

ii) If the value under the heading "PR > |T| " corresponding to the parameter of interest is less than the significance level, we will reject the hypothesis that the parameter equals zero. The |T| represents the absolute value of a t-statistic with appropriate degrees of freedom.

In Table 15 , the value under the heading "PR > |T|" corresponding to the T3 parameter is 0.0001. Assuming a level of significance of .05 we will reject the hypothesis that the T3 parameter equals zero.

Testing the parameter estimates is also referred to as testing for significance of regression. Another method of testing for significance of regression is to use the information given under the heading "PR > F". This is referred to in the literature as an F-test for significance of regression. In a manner analogous to that for the parameter estimates, if the value under the heading "PR > F" is less than the significance level chosen, we reject the hypothesis that the regression is not significant. While it is important to know whether or not a parameter estimate is different from zero, it is also useful to have an idea of how much we might expect that parameter estimate to change if we were to calculate it for another set of CFM56 rig data taken under identical conditions. An approximate measure of the variation in a parameter estimate can be found by taking the estimate plus or minus two times its standard error. In Table 15 then we find that our T3 estimate will vary over the range 0.00250325 ± 2 (.00002079) or from 0.002462 to 0.002544.

The information presented under the heading "SUM OF SQUARES" provides insight into how well the model fits the data. Suffice it to say that the CORRECTED TOTAL SUM OF SQUARES is a measure of the overall variation in the data. This total variation can be segregated into two parts: the first is the MODEL SUM OF SQUARES and the second is the ERROR SUM OF SQUARES. The MODEL SUM OF SQUARES is a measure of the portion of the total variation that can be attributed to the regression equation we have chosen. The ERROR SUM OF SQUARES is a measure of that portion of the total variation that is not accounted for by the regression equation. In general, we would like to see as much of the total variation in the data attributed to the model chosen. Thus if we have selected a reasonable model:

$$\mathrm{LN(NOX)} = a_0 + a_1\,\mathrm{T3} + a_2\,\mathrm{HAMB}$$

we would expect to reduce the "ERROR SUM OF SQUARES" to some minimal value, but never to zero because NOX formation is most probably a function to a limited extent of variables other than combustor inlet temperature and ambient humidity. As noted earlier, we would like to see the MODEL SUM OF SQUARES approach the value of the CORRECTED TOTAL SUM OF SQUARES which will consequently reduce the ERROR SUM OF SQUARES. We can write the relationship between the various sums of squares in equation form:

CORRECTED TOTAL SUM OF SQUARES = MODEL SUM OF SQUARES
+ ERROR SUM OF SQUARES

Another measure of how well the model fits the data is to examine the ratio:

$$R^2 = \text{(MODEL SUM OF SQUARES)/(CORRECTED TOTAL SUM OF SQUARES)}$$

noting that R^2 (R - SQUARE) will approach unity for a "good" fit. Referring again to Table 15 , we see that a significant portion of the CORRECTED TOTAL SUM OF SQUARES (86.73) is allocated to the MODEL SUM OF SQUARES (85.55) indicating that the model fits the data quite well. In fact, under the heading "R-SQUARE" we see that 98.64 percent of the total variation in the LN(NOX) data is attributable to the regression model we have chosen (e.g., variation in T3 and HAMB).

The statistic provided under the heading "C.V." expresses the variation in the data as a percentage of the mean of the data. This measure is called the coefficient of variation:

$$\text{C.V.} = \frac{\sigma}{\mu} * 100 \text{ percent}$$

where σ = the standard deviation of the data

μ = the mean of the data

Thus we see in Table 15 that the coefficient of variation for the idle to takeoff LN(NOX) data equals 3.8478 percent. It is interesting to compare this degree of variability in the LN(NOX) data to that presented in Section 6.2 for the untransformed NOX data where a coefficient of variation of 19% was found for the takeoff mode only. This reduction in variability is one of the properties of the logarithmic transformation which linearizes and rescales the test data by "compressing" the higher valued emission indices.

Comparing the regressions in Tables 13 to 16 we see that the best fit is with the LN(NOX) data -- this is reflected in both the MEAN SQUARE and the R-SQUARE values. The major reasons for this are (1) the effect of the log transformation in linearizing the data, and (2) the relatively low level of variation in the LN(NOX) data as reflected in the small coefficient of variation. The regression fits for LN(HC) and LN(CO) are still quite acceptable. Note that the error bounds on the parameter estimates (± 2 * STD ERROR OF ESTIMATE) are relatively small). Only for the LN(SMOKE) data do the regression statistics indicate a poor fit of the data. In Table 16 we see that only 4.99 percent (R-SQUARE) of the variation in the data is attributable to the model chosen. The parameter estimate for LN(P3) is significant, indicating a relationship between LN(P3) and LN(SMOKE), but the reasons for the poor R-SQUARE value are due to (1) the large amount of variation inherent in the LN(SMOKE) data as demonstrated by a large (66.39 percent) coefficient of variation, and (2) the low values of smoke number measured. Table 12, for instance, indicates the mean takeoff power smoke number was only 4.12. Due to the above limitations in the CFM56 smoke data, alternative data sources such as JT8D, JT9D, RB211-22B, SPEY 511 and the ALF502 were used to develop the smoke model, LN(SMOKE) = f(LN(P3)) which was chosen as the most representative predictor of variation in smoke number due to ambient and combustor inlet conditions.

In summation, this section of the report has presented a fairly comprehensive example illustrating the development and the performance of the emissions models developed for the CFM56 combustor rig. The intent of this section has been to illustrate, using extensive data from a single combustor, selected important facets of the data analysis process which are representative of many of the problems encountered and techniques applied to the entire ambient effects data base. Of particular importance in terms of overall representativeness are:

- The relative degree of variability in HC, CO, NOX and smoke emissions

  NOX CO SMOKE HC
  (Least Variable - - - - - - - - Most Variable)

- The emission response to combustor inlet conditions as expressed by the functional emissions models chosen. (See Figure 14.)

- The comparative degree of fit by the regression models for the four pollutants.

  NOX CO HC SMOKE
  (Best Fit - - - - - - - - - Poorest Fit)

7.0 GENERALIZED CORRECTION FACTORS

This section of the report summarizes the results of the generalized correction factor study for each of the four regulated pollutants - HC, CO, NOX, and EPA Smoke Number. Figure 28 illustrates the four basic steps used to develop these correction factors. First, regression analyses using the functional models discussed in Section 5.3 were performed on test data for each engine in the data base. Section 6 provides a detailed example of how these regressions were performed and an assessment of how well they typically predict emission response to changing combustor inlet conditions. For each engine (assuming data for each pollutant was available), five regression coefficients were determined.

Pollutant	Coefficient	Description
HC	T3COEF	HC combustor inlet temperature coefficient
CO	T3COEF	CO combustor inlet temperature coefficient
NOX	T3COEF	NOX combustor inlet temperature coefficient
	HAMBCOEF	NOX ambient humidity coefficient
SMOKE	P3COEF	Smoke combustor inlet pressure coefficient

The NOX combustor inlet temperature and ambient humidity coefficients, for example, are derived from a regression analysis of the form:

$$\mathrm{LN(NOX)} = \mathrm{CONSTANT} + \mathrm{T3COEF} * \mathrm{T3} + \mathrm{HAMBCOEF} * \mathrm{HAMB}, \quad \text{or}$$

$$\mathrm{NOX} = e^{(\mathrm{CONSTANT})} * e^{(\mathrm{T3COEF} * \mathrm{T3})} * e^{(\mathrm{HAMBCOEF} * \mathrm{HAMB})}$$

where LN(NOX) = the natural logarithm of the NOX emission index

CONSTANT = constant term in regression

T3 = combustor inlet temperature (Deg. F)

HAMB = ambient humidity (lb H_2O/lb day Air)

The T3COEF for NOX,therefore,provides a measure of the increase in the natural logarithm of the NOX emission index which should result from a one Deg. F increase in combustor inlet temperature. The effect of such a one degree change on the emission index itself is computed as exp (T3COEF). Similar analyses are applicable to both the HC and CO combustor inlet temperature coefficients and the NOX ambient humidity coefficient.

The smoke combustor inlet pressure coefficient P3COEF, on the other hand, developed using a model of the form:

$$\mathrm{LN(Smoke\ Number)} = \mathrm{CONSTANT} + \mathrm{P3COEF} * \mathrm{LN(P3)}$$

or

$$\mathrm{Smoke\ Number} = e^{\mathrm{CONSTANT}} * \mathrm{P3}^{\mathrm{P3COEF}}$$

where

LN(Smoke Number) = the natural logarithm of the EPA smoke number

CONSTANT = constant term in regression

P3 = combustor inlet pressure (PSIA)

The P3COEF for smoke,therefore,provides a measure of the increase in the natural logarithm of the smoke number which should result from a one unit increase in the logarithm of combustor inlet pressure.

The final step in the development of the proposed correction factors was to summarize salient engine operating parameters for each engine and relate these parameters to the combustor inlet regression coefficients determined above. Of particular interest in this phase of analysis were the rated engine pressure ratio (PR) and the idle pressure ratio (IPR). Although the usefulness of a variety of other engine parameters such as rated thrust and bypass ratio were analyzed, better correlation was found between the combustor coefficients and rated and idle pressure ratio. Primary outputs of this phase of the analysis are plots illustrating the variation in a particular coefficient as a function of rated or idle pressure ratio.

Each point plotted in these figures represents the results of one regression analysis on a given engine. The number of data points used to determine the regression line for each engine varied from approximately 10 to around 200. It is important to remember that the coefficients plotted in these figures represent the temperature, humidity or pressure sensitivity (slope) of a particular emission index or smoke number as a function of PR or IPR and not the magnitude of that emission index. Thus, while it is well known that the NOX emission index generally increases with rated engine pressure ratio, a plot of the NOX temperature coefficient T3COEF versus engine pressure ratio indicates how the slope of the NOX EI vs PR curve changes with rated pressure ratio. This slope is indicative of the response of a particular pollutant to the small changes in combustor inlet parameters commonly introduced by variations in ambient test conditions.

In the following, the results of the general correction factor analysis are summarized for each pollutant. Six basic types of information are presented:

- Correction Factor Coefficients in Tabular Form
- Correction Factor Coefficients Plotted versus Engine Operating Parameters
- Proposed Generalized Correction Factors
- Theoretical Background for Proposed Correction Techniques
- Relationship between Newer Technology Engines and Proposed Correction Techniques
- Sensitivity and Error Analysis

Figure 29 provides the nomenclature used throughout the presentation of this summary. A word of explanation is in order with regard to two parameters, T3MEAN and P3MEAN, which are used in this presentation. As stated earlier in the introduction to this section, the rated engine pressure ratio (PR) and idle pressure ratio (IPR) are used to correlate the correction factor coefficients with engine operating parameters. Since selected engines in the data base were not tested while operating in close proximity to "rated" standard day test conditions (e.g., the RB211-22B altitude data was run at a simulated 10,700 M pressure), two alternative parameters, T3MEAN and P3MEAN were introduced which are analogous to rated engine T3 and P3 but which also account for anomalies in the test data due to specifics of how the engines were tested. For example, the RB211-22B rated pressure ratio is 25. When this engine is operating in close proximity to standard day rated conditions, a P3MEAN of approximately 350 PSIA is observed. The same engine tested under high altitude conditions, however, exhibits a P3MEAN of approximately 260 PSIA. Similarly, a T3MEAN value of around 900 Deg. F is found for normal engine operation while a T3MEAN of 850 Deg.F is observed during altitude testing. In short, the use of T3MEAN and P3MEAN facilitates the correlation between correction factor coefficient and engine operating parameter by eliminating some of the confounding effects attributable to the fact that the engines analyzed were tested under a relatively diverse set of experimental designs. Figure 30 illustrates the relationship between T3MEAN and rated pressure ratio (PR) for the engines in the test data base.

7.1 Oxides of Nitrogen

Table 17 presents a summary of the NOX emission index correction factor coefficients developed for the model LN(NOX EI) = f(T3,HAMB). A description of the variables listed in this table was given in Figure 29. Summary statistics for these coefficients are provided in Table 18. The temperature and humidity correction factors developed from these data are presented and discussed below.

7.1.1 Temperature Correction Factor

In order to assess the potential influence of engine operating parameters on the NOX combustor inlet temperature coefficient T3COEF, this coefficient was plotted versus P3MEAN. Figure 31 illustrates the results of this analysis. Each point in this figure represents the T3 regression coefficient determined for a given engine. In selected cases, this plotted point represents the regression results for only a single operating mode (e.g., CFM56 Idle). As shown in this figure, the calculated combustor inlet temperature coefficients (T3COEF) rise linearly with P3MEAN. As combustor inlet pressure increases, therefore, the natural logarithm of the NOX emission index becomes more sensitive to changes in combustor inlet temperature.

A useful approach to analyzing the data presented in Figure 31 is to compare the results illustrated to those developed by Lipfert (Reference 6) and summarized in Figure 32 (Reference 13). In this figure, the NOX emission index for a variety of production engines is plotted versus compressor discharge temperature (T3). The slope of the Lipfert curve in log space represents the combustor inlet temperature coefficient T3COEF.

$$\mathrm{T3COEF} = \frac{\mathrm{LN(NOX\ EI)}_{\mathrm{T3}_2} - \mathrm{LN(NOX\ EI)}_{\mathrm{T3}_1}}{\mathrm{T3}_2 - \mathrm{T3}_1}$$

where $\mathrm{T3}_2 > \mathrm{T3}_1$ Deg. F.

In the Lipfert analysis, a constant NOX combustor inlet temperature coefficient of approximately 0.00385 was determined. This constant value of T3COEF is plotted as a horizontal line in Figure 31 and corresponds to approximately the mean value of the combustor inlet temperature coefficients determined in the present study.

In order to assess whether the observed NOX T3COEF trend is statistically significant (not necessarily significant from an engineering standpoint), the 95% upper and lower confidence bounds on the computed combustor inlet temperature coefficients were computed as follows:

Let: T3COEF = NOX combustor inlet temperature coefficient
$t_{.05}$ = t statistic at .05 significance level (≈2 for sample sizes greater than 30)
T3STD = T3COEF standard error
UCB = Upper Confidence Bound
LCB = Lower Confidence Bound

Then:

$$UCB = T3COEF + t_{.05} * T3STD$$

$$LCB = T3COEF - t_{.05} * T3STD$$

A confidence interval was constructed of the form:

$$LCB \leq T3COEF \leq UCB$$

The results of this analysis are presented in Figure 33 where the combustor inlet temperature coefficient and the corresponding upper and lower confidence bounds are plotted versus P3MEAN. A word of explanation is in order concerning the interpretation of these confidence intervals. The "true" value of T3COEF is a constant, not a random variable. In reality, therefore, this true T3COEF either is or is not contained in the confidence interval computed above. It is the interval as computed from the sample data which statistically varies. Both its midpoint and its width depend on the number and particular values obtained in the sample. If repeated regression analyses were performed on NOX data from a particular engine, and a confidence interval computed for the T3COEF determined from each, approximately 95% of the intervals so constructed would contain the "true" T3COEF. It is in this sense that the confidence intervals presented in Figure 33 should be interpreted. With this in mind, an examination of Figure 33 reveals that even when the confidence bounds on T3COEF are considered, a well defined upward trend between T3COEF and P3MEAN is evident.

Using theoretical analyses, Blazowski et al (Reference 5) also predicted an increasing temperature sensitivity with increasing combustor inlet pressure. This analysis was previously summarized in Section 4.1 and in Figure 4 where the required NOX temperature correction increased as rated engine pressure ratio increased from 10 to 25.

Figure 34 presents the NOX temperature coefficient plotted versus rated engine pressure ratio. The data presented in this figure provide the basis for the proposed NOX temperature correction factor. A least squares equation was determined which relates T3COEF to rated engine pressure ratio (PR). This equation is summarized below and plotted on Figure 34.

$$\text{NOX}\quad \text{T3COEF} = .001735 + .000107 * \text{PR}$$

$$R^2 = 0.77$$

Standard Errors of Regression Coefficients

Intercept = .000139
PR = .000010

The proposed NOX temperature correction factor is therefore a function of rated engine pressure ratio. In equation form, this temperature correction factor ($C_{T3_{NOX}}$) can be expressed as:

$$C_{T3_{NOX}} = e^{\text{T3COEF} * (T3_{\text{Reference}} - T3_{\text{Meas}})}$$

where

$$\text{T3COEF} = .00175 + .000107 * \text{PR}$$

Figure 35 illustrates the variation in T3COEF as a function of NOX MEAN (see Figure 29 for definition). As shown in this figure, the computed temperature coefficient rises uniformly with mean NOX levels. The only exception to this trend is the highly temperature sensitive SPEY 511, an older design engine, with high HC and CO emission levels but comparatively low NOX emissions. Also of note in this figure is the JT9D-7 Vorbix which employs an advanced technology staged combustor to reduce emissions. A comparison of the JT9D-7 Vorbix temperature coefficient with those of the conventional JT9D-7A and JT9D-7F engines reveals that the newer technology Vorbix exhibits a decreased NOX combustor inlet temperature sensitivity. An alternative method of presenting this finding is illustrated in Figure 36 where T3MEAN is plotted versus NOXMEAN. As seen in this figure, two basic engine groupings appear which roughly correspond to the levels of technology employed to control NOX emissions.

The first groups represents newer technology engines such as the JT9D-7 Vorbix, the CFM56 combustor rig, and the T63-A-5A advanced combustor engines. A primary objective of an NOX emission control strategy is the ability to operate at a given combustor inlet temperature and pressure and still reduce NOX emission levels. In simplified terms, the modification required to achieve this objective can involve lowering the NOX emission index vs combustor inlet temperature curve as shown in Figure 37. Two features on this curve are important. First, for a given combustor inlet temperature (T3) controlled engines exhibit a lower NOX emission index. Second, and more importantly, to achieve this reduced emission index, the temperature sensitivity (slope of the NOX vs T3 curve) must also be decreased. This phenomenon is manifested in Figures 35 and 36 for the JT9D-7 Vorbix and JT9D-7 conventional engines. Additional insights into the reduced NOX temperature sensitivity of new technology engines is provided in Reference 14.

The second group of engines in Figure 36 are representative, for the most part, of conventional engine designs with limited NOX emission controls. These engines typically exhibit a higher NOX temperature sensitivity for a given NOX emission level than the newer technology engines.

7.1.2 Humidity Correction Factor

Ambient humidity variations have a significant impact of NOX emission levels. This observation was illustrated in Figure 1 where a 25 percent change in the ALF502 NOX emission index was induced by changes in ambient humidity. As ambient humidity increased, NOX emission levels decreased, primarily because of the resulting reduced combustor inlet temperatures.

In developing a NOX EI humidity correction factor, attempts were made to determine the influence of engine operating parameters on the ambient humidity regression coefficient HAMBCOEF presented in Table 17. Theoretical insights provided by the research of Blazowski (Reference 5 and summarized in Section 4.1 and Figure 4) indicate that the NOX humidity coefficient should increase with rated engine pressure ratio. No evidence of this phenomenon could be found in the test data analyzed. Instead, it is felt that the mean value of the observed humidity coefficients provides a useful guideline in the choice of a humidity correction coefficient. This mean value was found to be -18.3 ± 8.0 (95% confidence level) for the 10 engines for which adequate humidity variation permitted computation of a humidity coefficient. This predicted range in the NOX humidity coefficient is comparable to that found by Shaw (Reference 15) of -22 ±8 and is close to the frequently quoted value of -19. The proposed NOX humidity correction factor is therefore:

$$C_{HAMB_{NOX}} = e^{HAMBCOEF * (HAMB_{Reference} - HAMB_{Meas})}$$

where

$HAMBCOEF = 18.3 \pm 8.0$

$HAMB_{Reference} = .00634$ lb H_2O/lb Dry Air

7.2 HYDROCARBONS

Table 19 presents a summary of the HC emission index correction factor coefficients developed using the model LN(HC EI) = f(T3). A description of the variables listed in this table was given in Figure 29. Summary statistics for these coefficients are provided in Table 20. The proposed HC temperature correction factor developed from these data is presented and discussed below.

Efforts were made to correlate the HC combustor inlet temperature T3COEF with a variety of engine operating parameters. The most successful of these engine correlation parameters was the Idle Pressure Ratio (IPR). Figure 38 presents a plot of the HC combustor inlet temperature coefficient versus engine idle pressure ratio. Two features of this figure are of importance in developing a generalized correction factor for hydrocarbons. First, as idle pressure ratio increases the HC temperature sensitivity as reflected in T3COEF increases in a negative direction. Since the HC combustor inlet temperature is defined as:

$$\text{T3COEF} = \frac{\text{LN(HC EI)}_{\text{T3}_2} - \text{LN(HC EI)}_{\text{T3}_1}}{\text{T3}_2 - \text{T3}_1}$$

where $\text{T3}_2 > \text{T3}_1$ Deg. F.

the observed negative increase in T3COEF indicates that higher idle pressure ratio engines exhibit larger decreases in HC emission levels for a given increase in combustor inlet pressure. This observation is consistent with the theoretical analysis presented by Blazowski et al (Reference 9 and summarized in Section 4.2 and Figure 5) where he demonstrates that a larger HC temperature correction factor is required for higher idle pressure ratio engines than for lower pressure ratio engines.

The second feature of Figure 38 of interest is the relationship between the coefficients determined for older technology engines with those of newer technology engines such as the JT9D-7 Vorbix and the CFM56 combustor rig. By an argument analogous to that presented in Section 7.1.1 where decreasing NOX temperature sensitivity was hypothesized for newer engines, an increasing HC temperature sensitivity would be expected for newer technology engines. Since hydrocarbon emissions are inversely proportional to combustor inlet temperature, a low HC emission engine designed to operate at a given idle pressure ratio could be expected to show more temperature sensitivity than an older technology engine. An examination of Figure 38 reveals that the JT9D-7 Vorbix and CFM56 combustor rig do, in fact, demonstrate high combustor inlet temperature sensitivity.

The data presented in Figure 38 form the basis for the proposed HC temperature correction factor. A line was drawn which represents the general coefficient trend between the HC temperature coefficient T3COEF and idle pressure ratio (IPR). This line is shown in Figure 38. The proposed HC temperature correction factor is, therefore, a function of engine idle pressure ratio and can be expressed as:

$$C_{T3_{HC}} = e^{T3COEF * (T3_{Reference} - T3_{Meas})}$$

where T3COEF is determined from Figure 38 and the appropriate idle pressure ratio.

7.3 CARBON MONOXIDE

An analysis similar to that outlined in Section 7.2 for hydrocarbons was also performed for carbon monoxide (CO). Table 21 presents a summary of the CO emission index correction factor coefficients developed using the LN(CO EI) = f(T3). A description of the variables listed in this table was given in Figure 29. Summary statistics for these coefficients are provided in Table 22. The proposed CO correction factor is outlined below.

Figure 39 presents a plot of the CO combustor inlet temperature coefficient T3COEF versus rated engine idle pressure ratio. Comments similar to those presented in Section 7.2 for HC are generally applicable to data presented in this figure. First, CO temperature sensitivity increases with rated engine pressure ratio. Second, newer technology engines tend to exhibit more temperature sensitivity for a given IPR. This observation is demonstrated by the high degree of CO temperature dependence found for the JT9D-7 Vorbix. It should be pointed out, however, that HC and CO correction factor coefficients do not always parallel each other. This observation is demonstrated by the relationship between the CFM56 combustor rig HC coefficient which is quite large and the CO coefficient which falls on the general trend line for engines of comparable idle pressure ratio.

The data presented in Figure 39 form the basis for the proposed CO temperature correction factor. A line was drawn which represents the general coefficient trend between the CO combustor inlet temperature coefficient T3COEF and idle pressure ratio IPR. This equation is plotted in Figure 39. The proposed CO temperature correction factor is, therefore, a function of engine idle pressure ratio. In equation form, this temperature correction factor ($C_{T3_{CO}}$) can be expressed as

$$C_{T3_{CO}} = e^{T3COEF * (T3_{Reference} - T3_{Meas})}$$

where T3COEF is determined from Figure 39 and the appropriate idle pressure ratio.

7.4 SMOKE NUMBER

Table 23 presents a summary of the EPA smoke number correction factor coefficients developed using the model LN (Smoke Number) = f(LN(P3)). A description of the variables in this table is given in Figure 29. Summary statistics for these coefficients are provided in Table 24. The proposed smoke number correction factor is outlined below.

Efforts were made to find a suitable engine operating parameter which correlated with the smoke number combustor inlet pressure coefficient P3COEF. Figure 40 presents a plot of this pressure coefficient versus rated engine pressure ratio (PR). Although a general trend of decreasing pressure coefficient with increasing rated pressure ratio is evidenced, this trend is for the most part the result of the smoke coefficient for a single engine, the ALF502 which exhibits a high smoke coefficient. The remaining engines in this figure represent large gas turbines (Class T2, T4) and have smoke coefficients in the range 0.5 to 1.5 with a mean P3COEF of approximately 1.0. These figures can be compared to the G.E. smoke coefficient of 1.5 which was discussed in Section 4.4.

An additional facet of the behavior for the smoke number combustor inlet pressure coefficient is provided in Figure 41 where the P3COEF is plotted versus SMKMEAN or the mean maximum power smoke number. As mean smoke emissions rise, combustor inlet pressure sensitivity also rises. Of note in this figure are the smoke levels exhibited by the JT9D-7 Vorbix.

The discussion above and the data in Figures 40 and 41 provide the basis for the proposed smoke correction factor. Using the smoke pressure coefficient which is defined in general terms as:

$$\text{P3COEF} = \frac{\text{LN(Smoke Number)}_{\text{P3}_2} - \text{LN(Smoke Number)}_{\text{P3}_1}}{\text{LN}(\text{P3}_2) - \text{LN}(\text{P3}_1)}$$

where $\text{P3}_2 > \text{P3}_1$ PSIA .

The smoke number correction factor ($C_{\text{P3}_{\text{Smoke}}}$) can be expressed as

$$C_{\text{P3}_{\text{Smoke}}} = \left(\frac{\text{P3}_{\text{Reference}}}{\text{P3}_{\text{Meas}}} \right)^{\text{P3COEF}}$$

where P3COEF = 1.0.

7.5 CORRECTION FACTOR SENSITIVITY ANALYSIS

In this section of the report, the sensitivity of each proposed correction factor will be analyzed in light of a variety of sources of error. Several of the more important considerations in analyzing these sources of error in ambient effects data correction are listed below:

- Test-to-Test Variability
- Engine-to-Engine Variability
- Model Formulation Error
- T3, P3, HAMB Coefficient Selection Error

Test-to-test and engine-to-engine variability were previously discussed in Sections 5.4.1 and 5.4.2. Model formulation error represents the inaccuracy introduced into the correction factor process because of the use of relatively basic emissions models as outlined in Figure 14. The errors introduced by these fundamental models can be assessed by examining mean RSQ (R^2) values presented in coefficient summary Tables 18, 20, 22 and 24. R^2 or the coefficient of determination provides a measure of the percent of the variation in a given set of data explained by the regression model selected. For the regressions performed in the present study, the mean R^2 values are summarized below. Also included in this summary is the estimated test-to-test variability. This test-to-test variability provides a reference against which to judge the overall performance of the regression models selected.

MODEL FORMULATION ERROR ASSESSMENT

Pollutant	Model	Percent Variation Explained $R^2 * 100$			Estimated Test-to-Test Variability %
		MIN	MAX	MEAN	
HC	LNHC = f(T3)	21	99	82	16
CO	LNCO = f(T3)	17	99	86	4
NOX	LNNOX = f(T3,HAMB)	73	99	91	3
SMOKE	LNSMK = f(LNP3)	5	96	60	33

A quantitative discussion of coefficient selection error is presented below. Correction factors for EI's are given as follows: For example, let:

$$\text{Smoke Number} = A0 * P3^{P3COEF}$$

where:

Smoke Number = EPA Smoke Number

$P3$ = Combustor Inlet Pressure (PSIA)

The smoke pressure correction factor would then be:

$$CF_{P3} = \left(\frac{P3_{Reference}}{P3_{Measured}} \right)^{P3COEF}$$

where:

$P3_{Reference}$ = Combustor Inlet Pressure at standard day conditions

$P3_{Measured}$ = Combustor Inlet Pressure as measured under non-reference conditions

In a similar manner, a temperature correction factor can be generated:

$$\text{NOX EI} = A0 * e^{T3COEF * T3}$$

where:

$T3$ = Combustor Inlet Temperature (Deg. F)

Then:

$$CF_{T3} = e^{T3COEF * (T3_{Reference} - T3_{Measured})}$$

An ambient humidity correction factor is generated in a manner similar to that for T3.

$$CF_{HAMB} = e^{HAMBCOEF * (HAMB_{Reference} - HAMB_{Measured})}$$

A sensitivity analysis can be performed on the correction factors by selecting values for the correction coefficients and allowing the inlet (P3, T3) and ambient (HAMB) conditions to vary over ranges typically experienced by production engines. Plots of correction factors as a function of inlet and ambient conditions are given in Figures 42 through 46. For example, Figure 42 demonstrates NOX combustor inlet temperature correction sensitivity. The values selected for the parameter T3COEF cover the range of T3 coefficients found for the various engine regressions done in this study. $T3_{Reference} - T3_{Measured}$ represents the difference between reference and measured combustor inlet temperatures which typically occur when testing engines at other than standard day conditions. Thus if $T3_{(Reference)} - T3_{(Measured)} = -100$, one would find a range of temperature correction factors of (0.905 - 0.607) corresponding to a range of (0.001 - 0.005) for the T3 coefficient.

Figure 47 shows the percent error in the NOX temperature correction factor as a result of using an incorrect T3 coefficient. In this case, it is assumed that the true value of T3COEF is .002, but a value of .004 was used to calculate the correction factor. The range of T3 coefficients for NOX regressions for the data used in this study is approximately .001 to .005. If we had picked a single T3 coefficient (to use for all engines), say .003, then the maximum difference between the "true" coefficient and .003 would be .002. This plot, then, represents the maximum error due to incorrect temperature coefficient selection one might expect to find if a general model of the form $NOX\ EI = A0 * e^{(T3COEF * T3)}$ is used for a group of engines.

Figures 48 through 51 give similar plots for HC and CO temperature correction, NOX humidity correction, and SMOKE pressure correction.

7.6 CORRECTION FACTOR PERFORMANCE ANALYSIS

Figures 52 through 55 indicate representative performance figures for both the single engine correction factor coefficients and the general trend line coefficients. Data are presented in these tables for the CFM56 combustor rig and the ALF502 combustor rig. The reduction in emissions variability achieved for these engines is comparable to that found when multiple tests are performed on a single engine. In other words, the major sources of variability in the emissions measurements for data presented in these tables are ambient conditions and test-to-test variability. The specific performance figures used to assess the correction factor performance are the uncorrected data coefficient of variation or

$$CV_{uncorrected} = \frac{\sigma_{uncorrected}}{\mu_{uncorrected}}$$

and the corrected data coefficient of variation

$$CV_{corrected} = \frac{\sigma_{corrected}}{\mu_{corrected}}$$

where σ = the standard deviation of the emissions data

μ = the mean of the emissions data

Ideally, since the correction factor process attempts to reduce $\sigma_{corrected}$ as much as possible, $CV_{corrected}$ will approach 0 for perfect correction to standard day conditions. The primary limitations on the ability to achieve this ideal correction have been discussed in previous sections and are amplified below. First, the inherent test-to-test variability in emissions data which is typically on the order of magnitude of 5% for NOX, 10% to 20% for HC and CO, and 40% for SMOKE provides a lower bound on the achievable reduction in emissions variation. Second, the use of simplified emissions models provides a further limitation on the correction factor performance. Finally, the correction coefficient selection error introduces a final major limitation on the correction process. This coefficient selection error is illustrated by the differences in performance between data correction using a correction coefficient developed for a specific engine and data correction using a general trend line coefficient.

The effect of these limitations on the emissions correction process can be further illustrated by Figure 56 where a hypothetical emission index Y (e.g., NOX EI) is plotted versus a typical correction factor correlating parameter X (e.g., T3). As shown in this figure, the uncorrected or measured emission data increases linearly with the correlating parameter. This phenomenon can be expressed in equation form as $Y = a + bX$ where a and b are regression coefficients. The principal effect of the data correction process is to transform this emissions data so that the corrected emission index is independent of the correlating parameter. Graphically, the ideal correction should transform the corrected data onto a perfect horizontal line. (See Appendix F for sample emission index corrections.) The use of simplified emissions models and test-to-test variability, however, provide limitations on how much reduction in variability can be practically achieved. The nature and extent of these limitations can be evaluated in quantitative terms as follows:

Let y_i = i^{th} uncorrected emission index measurement

x_i = i^{th} correlating parameter measurement

N = number of measurements

Then

$\hat{\sigma}_y^2$ = variance of uncorrected emission indices

$$= \frac{\sum_i (y_i - \bar{y})^2}{N - 1}$$

$\hat{\sigma}_{yx}^2$ = variance of the uncorrected emissions indices around the computed emission index line (residual variance)

$$= \frac{\sum_i (y_i - Y)^2}{N - 2}$$

where: Y = Estimate of the emission index y_i computed from the regression equation

$$Y = a + bx_i$$

$\bar{y}$ = Mean uncorrected emission index

The relationship between $\hat{\sigma}_y$ and σ_{yx} can be shown to be:

$$\sigma_{yx} = \sigma_y \sqrt{1 - R^2} \quad \frac{N-1}{N-2}$$

where R = Correlation coefficient between y and x

R^2 = Coefficient of determination (see Section 5.3)

$\hat{\sigma}_{yx}^2$ Provides a measure of the variance in the emissions data not accounted for by the regression model chosen and principally includes the effects due to test-to-test variability and the use of simplified emissions models. The effect of coefficient selection error provides an additional source of variability in this analysis. An assessment of the magnitude of this error component was presented in Section 7.5 and Figures 47 to 51.

The residual variance component as shown in the lower half of Figure 56 will remain even after the emissions data is corrected to reference conditions. The relationship between $CV_{uncorrected}$ and $CV_{corrected}$ (assuming $\mu_{uncorrected} = \mu_{corrected}$, N is large, $\sigma_{xy} \rightarrow \sigma_{corrected}$) can be expressed as

$$CV_{corrected} = \sqrt{1 - R^2} \; CV_{uncorrected}$$

In order to assess the implications of the above relationship on the correction factor process, the mean, maximum and minimum R^2 values presented in Section 7.5 for the entire emissions data base were used to compute the range of expected reduction in emission index variability for each of the four pollutants.

$$\text{Percent Reduction} = \frac{CV_{uncorrected} - CV_{corrected}}{CV_{uncorrected}} * 100\%$$

$$= (1 - \sqrt{1 - R^2}) * 100\%$$

Pollutant	Mean R^2 Statistic	Percent Reduction Emission Index Variability		
		MIN	MAX	MEAN
NOX EI	.91	48	90	70
HC EI	.82	11	90	58
CO EI	.86	9	90	63
SMOKE NUMBER	.60	3	80	37

A comparison of the above expected percent reduction in emission index variability with that actually computed for the CFM56 and ALF502 combustor rigs for NOX, HC, CO and Smoke in Figures 52 to 55 reveals the following. First, the CFM56 and ALF502 NOX, HC and CO emissions corrections for the specific engine coefficients (NOX = 68%, HC = 54%, CO = 54%) and the NOX and HC general coefficients (NOX = 65%, HC = 53%) provide reductions in emission index variability close to the mean percent reduction expected for each pollutant. Second, correcting the CFM56 rig CO data using the general coefficient provides substantially less reduction in emission index variability (e.g., at idle, 24% reduction vs 52% reduction) than use of the coefficient developed specifically for this rig. The principal reason for this occurrence as seen in Figure 39 is the difference between the specific engine CFM56 CO temperature correction coefficient and that predicted by the general trend line. Finally, the ALF502 smoke number corrections (5-9% reduction in variability) perform significantly poorer than the mean expected percent reduction for smoke number emissions, 37%. The small and highly variable smoke numbers (due primarily to the availability of only low power data) measured for this engine provide an explanation of the performance of the smoke correction on this particular data set. In general, a reduction in smoke number variability on the order of 30-40 percent can be expected.

8. REFERENCES

1) "Control of Air Pollution from Aircraft and Aircraft Engines," Federal Register, Volume 38, No. 136, Part II, July 17, 1973.

2) Slogar, G.A., Determination of Effects of Ambient Conditions on Aircraft Engine Emissions Engine Testing - GTCP 85 APU, TPE331 Turboprop, Volume 1, EPA Report 460/3-76-009-a, March 1976.

3) Slogar, G.A. and Holder, R.G., Determination of Effects of Ambient Conditions on Aircraft Engine Emissions Engine Testing - GTCP85 APU, TPE331 Turboprop, Volume 2, EPA Report 460/3-76-009-b, March 1976.

4) McAdams, H.T., Analysis of Aircraft Exhaust Emission Measurements - Statistics, EPA Report NA5007-K-2.

5) Blazowski, W.S., Walsh, D.E. and Mach, K.D., "Operating and Ambient Condition Influences on Aircraft Gas Turbine NOX Emissions" Journal of Aircraft, Vol. 12, No. 2, February 1975, pp. 113.

6) Lipfert, F.W., "Correlation of Gas Turbine Emissions Data," ASME Paper 72-GT-60, 1972.

7) Sarli, V.J., Eiler, D.C., and Marshal, R.L., "Effects of Operating Variables on Gaseous Emissions," Paper presented at Air Pollution Control Association (APCA) Specialty Conference on Air Pollution Measurement Accuracy as it Relates to Regulation Compliance, New Orleans, October 1975.

8) Durkee, K.R., Noble, E.A., and Jenkens, R., Standards Support and Environmental Impact Statement - An Investigation of the Best Systems of Emission Reduction for Stationary Gas Turbines, EPA Office of Air Quality Planning and Standards Preliminary Report, July 1976, pp. 3-60.

9) Blazowski, W.A. and Marzewski, J.W., Ambient Correction Factors for Aircraft Gas Turbine Idle Emissions, Interim Technical Report for the Period January 1975-March 1976, Technical Report AFAPL-TR.

10) Op. Cit., Reference 8, pp. 3-55.

11) Souza, A.F., Reckner, Louis, R., Variability in Aircraft Turbine Engine Emissions Measurements, EPA Report No. 460/3/74-006, January 1974.

12) Souza, A.F., Further Investigation Into the Causes of Variability in Aircraft Turbine Emission Measurement, EPA Report No. 460/3-75-011, November 1975.

13) Munt, R. and Danielson, E., *Aircraft Technology Assessment - Status of the Gas Turbine Program,* EPA Division of Emission Control Technology Report, December 1976.

14) Op. Cit, Reference 13, pp. 80.

15) Shaw, H., "The Effect of Water on Nitric Oxide Production in Gas Turbines," ASME Paper 75-GT-70, 1975.

9. TABLES

Table 1
ENGINE/COMBUSTOR RIG SUMMARY – EPA SPONSORED DATA

ENGINE/RIG	TESTS (1)	EPA CLASS	TEST CONTRACTOR	TEST TYPE	RATED POWER
TPE331-5-251	336	P2	AiResearch	Controlled	706 SHP (2)
GTCP85-98CK	240	APU	AiResearch	Controlled	260 HP (3)
ALF502 Engine	56	T1	AVCO-Lycoming	Uncontrolled	6,500 lb thrust
ALF502 Rig	66	T1	AVCO-Lycoming	Controlled	6,500 lb thrust
CFM56 Rig	214	T2	General Electric	Controlled	22,000 lb thrust
	912				

(1) Test is defined as a given thrust/ambient condition combination (e.g., Idle represents one test, 1.5 Idle represents a second).

(2) Derated from 840 SHP.

(3) Maximum power operation (45.7 SHP + 214.3 Bleed-Air HP).

ENGINE		HC	EPAP CO	NOX	SMOKE NUMBER
TPE331-5-251	1979 Standard	4.9	26.8	12.9	47
	Measured[A]	3.6	12.8	8.9	15
	(lb/1000 hp-hr/LTO)				
GTCP85-98CK	1979 Standard	0.4	5.0	3.0	None
	Measured[B]	0.2	7.5	6.4	-
	(lb/1000 hp-hr)				
ALF502	1979 Standard	1.6	9.4	3.7	34
	Measured[C]	1.5	12.5	3.0	23
	(lb/1000 lbf/hr/LTO)				
CFM56	1979 Standard	0.8	4.3	3.0	23
	Measured[D]	1.7	12.8	4.7	-
	(lb/1000 lbf-hr/LTO)				

LTO = Landing Takeoff Cycle

[A] Taxi - Idle operation with primary atomizers only, Reference 2

[B] Reference 2

[C] ALF502 Test Data - TAMB=63°F, PAMB=29.88 in Hg, HAMB=0.0088 lb H_2O/lb Air

[D] PFRT baseline engine reported in Reference 13; no smoke number reported

Preceding page blank

Table 2
INDUSTRY CONTRIBUTED DATA – SELECTED EXPERIMENTAL DESIGN FEATURES

Single Engine

- Generally uncontrolled ambient conditions (e.g., TF30).
- Provides a measure of test-to-test variability if replicates included.
- Test points correspond to normal engine operation (e.g., Idle, Takeoff).

Multiple Engine

- Generally uncontrolled ambient conditions (e.g., Pratt & Whitney JT8D and JT9D Pilot Lot Data).
- Provides a measure of engine-to-engine variability.
- Test points correspond to normal engine operation (e.g., Idle, Takeoff).

Parametric Tests

- Always controlled ambient conditions (e.g., T56 Rig and T63-A-5A Rig).
- Independent pressure, temperature or humidity variation.
- Combustor rigs only.
- Test points generally do not correspond to normal engine operation (e.g., Idle, Takeoff).

Table 3

AMBIENT TEST CONDITIONS
TPE331-5-251 AND GTCP85-98CK APU

Test Point	Temperature		Humidity		Barometric Pressure	
	°C	°F	Grams H_2O/ Kilogram Air	Grains H_2O/ Pound Air	Mm Hg	Inches Hg
1	-7.0	19	1.0	7.0	Hold constant at standard condition as specified in the United States Standard Atmosphere, 1962 for the test cell altitude.	
2	-7.0	19	2.0	14.0		
3	4.0	39	2.0	14.0		
4	4.0	39	5.0	35.0		
5	15.0	59	2.0	14.0		
6	15.0	59	5.0	35.0		
7	15.0	59	7.5	52.5		
8	15.0	59	10.0	70.0		
9	33.0	91	10.0	70.0		
10	33.0	91	15.0	105.0		
11	33.0	91	20.0	140.0		
12	33.0	91	25.0	175.0		
13	15.0	59	7.5	52.5	580	22.83
14	15.0	59	7.5	52.5	650	25.98
15	15.0	59	7.5	52.5	740	29.13
16	15.0	59	7.5	52.5	500	19.69

Table 4

TPE 331-5-251 ENGINE LOAD CONDITIONS
(CORRECTED TO 59°F AND 29.92 IN. HG ABS)

Condition	Load	Percent of Rated Power	Corrected Total Shaft Horsepower
1*	(Taxi) Idle	5	35
2*	1.5 x Idle	7.5	53
3*	2.0 x Idle	10.0	76
4	Approach	30.0	212
5	Cruise	70.0	494
6	Climb-Out	90.0	635
7 **	Takeoff	100.0	706

*Engine operation on primary fuel atomizers only.

**A derated takeoff load of 706 shp/$\sqrt{\theta}\delta$ was necessary to protect the engine from turbine interstage overtemperature.

Table 5

GTCP85-98CK APU ENGINE LOAD CONDITIONS (CORRECTED TO 59°F AND 29.92 IN. HG ABS)

Condition	Load	Horsepower		
		Shaft	Bleed-Air	Total
1	Idle	-	-	-
2	Pure Shaft Power	79.5	0	79.5
3	Rated Power	198.6	0	198.6
4	Pure Bleed	-	245.0	245.0
5	Combination	45.7	214.3	260.0

Table 6
AMBIENT TEST CONDITIONS - ALF502 FULL-SCALE ENGINE UNCONTROLLED AMBIENT CONDITIONS

Ambient Temperature °F	Ambient Pressure in HG	Ambient Specific Humidity Lb Water/Lb Dry Air
77	30.00	.01445
71	30.00	.01632
76	29.80	.01530
78	29.75	.01770
73	29.70	.01725
78	29.75	.01582
63	29.85	.0089

7 Power Levels for Each Ambient Test Condition

1) IDLE
    a) Taxi-Out
    b) Taxi-In
2) 1.5 IDLE
3) Approach (30% rated)
4) 40% Rated
5) 50% Rated
6) CLIMB (90% Rated)
7) TAKEOFF (100% Rated)

Table 7
AMBIENT TEST CONDITIONS - ALF502 COMBUSTOR RIG

TEST	AMBIENT TEMPERATURE °F	AMBIENT PRESSURE in HG	AMBIENT SPECIFIC HUMIDITY Grains H_2O/lb Air
0	59	29.92	44 (Reference Day)
1	19	25.98	25
2	19	29.92	25
3	19	32.28	25
4	39	29.92	25
5	39	29.92	25
6	59	25.98	52.5
7	59	29.92	25
8	59	29.92	52.5
9	59	29.92	70
10	59	32.28	52.5
11	85	29.92	25
12	85	29.92	52.5
13	85	29.92	105
14	85	29.92	175
15	105	25.98	25
16	105	25.98	175
17	105	29.92	25
18	105	29.92	52.5
19	105	29.92	105
20	105	29.92	175
21	105	32.28	25
22	105	32.28	175

3 Power Levels for Each Ambient Test Condition

1)	IDLE	5% Rated
2)	1.5 IDLE	7.5% Rated
3)	APPROACH	30% Rated

Table 8

AMBIENT EFFECTS TEST CONDITIONS - CFM56 COMBUSTOR RIG

	Temperature		Humidity		Pressure	
Test Point	°C	°F	Grams H_2O Per Kilogram Air	Grains H_2O Per Pound Air	KPa,	Inches Hg
1	-7	19	2	14	Hold constant as specified in the United States Standard Atmosphere 1962 for the test Cell Altitude	
2	4	39	2	14		
3	15	59	2	14		
4	29.5	85	2	14		
5	40	105	2	14		
6	4	39	5	35		
7	15	59	7.5	52.5		
8	29.5	85	7.5	52.5		
9	40.5	105	7.5	52.5		
10	15	59	10	70		
11	29.5	85	15	105		
12	40.5	105	15	105		
13	29.5	85	25	175		
14	40.5	105	25	175		
15	-7	19	2	14	109.32	32.28
16	15	59	7.5	52.5	109.32	32.28
17	40.5	105	2	14	109.32	32.28
18	40.5	105	25	175	109.32	32.28
19	-7	19	2	14	88	25.98
20	15	59	7.5	52.5	88	25.98
21	40.5	105	2	14	88	25.98
22	40.5	105	25	175	88	25.98

22 - Test points - given above.

5 - Power settings - idle, 1-1/2 times idle, approach, climbout, takeoff.

1 - Replication of each test point - Each point will therefore, be run twice.

214 - Total measurements (22 x 5 x 2 = 220) Less 6 unrealizable takeoff points.

Table 9

CFM56 COMBUSTOR RIG REPLICATE ANALYSIS

MEAN REPLICATION COEFFICIENT OF VARIATION BY MODE
2 REPLICATES/TEST POINT, 22 TEST POINTS/MODE

Coefficient of Variation for Test Point = $\hat{\sigma}_k/\bar{X}_k$

where $\bar{X}_k$ = mean value of the 2 replicates
$\hat{\sigma}_k$ = standard deviation of the 2 replicates

Pollutant MODE (% Rated)	HC EI	CO EI	NOX EI	SMOKE
IDLE (5)	.2232	.0365	.0401	.4467
1.5 IDLE (9)	.1872	.0393	.0277	.3676
APPROACH (30)	.1941	.1413	.0355	.5743
CLIMBOUT (85)	-	-	.0336	.2656
TAKEOFF (100)	-	-	.0351	.2186
TOTAL	.2015	.0724	.0344	.3746

Table 10
TPE331-5-251 FULL SCALE ENGINE REPLICATE ANALYSIS

3 REPLICATES/TEST POINT, 16 TEST POINTS/MODE

Coefficient of Variation for Test Point = $\hat{\sigma}_K / \bar{X}_K$

where $\bar{X}_K$ = mean value of the 3 replicates
$\hat{\sigma}_K$ = standard deviation of the 3 replicates

Pollutant MODE (% Rated)	HC EI	CO EI	NOX EI	SMOKE
IDLE (5)	.1086	.0363	.0365	.1430
1.5 IDLE (7.5)	.0843	.0276	.0340	.1594
2.0 IDLE (10)	.0969	.0325	.0302	.1710
APPROACH (30)	.1510	.0522	.0223	.0649
CRUISE (70)	-	-	.0176	.0556
CLIMBOUT (90)	-	-	.0181	.0605
TAKEOFF (100)	-	-	.0159	.0584
TOTAL	.1102	.0372	.0249	.1018

Table 11

TEST TO TEST VARIABILITY MEAN IDLE COEFFICIENT OF VARIATION BY ENGINE

			MEAN COEFFICIENT OF VARIATION			
ENGINE	NUMBER TESTS	NUMBER REPLICATES	HC EI	CO EI	NOX EI	SMOKE
TPE331-5-251 FULL SCALE	16	3	.1086	.0363	.0365	.1430
CFM56 COMBUSTOR RIG	22	2	.2232	.0365	.0401	.4467
ALF502 FULL SCALE	7	2	.0771	.0315	.0070	.3646
WEIGHTED AVERAGE	45		.1597	.0357	.0338	.3259

Table 12

CFM56 COMBUSTOR RIG - SUMMARY STATISTICS BY MODE

VARIABLE	N	MEAN	STANDARD DEVIATION	MINIMUM VALUE	MAXIMUM VALUE	VARIANCE	STD ERROR OF MEAN	C.V.
IDLE								
PTHRUST	44	5.70414091	0.10116185	5.51820000	5.85820000	0.01023372	0.01525072	1.773
P3	44	48.33931818	3.16793998	42.36000000	53.95000000	10.03584371	0.47758492	6.551
T3	44	363.67498864	43.97538157	292.00000000	427.70000000	1933.92213617	6.62968837	11.896
FA	44	0.01575455	0.00078950	0.01410000	0.01760000	0.00000062	0.00011904	5.012
CO	44	25.68772727	6.48564644	16.82000000	44.58000000	42.06620402	0.97777814	25.249
HC	44	1.30363636	1.28110434	0.17000000	6.22000000	1.64122833	0.19313375	98.272
NOX	44	3.15568182	0.47909021	2.36000000	4.17000000	0.22952743	0.07222557	15.182
SMOKE	44	2.72272727	1.19861519	0.20000000	5.58000000	1.43668076	0.18069819	44.023
1.5 IDLE								
PTHRUST	44	8.97313636	0.22195820	8.57730000	9.33642000	0.04926988	0.03346297	2.474
P3	44	63.39704545	4.14643954	55.09000000	70.92000000	17.19296084	0.62509929	6.540
T3	44	437.41590682	47.47938219	352.39390000	496.39590000	2254.29173272	7.15778618	10.855
FA	44	0.01480455	0.00059998	0.01360000	0.01640000	0.00000036	0.00009045	4.053
CO	44	12.94659091	3.03402714	9.11000000	21.80000000	9.20532057	0.45739689	23.435
HC	44	0.15636364	0.17288376	0.02000000	0.81000000	0.02988879	0.02606321	110.565
NOX	44	4.12090909	0.72391641	2.74000000	5.76000000	0.52405457	0.10913451	17.567
SMOKE	44	2.61363636	0.91894553	0.20000000	4.70000000	0.84446089	0.13853625	35.160
APPROACH								
PTHRUST	44	30.00000000	0.00000000	30.00000000	30.00000000	0.00000000	0.00000000	0.000
P3	44	138.98681818	9.12909272	122.79000000	154.04000000	83.34033383	1.37626251	6.568
T3	44	654.18182727	59.05725993	547.00000000	719.20000000	3487.75925043	8.90321692	9.028
FA	44	0.01788864	0.00085313	0.01620000	0.01900000	0.00000074	0.00012937	4.797
CO	44	2.95272727	0.64760871	1.65000000	4.65000000	0.41939704	0.09763069	21.933
HC	44	0.01659091	0.01539302	0.01000000	0.09000000	0.00023695	0.00232058	92.780
NOX	44	7.47568182	1.22013419	5.30000000	10.10000000	1.48872743	0.18394215	16.321
SMOKE	44	2.24318182	1.39723943	0.30000000	6.10000000	1.95227891	0.21064177	62.288
CLIMB								
PTHRUST	44	65.00000000	0.00000000	65.00000000	65.00000000	0.00000000	0.00000000	0.000
P3	44	165.95681818	10.88540324	146.45000000	184.07000000	118.49200359	1.64103623	6.559
T3	44	918.45362955	68.20577294	791.30000000	994.00000000	4652.02718354	10.28240685	7.426
FA	44	0.02575682	0.00151893	0.02290000	0.02830000	0.00000231	0.00022899	5.897
CO	44.	2.74113636	0.82770963	1.39000000	4.59000000	0.68510333	0.12478193	30.196
HC	44	0.01000000	0.00000000	0.01000000	0.01000000	0.00000000	0.00000000	0.000
NOX	44	13.19318182	2.39343945	9.82000000	18.50000000	5.72855243	0.36082457	18.141
SMOKE	44	3.96590909	1.77880848	1.50000000	10.30000000	3.16415962	0.26816547	44.852
TAKEOFF								
PTHRUST	38	100.00023684	0.00101832	100.00000000	100.00450000	0.00000104	0.00016519	0.001
P3	38	171.56657895	10.42613719	152.51000000	191.07000000	108.70433663	1.69134279	6.077
T3	38	958.38158158	68.66312081	840.50000000	1049.00000000	4714.62553322	11.13863056	7.164
FA	38	0.02714474	0.00164213	0.02410000	0.02940000	0.00000270	0.00026639	6.050
CO	38	3.06052632	1.08758087	1.44000000	5.43000000	1.18283215	0.17642891	35.536
HC	38	0.01000000	0.00000000	0.01000000	0.01000000	0.00000000	0.00000000	0.000
NOX	38	15.23500000	2.87716241	11.97000000	21.91000000	8.27806351	0.46673737	18.885
SMOKE	38	4.11578947	1.27672013	1.70000000	8.30000000	1.63001422	0.20711135	31.020

Table 13

CFM56 COMBUSTOR RIG - HC REGRESSION SUMMARY

```
                                              GENERAL LINEAR MODELS PROCEDURE

DEPENDENT VARIABLE: LNHC        NATURAL LOG(HC)

SOURCE                   DF      SUM OF SQUARES          MEAN SQUARE        F VALUE          PR > F          R-SQUARE            C.V.

MODEL                     1        155.02251252         155.02251253         584.17          0.0001          0.871675         42.1495

ERROR                    86         22.82196483           0.26537168                          STD DEV                        LNHC MEAN

CORRECTED TOTAL          87        177.84447741                                            0.51514239                      -1.22217993

                                   T FOR H0:           PR > |T|            STD ERROR OF
PARAMETER             ESTIMATE    PARAMETER=0                                 ESTIMATE

INTERCEPT           8.23545584          20.85            0.0001              0.39595633
T3                 -0.02348592         -24.17            0.0001              0.00097171
```

Table 14

CFM56 COMBUSTOR RIG - CO REGRESSION SUMMARY

```
                                                  GENERAL LINEAR MODELS PROCEDURE

DEPENDENT VARIABLE: LNCO        NATURAL LOG(CO)

SOURCE                  DF       SUM OF SQUARES          MEAN SQUARE         F VALUE          PR > F          R-SQUARE          C.V.

MODEL                    1          11.66575450          11.66575450          337.12          0.0001          0.796749        6.4658

ERROR                   86           2.97593238           0.03460386                         STD DEV                        LNCO MEAN

CORRECTED TOTAL         87          14.64168688                                            0.18602114                      2.87699378

PARAMETER                 ESTIMATE        T FOR H0:       PR > |T|          STD ERROR OF
                                        PARAMETER=0                          ESTIMATE

INTERCEPT               5.47590815            38.30         0.0001          0.14298231
T3                     -0.00644263           -18.36         0.0001          0.00035089
```

Table 15

CFM56 COMBUSTOR RIG - NOX REGRESSION SUMMARY

```
                                          GENERAL LINEAR MODELS PROCEDURE
DEPENDENT VARIABLE: LNNOX      NATURAL LOG(NOX)
SOURCE                  DF       SUM OF SQUARES       MEAN SQUARE        F VALUE          PR > F        R-SQUARE           C.V.
MODEL                    2          85.55307798       42.77653899        7668.83          0.0001        0.986430         3.8478
ERROR                  211           1.17695298        0.00557798                         STD DEV                    LNNOX MEAN
CORRECTED TOTAL        213          86.73003096                                       0.07468585                     1.94101868

PARAMETER                ESTIMATE        T FOR H0:      PR > |T|        STD ERROR OF
                                        PARAMETER=0                       ESTIMATE
INTERCEPT              0.45742286             30.28        0.0001         0.01543587
T3                     0.00250325            120.40        0.0001         0.00002079
HAMB                 -20.70200748            -32.91        0.0001         0.62901159
```

Table 16

CFM56 COMBUSTOR RIG - SMOKE REGRESSION SUMMARY

```
                                             GENERAL LINEAR MODELS PROCEDURE

DEPENDENT VARIABLE: LNSMK        NATURAL LOG(SMOKE)

SOURCE                   DF       SUM OF SQUARES         MEAN SQUARE        F VALUE          PR > F         R-SQUARE            C.V.

MODEL                     1           4.64120782          4.64120782          11.15          0.0010         0.049957         66.3910

ERROR                   212          88.26363650          0.41633791                        STD DEV                      LNSMK MEAN

CORRECTED TOTAL         213          92.90484432                                         0.64524252                      0.97188252

                                     T FOR H0:      PR > |T|        STD ERROR OF
PARAMETER              ESTIMATE     PARAMETER=0                        ESTIMATE

INTERCEPT           -0.31230670           -0.81       0.4207          0.38714494
LNP3                 0.27750009            3.34       0.0010          0.08311332
```

Table 17

NOX CORRECTION FACTOR COEFFICIENTS - TABULAR SUMMARY

NOX CORRECTION COEFFICIENT SUMMARY

ENGINE	MODES	CLASS	SAMPLES	CONSTANT	T3COEF	T3STD	HAMBCOEF	HAMBSTD	RSQ	T3MEAN	P3MEAN	NOXMEAN	PR
GTCP85-98CK APU	BLEED & SHAFT	APU	9	1.0507	0.001677	0.000331	-22.84	2.360	0.7859	357	56.4	5.20	4.00
T56 STANDARD JETA	PR=2	P2	16	0.0120	0.001785	0.000292	.	.	0.7278	190	30.0	1.43	2.00
T56 LEAN JETA	PR=2	P2	16	0.3258	0.002018	0.000181	.	.	0.8993	188	30.0	2.04	2.00
T56 STANDARD JETA	PR=3	P2	16	0.0567	0.002853	0.000220	.	.	0.9232	283	45.0	2.42	3.00
T56 LEAN JETA	PR=3	P2	16	0.5212	0.001469	0.000193	.	.	0.8054	282	45.0	2.56	3.00
T56 STANDARD JETA	PR=4	P2	16	0.3925	0.001945	0.000199	.	.	0.8722	355	60.0	2.99	4.00
T56 LEAN JETA	PR=4	P2	16	0.3400	0.002173	0.000208	.	.	0.8867	356	60.0	3.09	4.00
T56 STANDARD JETA	PR=5	P2	16	0.6065	0.001627	0.000210	.	.	0.8107	417	75.0	3.65	5.00
T56 LEAN JETA	PR=5	P2	16	0.1884	0.002699	0.000166	.	.	0.9499	417	75.0	3.81	5.00
T63-A-5A	WALL FILM(FA IN EQ)	P2	9	-9.9541	0.003030	0.001026	.	.	0.9478	622	60.7	5.33	6.20
T63-A-5A	PRES ATOM(FA IN EQ)	P2	9	-5.2671	0.001999	0.000622	.	.	0.8229	600	60.2	5.83	6.20
T63-A-5A	AIR BLAST(FA IN EQ)	P2	9	-5.3716	0.001925	0.000487	.	.	0.8827	600	60.5	5.51	6.20
PT6A-50	IDLE TO TAKEOFF	P2	15	0.7037	0.002668	0.000072	.	.	0.9906	637	126.0	11.17	8.70
ALLISON 501K	LOW RPM	P2	7	0.3612	0.003046	0.000369	.	.	0.9317	403	66.3	5.02	9.40
ALLISON 501K	HIGH RPM GT 90% RATE	P2	19	0.5855	0.002882	0.000292	.	.	0.8514	599	135.9	20.23	9.40
TPE331-5-251	APPROACH TO TAKEOFF	P2	192	0.5517	0.002864	0.000301	-14.13	0.094	0.7584	655	142.0	10.56	10.37
TYNE	IDLE TO CRUISE	P2	28	0.4647	0.002602	0.000486	-17.83	1.580	0.8419	700	180.0	7.70	13.50
ALF502 COMBUSTOR RIG	IDLE TO APPROACH	T1	66	0.5328	0.002725	0.000097	-20.09	1.220	0.9316	456	75.0	4.99	5.11
JT15D-4 P&W CANADA	IDLE TO TAKEOFF	T1	12	0.3697	0.003205	0.000109	-24.35	5.040	0.9898	624	152.0	9.44	9.65
ALF502 ENGINE	IDLE TO TAKEOFF	T1	56	0.7147	0.002400	0.000051	-15.01	3.100	0.9773	698	154.0	8.19	10.70
TFE731-2	IDLE TO TAKEOFF	T1	28	0.4411	0.002936	0.000097	.	.	0.9722	754	186.0	15.88	13.00
TFE731-3	IDLE TO TAKEOFF	T1	14	0.5427	0.002881	0.000125	.	.	0.9780	792	197.0	18.49	14.60
CFM56 COMBUSTOR RIG	IDLE	T2	44	0.5638	0.001994	0.000189	-17.96	0.970	0.8954	370	48.4	3.16	.
CFM56 COMBUSTOR RIG	1.5*IDLE	T2	44	0.5989	0.002267	0.000171	-21.55	0.940	0.9289	437	63.4	4.12	.
CFM56 COMBUSTOR RIG	APPROACH	T2	44	1.0522	0.001744	0.000155	-21.38	1.080	0.9062	654	139.0	7.48	.
CFM56 COMBUSTOR RIG	CLIMB	T2	44	0.5770	0.002352	0.000114	-19.31	0.910	0.9356	918	166.0	13.19	.
CFM56 COMBUSTOR RIG	TAKEOFF	T2	38	0.4949	0.002425	0.000121	-16.95	1.350	0.9292	958	171.6	15.24	.
CFM56 COMBUSTOR RIG	IDLE TO TAKEOFF	T2	214	0.4674	0.002503	0.000021	-20.70	0.630	0.9864	958	172.0	15.24	11.70
TF30	IDLE TO TAKEOFF	T2	178	0.2605	0.003324	0.000036	-12.01	1.340	0.9801	740	210.0	13.44	14.20
SPEY 511	IDLE TO TAKEOFF	T2	120	-0.8503	0.004674	0.000142	.	.	0.9016	826	265.0	8.02	18.90
JT9D-7 VORBIX	PILOT FA LT .009	T2	61	-0.5154	0.003514	0.000125	.	.	0.9301	887	314.0	13.99	20.40
JT9D-7A	IDLE TO TAKEOFF	T2	181	-0.1987	0.004156	0.000048	-19.94	2.370	0.9771	845	258.7	24.68	20.40
JT9D-7F	IDLE TO TAKEOFF	T2	94	-0.3103	0.004422	0.000081	-16.12	4.240	0.9714	820	268.9	27.45	21.20
JT9D-7 OVERHAUL	IDLE TO TAKEOFF	T2	114	-0.4312	0.004307	0.000064	.	.	0.9760	899	283.0	34.19	22.30
RB211-22B COMBUST #1	IDLE TO TAKEOFF	T2	51	-0.6017	0.004290	0.000093	.	.	0.9888	907	351.0	27.98	25.00
RB211-22B COMBUST #2	IDLE TO TAKEOFF	T2	16	-0.7541	0.004412	0.000133	.	.	0.9874	901	341.0	27.13	25.00
RB211-22B ALTITUDE	IDLE TO TAKEOFF	T2	21	-0.7016	0.004357	0.000119	.	.	0.9857	849	260.0	20.89	25.00
JT8D-9	IDLE TO TAKEOFF	T4	134	0.3033	0.003204	0.000082	.	.	0.9209	719	198.4	20.94	15.90
JT8D-17	IDLE TO TAKEOFF	T4	85	0.4502	0.002989	0.000109	.	.	0.9013	740	207.8	15.27	17.00

Table 18

NOX CORRECTION FACTOR COEFFICIENTS - SUMMARY STATISTICS

NOX CORRECTION COEFFICIENT SUMMARY

VARIABLE	LABEL	N	MEAN	STANDARD DEVIATION	MINIMUM VALUE	MAXIMUM VALUE	RANGE
SAMPLES	SAMPLE SIZE	34	55.00000000	61.56888234	7.00000000	214.00000000	207.00000000
CONSTANT	REGRESSION CONSTANT	34	-0.43273824	2.18601102	-9.95410000	1.05070000	11.00480000
T3COEF	NOX TEMPERATURE COEFFICIENT	34	0.00292826	0.00090684	0.00146900	0.00467400	0.00320500
T3STD	T3COEF STANDARD ERROR	34	0.00021138	0.00020130	0.00002100	0.00102600	0.00100500
HAMBCOEF	NOX HUMIDITY COEFFICIENT	10	-18.30200000	3.96678095	-24.35000000	-12.01000000	12.34000000
HAMBSTD	HAMBCOEF STANDARD ERROR	10	2.19740000	1.56617611	0.09400000	5.04000000	4.94600000
RSQ	COEFFICIENT OF DETERMINATION(R-SQUARED)	34	0.91306471	0.07437623	0.72780000	0.99060000	0.26280000
T3MEAN	MEAN COMBUSTOR INLET TEMPERATURE(DEG.F)	34	519.88235294	225.39094181	188.00000000	958.00000000	770.00000000
P3MEAN	MEAN COMBUSTOR INLET PRESSURE(PSIA)	34	152.99411765	97.11157888	30.00000000	351.00000000	321.00000000
NOXMEAN	MEAN NOX EMISSION INDEX	34	11.90441176	9.05046330	1.43000000	34.19000000	32.76000000
PR	RATED ENGINE PRESSURE RATIO	34	11.53029412	7.32116131	2.00000000	25.00000000	23.00000000

NOTE: ONLY CFM56 IDLE TO TAKEOFF COEFFICIENT FROM TABLE 17 INCLUDED IN ABOVE SUMMARY

Table 19
HC CORRECTION FACTOR COEFFICIENTS - TABULAR SUMMARY

HC CORRECTION COEFFICIENT SUMMARY

ENGINE	MODES	CLASS	SAMPLES	CONSTANT	T3COEF	T3STD	RSQ	HCMEAN	PR	IPR
GTCP85-98CK APU	BLEED & SHAFT	APU	9	9.5625	-0.029100	0.004059	0.8801	0.49	4.00	4.00
T63-A-5A	WALL FILM INJECTION	P2	9	34.4800	-0.010745	0.003386	0.8232	4.68	6.20	.
T63-A-5A	PRESSURE ATOMIZER	P2	7	16.3600	-0.008126	0.003307	0.8034	0.69	6.20	.
ALLISON 501K	HIGH RPM LT 30%RATED	P2	21	6.0081	-0.009915	0.001105	0.8091	2.32	9.40	.
PT6A-50	IDLE TO APPROACH	P2	8	6.2118	-0.019231	0.000619	0.9938	12.04	8.70	2.20
TPE331-8	IDLE	P2	4	6.6488	-0.017719	0.002916	0.2064	1.54	10.30	3.20
ALF502 COMBUSTOR RIG	IDLE TO APPROACH	T1	66	3.8194	-0.008304	0.000486	0.8201	5.22	5.11	1.73
JT15D-4 P&W CANADA	IDLE TO APPROACH	T1	6	6.9240	-0.016619	0.002715	0.9035	2.84	9.65	1.85
TFE731-2	IDLE TO APPROACH	T1	21	4.4835	-0.006693	0.000618	0.9214	20.58	13.00	1.87
TFE731-3	IDLE TO APPROACH	T1	16	4.4715	-0.008575	0.002653	0.7231	8.96	14.60	2.00
ALF502 ENGINE	IDLE TO APPROACH	T1	28	4.4205	-0.011038	0.000387	0.9690	5.16	10.70	2.30
SPEY 511	T3 LE 600 DEG.F	T2	77	6.7523	-0.009061	0.000343	0.9029	121.50	18.90	2.20
TF30	IDLE & APPROACH	T2	82	5.6067	-0.012370	0.000378	0.9362	12.45	14.20	2.70
CFM56 COMBUSTOR RIG	IDLE & 1.5 IDLE	T2	88	8.2555	-0.023486	0.000972	0.8717	1.30	11.70	3.40
RB211-22B COMBUST #2	IDLE	T2	8	7.3528	-0.010160	0.001919	0.8236	50.09	25.00	3.50
RB211-22B ALTITUDE	IDLE & APPROACH	T2	6	9.8035	-0.014348	0.000607	0.9929	66.96	25.00	3.50
JT9D-7 VORBIX	PILOT FA GE 0.009	T2	23	6.4740	-0.018116	0.004094	0.4825	1.46	20.40	3.95
JT9D-7 OVERHAUL	IDLE & APPROACH	T2	62	8.7491	-0.015041	0.000397	0.9599	27.00	22.30	3.95
JT9D-7A	IDLE	T2	49	7.6726	-0.011815	0.000839	0.8083	23.48	20.40	3.95
JT9D-7F	IDLE	T2	28	8.3483	-0.014810	0.000748	0.9378	17.87	21.20	3.95
JT8D-9	IDLE	T4	66	5.3951	-0.011670	0.001033	0.6659	16.56	15.90	2.24
JT8D-17	IDLE	T4	36	5.9325	-0.014036	0.001049	0.8404	10.37	17.00	2.47

Table 20
HC CORRECTION FACTOR COEFFICIENTS SUMMARY STATISTICS

HC CORRECTION COEFFICIENT SUMMARY 3

VARIABLE	LABEL	N	MEAN	STANDARD DEVIATION	MINIMUM VALUE	MAXIMUM VALUE	RANGE
SAMPLES	SAMPLE SIZE	22	32.72727273	28.24077063	4.00000000	88.00000000	84.00000000
CONSTANT	REGRESSION CONSTANT	22	8.35147727	6.40408561	3.81940000	34.48000000	30.66060000
T3COEF	HC TEMPERATURE COEFFICIENT	22	-0.01368082	0.00543549	-0.02910000	-0.00669300	0.02240700
T3STD	T3COEF STANDARD ERROR	22	0.00157409	0.00129571	0.00034300	0.00409400	0.00375100
RSQ	COEFFICIENT OF DETERMINATION(R-SQUARED)	22	0.82160000	0.18049226	0.20640000	0.99380000	0.78740000
HCMEAN	MEAN HC EMISSION INDEX	22	18.79818182	28.33646257	0.49000000	121.50000000	121.01000000
PR	RATED ENGINE PRESSURE RATIO	22	14.08454545	6.47804845	4.00000000	25.00000000	21.00000000
IPR	IDLE PRESSURE RATIO	19	2.89263158	0.85054781	1.73000000	4.00000000	2.27000000

Table 21

CO CORRECTION FACTOR COEFFICIENTS TABULAR SUMMARY

CO CORRECTION COEFFICIENT ANALYSIS

ENGINE	MODES	CLASS	SAMPLES	CONSTANT	T3COEF	T3STD	RSQ	COMEAN	PR	IPR
GTCP85-98CK APU	BLEED & SHAFT	APU	9	5.8608	-0.008326	0.000881	0.9274	18.15	4.00	4.00
T63-A-5A	WALL FILM(FA IN EQ)	P2	9	21.7700	-0.006354	0.001523	0.8734	16.17	6.20	.
T63-A-5A	PRES ATOM(FA IN EQ)	P2	9	16.1700	-0.004859	0.001742	0.7019	9.90	6.20	.
T63-A-5A	AIR BLAST(FA IN EQ)	P2	9	16.5900	-0.003449	0.000738	0.9116	10.79	6.20	.
ALLISON 501K	HIGH RPM LE 30% RATE	P2	22	5.3696	-0.005739	0.000829	0.7056	10.42	9.40	.
PT6A-50	IDLE TO APPROACH	P2	8	5.1577	-0.008222	0.000186	0.9969	35.08	8.70	2.20
TPE331-5-251	IDLE TO 2.0 IDLE	P2	144	4.9222	-0.006378	0.001201	0.1657	22.00	10.37	3.45
TYNE	IDLE TO CRUISE	P2	28	7.1201	-0.009577	0.001243	0.6953	26.84	13.50	4.00
ALF502 COMBUSTOR RIG	IDLE TO APPROACH	T1	66	4.7618	-0.004177	0.000267	0.7923	36.10	5.11	1.73
JT15D-4 P&W CANADA	IDLE TO APPROACH	T1	6	5.5153	-0.005613	0.000213	0.9943	26.83	9.65	1.85
TFE731-2	IDLE TO 50% RATED	T1	16	5.4579	-0.005752	0.000458	0.9184	58.94	13.00	1.87
TFE731-3	IDLE TO 50% RATED	T1	8	5.5458	-0.006097	0.000798	0.9068	47.07	14.60	2.00
ALF502 ENGINE	IDLE TO APPROACH	T1	28	5.3600	-0.006459	0.000171	0.9822	40.89	10.70	2.30
SPEY 511	IDLE TO TAKEOFF	T2	150	6.7451	-0.007242	0.000157	0.9349	132.30	18.90	2.20
TF30	IDLE TO TAKEOFF	T2	180	5.8252	-0.007146	0.000073	0.9820	56.31	14.20	2.70
CFM56 COMBUSTOR RIG	IDLE & 1.5 IDLE	T2	88	5.4769	-0.006443	0.000351	0.7967	25.69	11.70	3.40
RB211-22B COMBUST #1	IDLE TO TAKEOFF	T2	49	7.2056	-0.007024	0.000220	0.9559	99.55	25.00	3.50
RB211-22B COMBUST #2	IDLE TO TAKEOFF	T2	15	7.2690	-0.007149	0.000474	0.9459	107.33	25.00	3.50
RB211-22B ALTITUDE	IDLE TO TAKEOFF	T2	21	8.1424	-0.007864	0.000287	0.9753	163.42	25.00	3.50
JT9D-7 VORBIX	PILOT FA GE 0.009	T2	23	7.7941	-0.014862	0.001809	0.7627	14.83	20.40	3.95
JT9D-7 OVERHAUL	IDLE & APPROACH	T2	62	7.9885	-0.010337	0.000388	0.9222	66.13	22.30	3.95
JT9D-7A	IDLE TO APPROACH	T2	63	7.8671	-0.009779	0.000354	0.9203	60.42	20.40	3.95
JT9D-7F	IDLE TO APPROACH	T2	31	7.5716	-0.010320	0.000659	0.8942	45.83	21.20	3.95
JT8D-9	IDLE TO APPROACH	T4	79	4.9610	-0.005638	0.000182	0.9257	40.03	15.90	2.24
JT8D-17	IDLE TO APPROACH	T4	43	4.8839	-0.005335	0.000155	0.9667	33.05	17.00	2.47

Table 22

CO CORRECTION FACTOR COEFFICIENTS SUMMARY STATISTICS

CO CORRECTION COEFFICIENT ANALYSIS

VARIABLE	LABEL	N	MEAN	STANDARD DEVIATION	MINIMUM VALUE	MAXIMUM VALUE	RANGE
SAMPLES	SAMPLE SIZE	25	46.84000000	48.64726782	6.00000000	180.00000000	174.00000000
CONSTANT	REGRESSION CONSTANT	25	7.65326600	4.21369507	4.76180000	21.77000000	17.00820000
T3COEF	CO TEMPERATURE COEFFICIENT	25	-0.00720564	0.00240191	-0.01486200	-0.00344900	0.01141300
T3STD	T3COEF STANDARD ERROR	25	0.00061436	0.00051998	0.00007300	0.00180900	0.00173600
RSQ	COEFFICIENT OF DETERMINATION(R-SQUARED)	25	0.86217200	0.17264962	0.16570000	0.99690000	0.83120000
COMEAN	MEAN CO EMISSION INDEX	25	48.16280000	39.39699402	9.90000000	163.42000000	153.52000000
PR	RATED ENGINE PRESSURE RATIO	25	14.18520000	6.65251840	4.00000000	25.00000000	21.00000000
IPR	IDLE PRESSURE RATIO	21	2.98619048	0.85584155	1.73000000	4.00000000	2.27000000

Table 23

SMOKE NUMBER CORRECTION FACTOR COEFFICIENTS TABULAR SUMMARY

EPA SMOKE NUMBER CORRECTION COEFFICIENT SUMMARY

ENGINE	MODES	CLASS	SAMPLES	CONSTANT	P3COEF	P3STD	RSQ	SMKMEAN	PR
GTCP85-98CK APU	BLEED & SHAFT	APU	15	1.2375	0.6394	0.1964	0.4492	41.49	4.00
TPE331-5-251	APPROACH TO TAKEOFF	P2	192	-0.5323	0.6471	0.1011	0.1774	14.06	10.37
ALF502 ENGINE	IDLE TO TAKEOFF	T1	55	-6.9848	2.0754	0.0940	0.9020	23.50	10.70
CFM56 COMBUSTOR RIG	IDLE TO TAKEOFF	T2	214	-0.3123	0.2775	0.0831	0.0500	4.12	11.70
SPEY 511	IDLE TO TAKEOFF	T2	120	-0.3525	0.7771	0.0445	0.7780	17.15	18.90
JT9D-7 VORBIX	PILOT FA LT 0.009	T2	24	-3.4921	1.1907	0.0793	0.9112	29.84	20.40
JT9D-7A	IDLE TO TAKEOFF	T2	69	-3.6831	0.9507	0.1439	0.3945	6.04	20.40
JT9D-7 OVERHAUL	IDLE TO TAKEOFF	T2	36	-3.5236	0.9207	0.1937	0.3993	7.80	22.30
RB211-22B COMBUST #1	IDLE TO TAKEOFF	T2	42	-0.8485	0.4992	0.0729	0.5357	8.67	25.00
RB211-22B COMBUST #2	IDLE TO TAKEOFF	T2	13	-3.2239	0.9057	0.1803	0.6984	10.60	25.00
JT8D-9	IDLE TO TAKEOFF	T4	94	-3.8398	1.3038	0.0285	0.9579	21.26	15.90
JT8D-17	IDLE TO TAKEOFF	T4	61	-4.3727	1.4063	0.0640	0.8929	22.95	17.00

Table 24

SMOKE NUMBER CORRECTION FACTOR COEFFICIENTS SUMMARY STATISTICS

EPA SMOKE NUMBER CORRECTION COEFFICIENT SUMMARY

VARIABLE	LABEL	N	MEAN	STANDARD DEVIATION	MINIMUM VALUE	MAXIMUM VALUE	RANGE
SAMPLES	SAMPLE SIZE	12	77.91666667	66.45635387	13.00000000	214.00000000	201.00000000
CONSTANT	REGRESSION CONSTANT	12	-2.49400833	2.32255414	-6.98480000	1.23750000	8.22230000
P3COEF	SMOKE PRESSURE COEFFICIENT	12	0.96646667	0.47964638	0.27750000	2.07540000	1.79790000
P3STD	P3COEF STANDARD ERROR	12	0.10680833	0.05789169	0.02850000	0.19640000	0.16790000
RSQ	COEFFICIENT OF DETERMINATION(R-SQUARED)	12	0.59554167	0.30652553	0.05000000	0.95790000	0.90790000
SMKMEAN	MEAN EPA SMOKE NUMBER	12	17.29000000	11.07448993	4.12000000	41.49000000	37.37000000
PR	RATED ENGINE PRESSURE RATIO	12	16.80583333	6.49695377	4.00000000	25.00000000	21.00000000

10. FIGURES

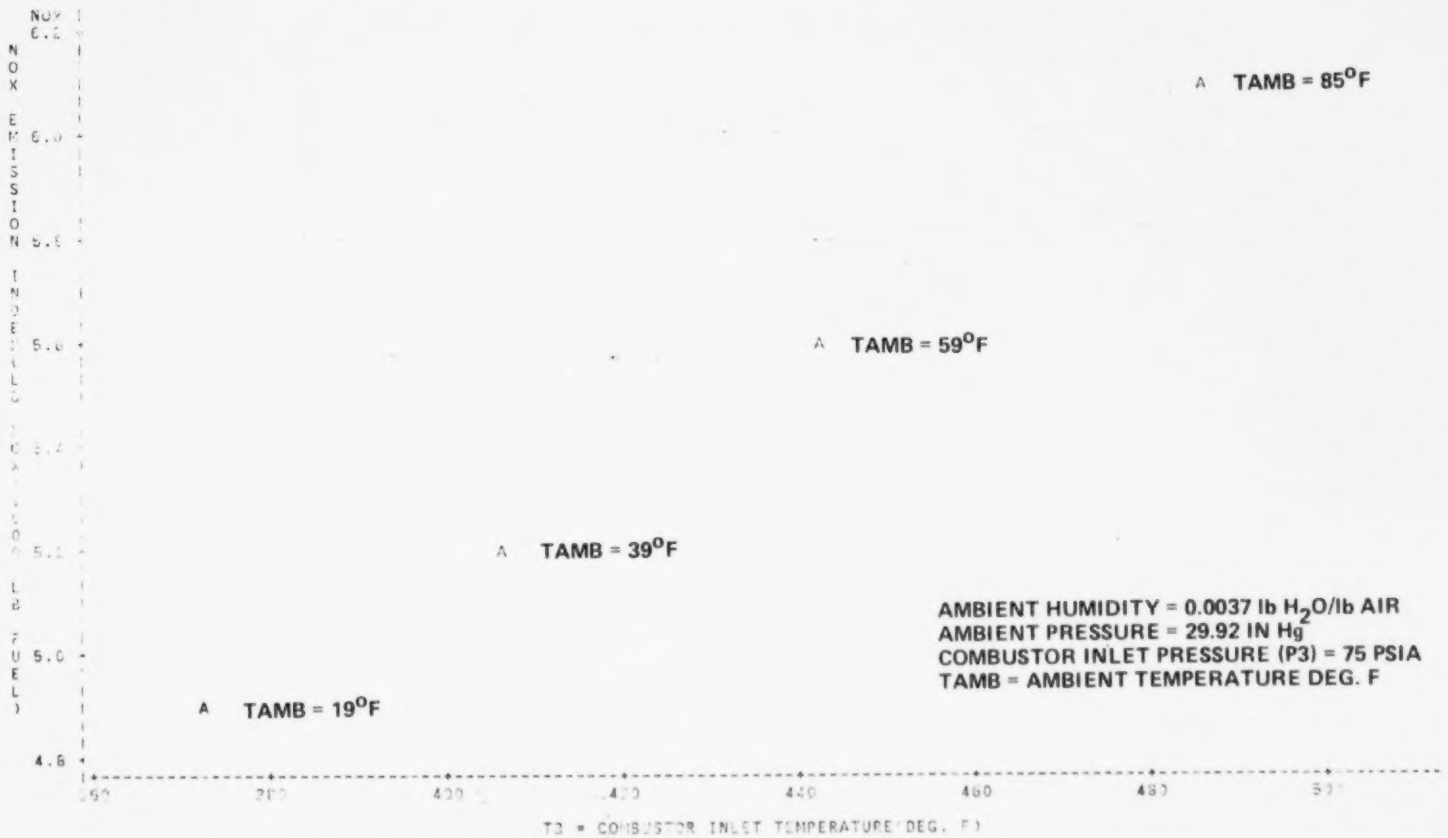

Figure 1 VARIATION OF OXIDES OF NITROGEN (NOX) EMISSION INDEX WITH AMBIENT TEMPERATURE – ALF 502 COMBUSTOR RIG, APPROACH MODE

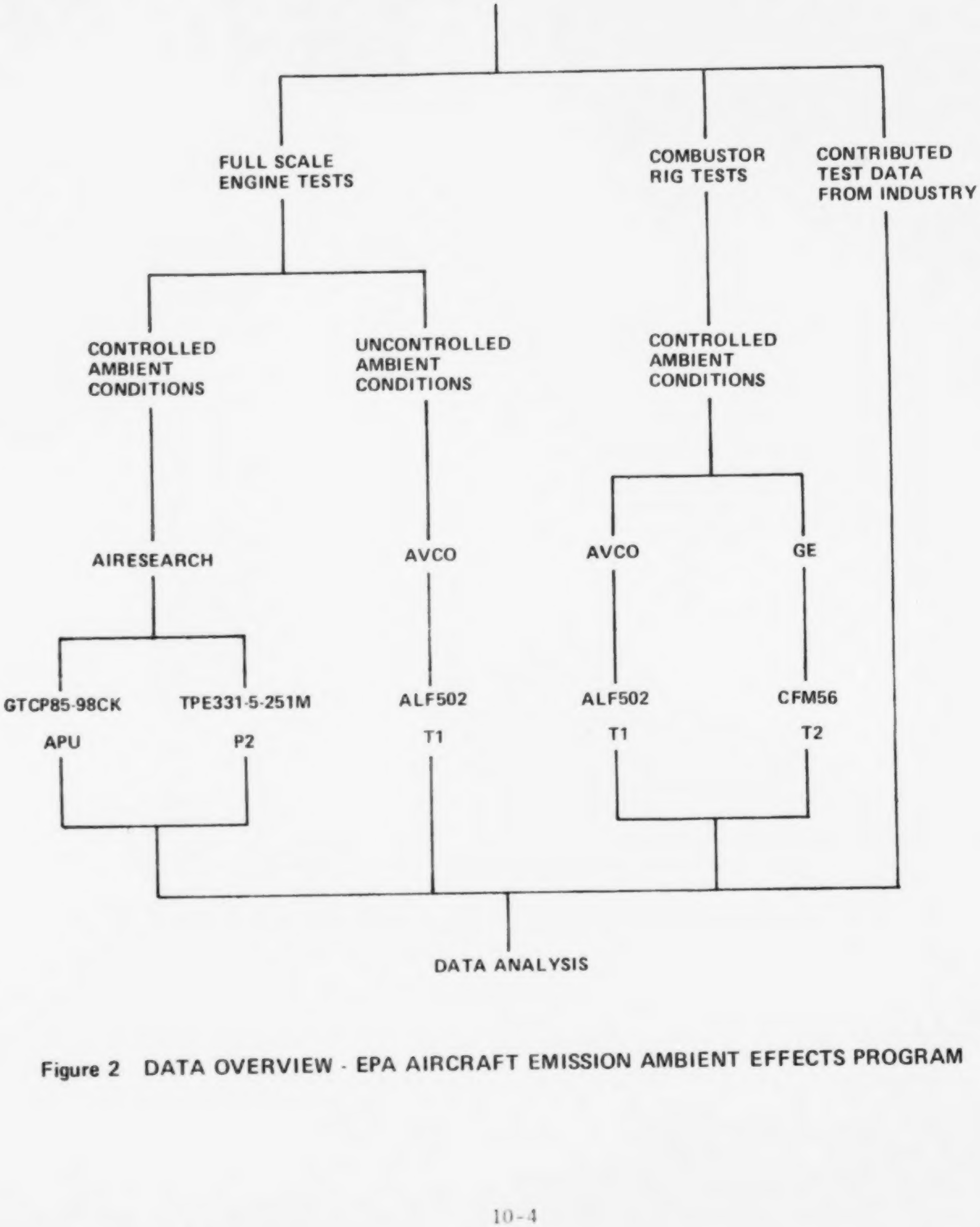
FULL SCALE
ENGINE TESTS
COMBUSTOR
RIG TESTS
CONTRIBUTED
TEST DATA
FROM INDUSTRY
CONTROLLED
AMBIENT
CONDITIONS
UNCONTROLLED
AMBIENT
CONDITIONS
CONTROLLED
AMBIENT
CONDITIONS
AIRESEARCH
AVCO
AVCO
GE
GTCP85-98CK
APU
TPE331-5-251M
P2
ALF502
T1
ALF502
T1
CFM56
T2
DATA ANALYSIS

Figure 2 DATA OVERVIEW - EPA AIRCRAFT EMISSION AMBIENT EFFECTS PROGRAM

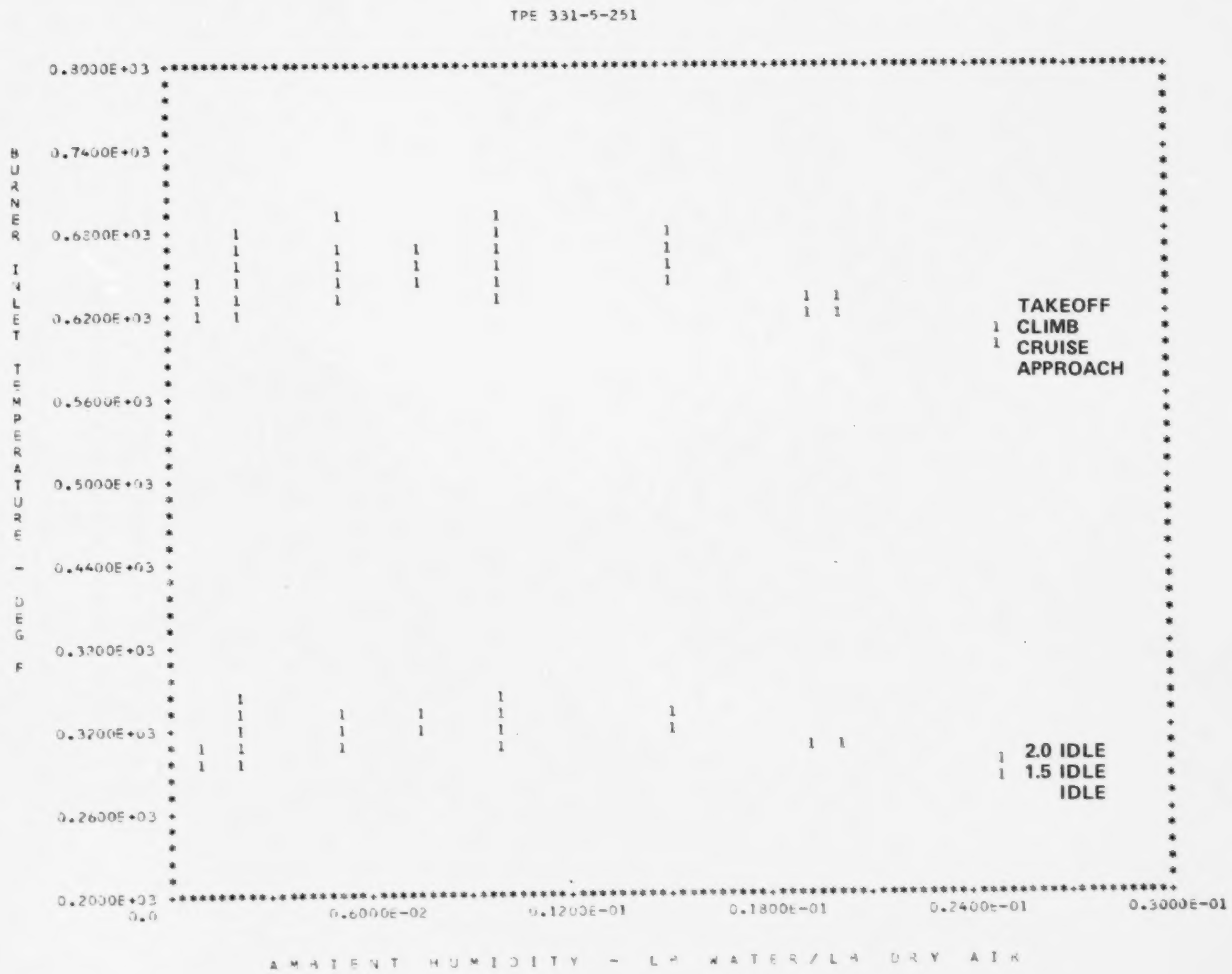

Figure 3 BURNER INLET TEMPERATURE VERSUS AMBIENT HUMIDITY - TPE 331-5-251

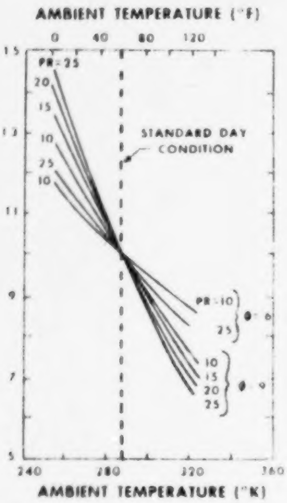

Ambient temperature correction factors (φ = 0.9 and φ = 0.6).

(a)

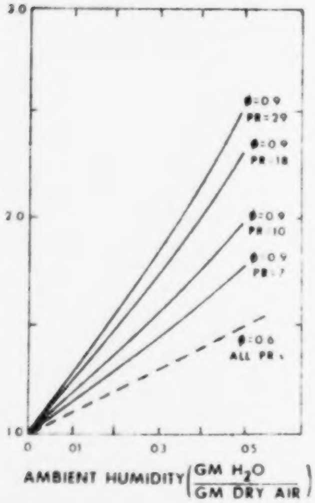

Ambient humidity correction factors (φ = 0.9 and φ = 0.6).

(b)

Figure 4 EFFECT OF ENGINE PRESSURE RATIO AND EQUIVALENCE RATIO ON NOX TEMPERATURE AND HUMIDITY CORRECTION FACTORS - FROM BLAZOWSKI REFERENCE 5

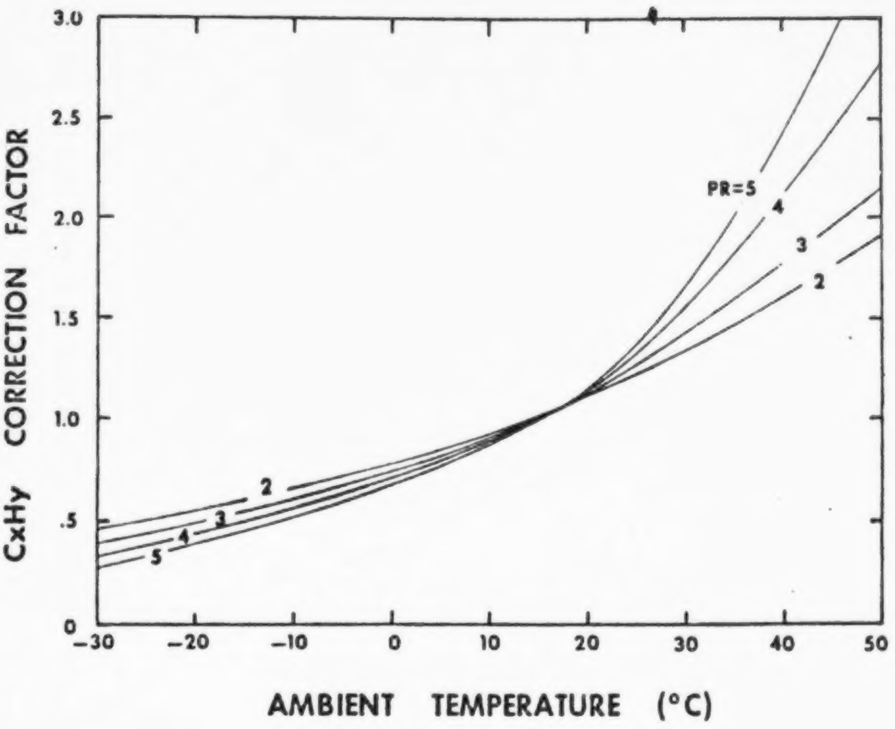

Figure 5 ANALYTICALLY PREDICTED AMBIENT TEMPERATURE CORRECTION FACTORS FOR HYDROCARBONS. FROM BLAZOWSKI AND MARZEWSKI REFERENCE 9.

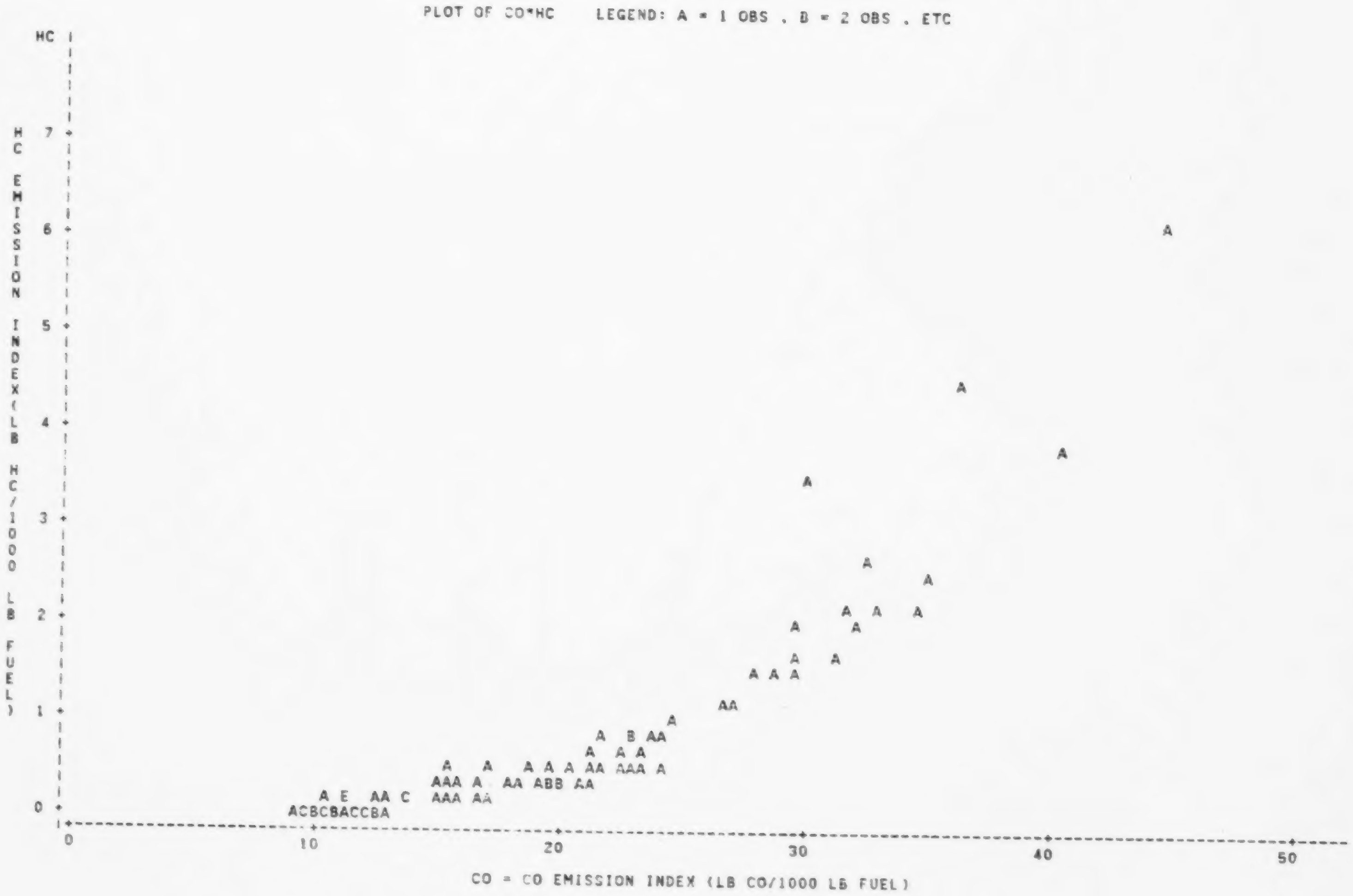

Figure 6 HC EI VERSUS CO EI - CFM56 COMBUSTOR RIG @ IDLE AND 1.5 IDLE

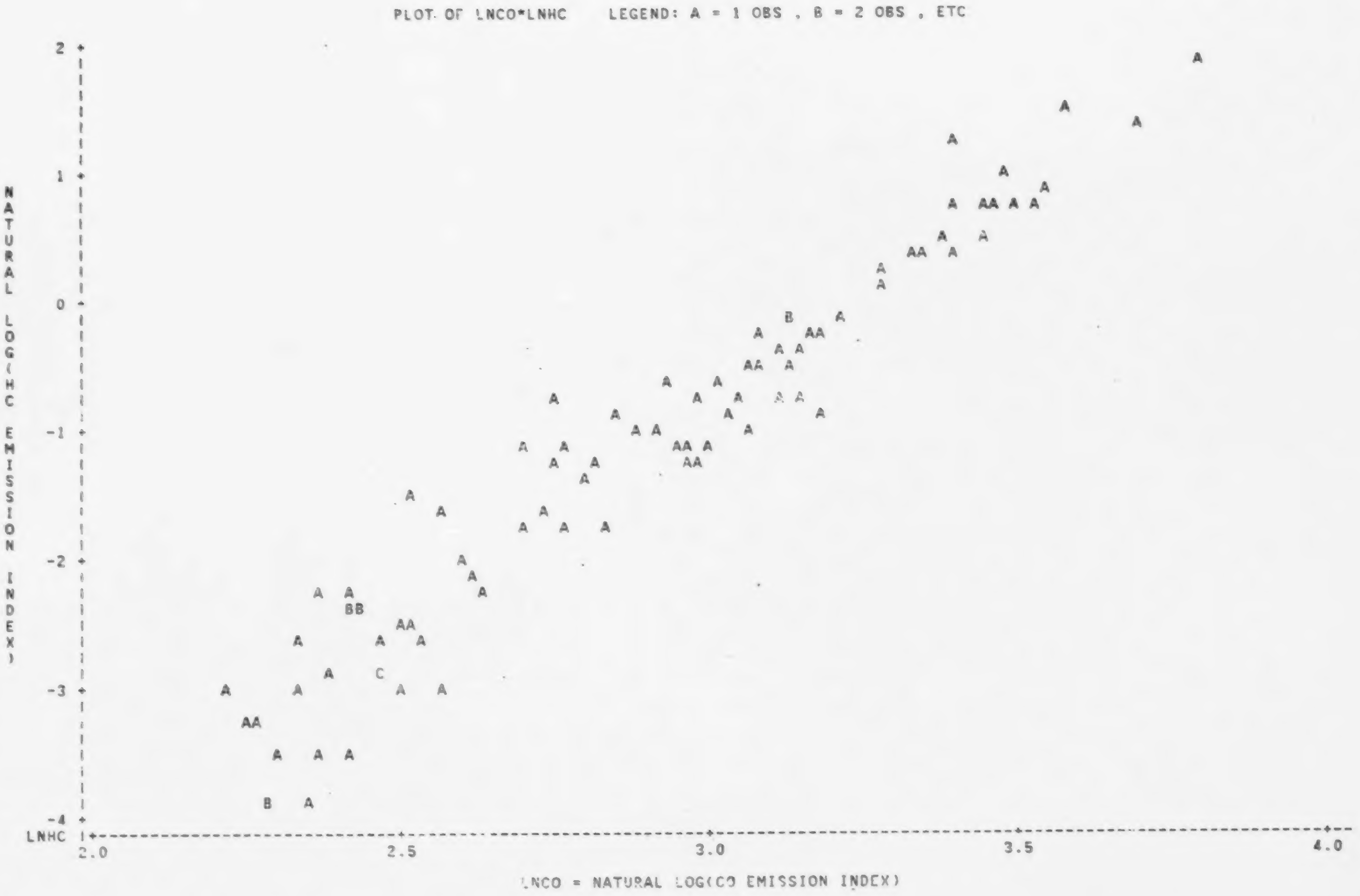

Figure 7 NATURAL LOG OF HC EI VERSUS NATURAL LOG OF CO EI - CFM56 COMBUSTOR RIG @ IDLE AND 1.5 IDLE

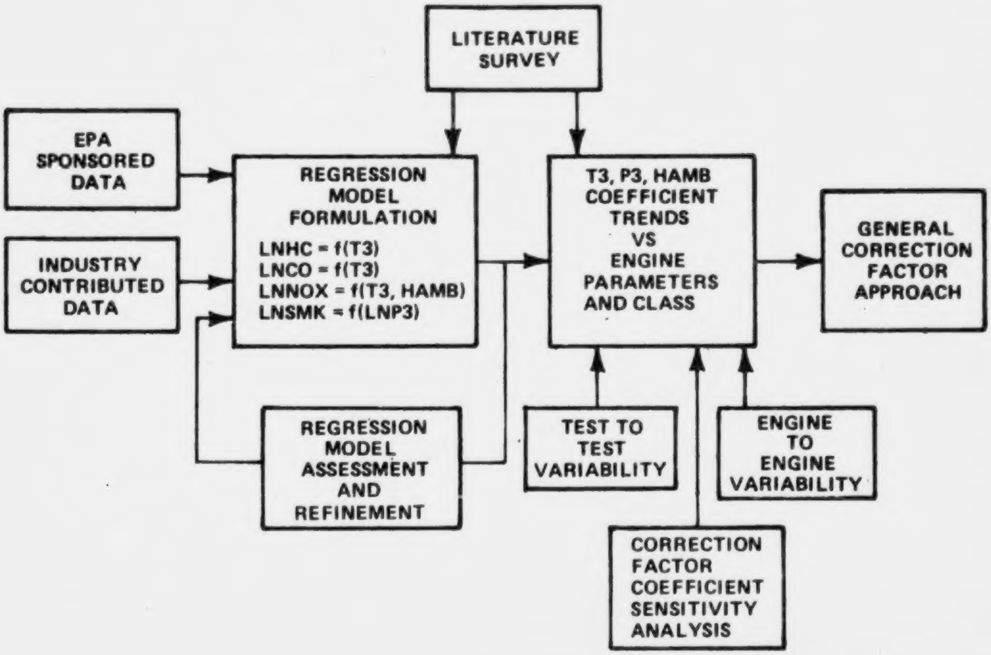
LITERATURE SURVEY
EPA SPONSORED DATA
INDUSTRY CONTRIBUTED DATA
REGRESSION MODEL FORMULATION
LNHC = f(T3)
LNCO = f(T3)
LNNOX = f(T3, HAMB)
LNSMK = f(LNP3)
T3, P3, HAMB COEFFICIENT TRENDS VS ENGINE PARAMETERS AND CLASS
GENERAL CORRECTION FACTOR APPROACH
REGRESSION MODEL ASSESSMENT AND REFINEMENT
TEST TO TEST VARIABILITY
ENGINE TO ENGINE VARIABILITY
CORRECTION FACTOR COEFFICIENT SENSITIVITY ANALYSIS

Figure 8 GENERAL CORRECTION FACTOR DEVELOPMENT OVERVIEW

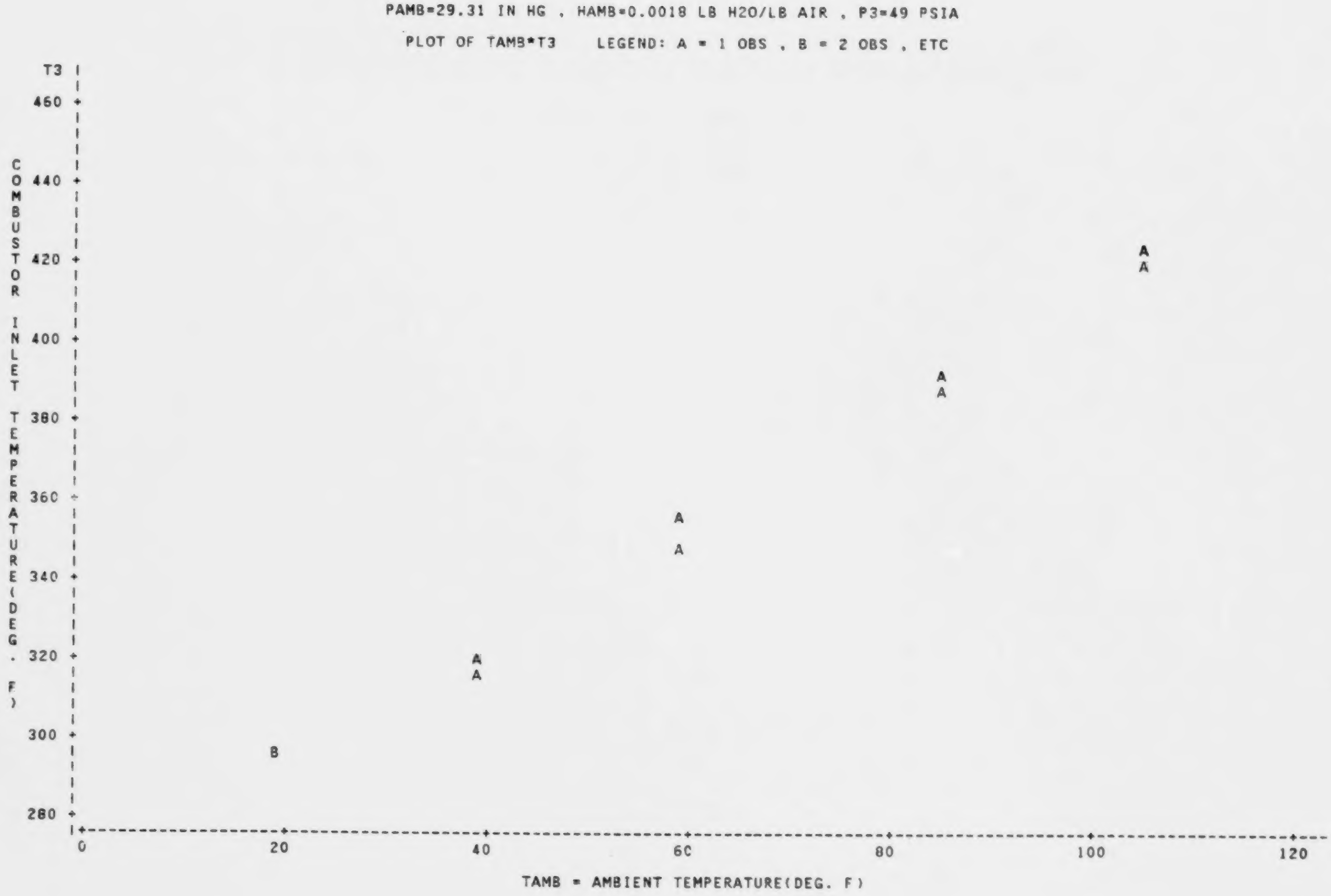

Figure 9 COMBUSTOR INLET TEMPERATURE VERSUS AMBIENT TEMPERATURE - CFM56 COMBUSTOR RIG AT IDLE

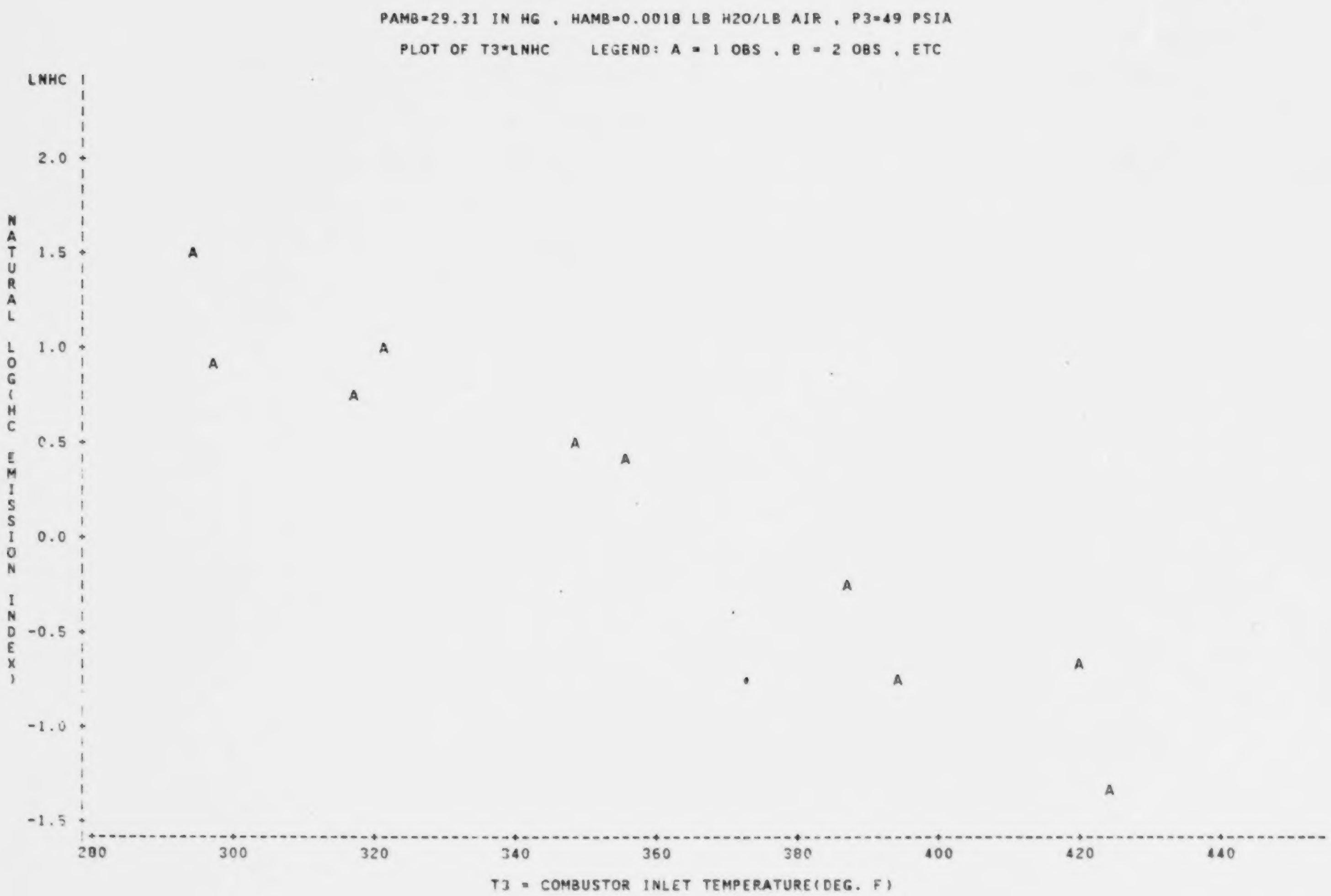

Figure 10 NATURAL LOG OF HC EI VERSUS COMBUSTOR INLET TEMPERATURE - CFM56 COMBUSTOR RIG AT IDLE (PRESSURE AND HUMIDITY FIXED)

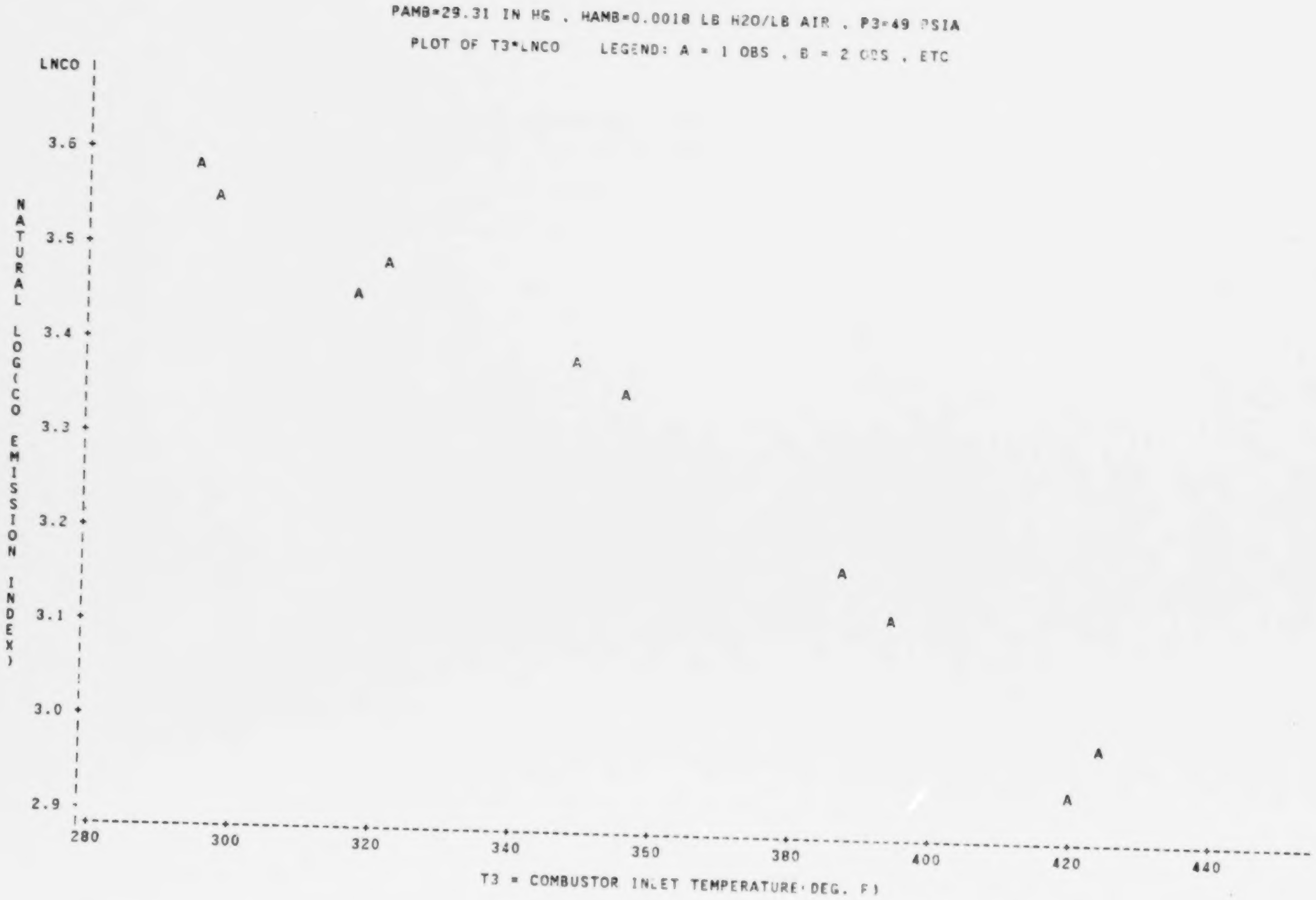

Figure 11 NATURAL LOG OF CO EI VERSUS COMBUSTOR INLET TEMPERATURE - CFM56 COMBUSTOR RIG AT IDLE (PRESSURE AND HUMIDITY FIXED)

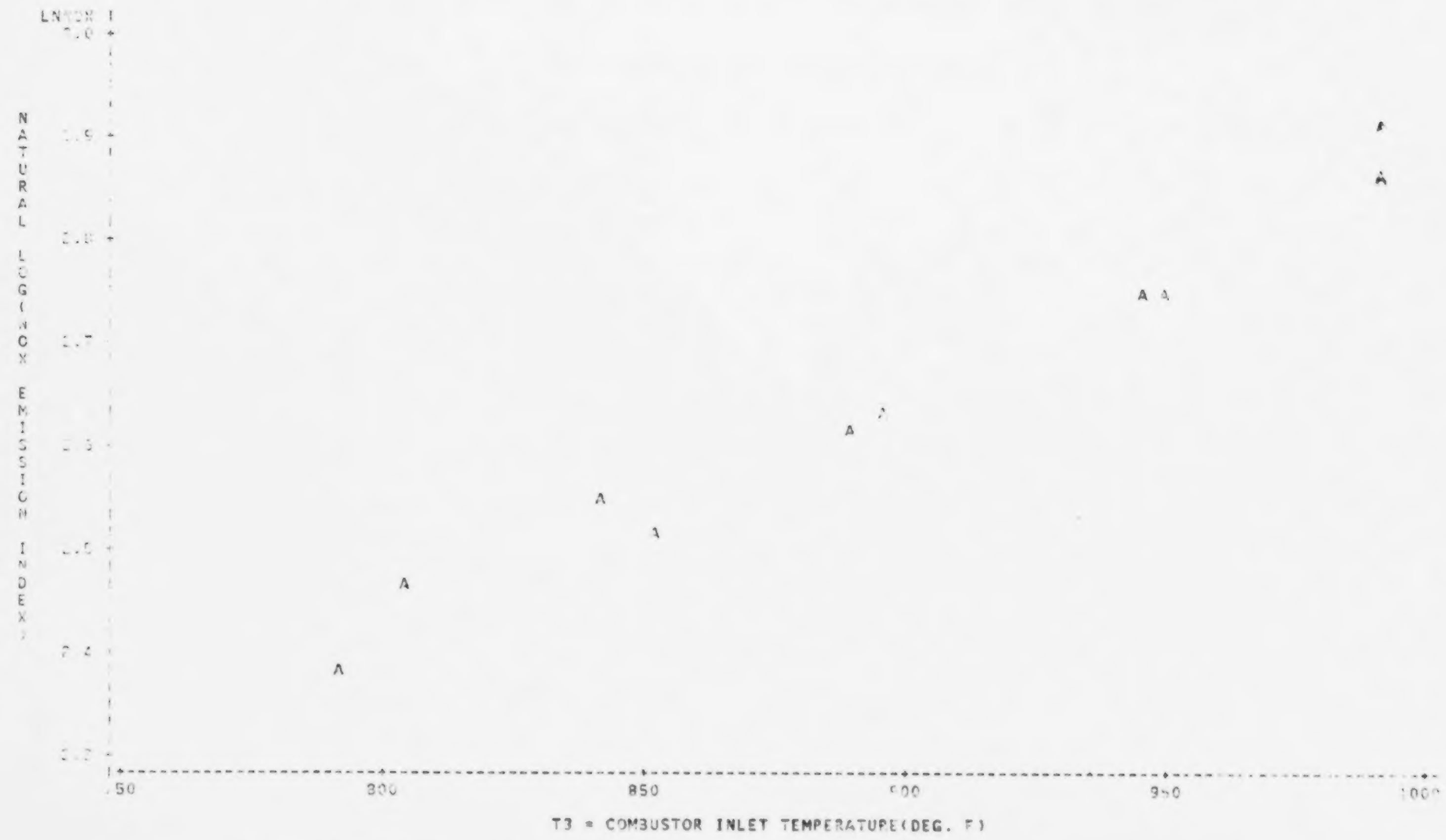

Figure 12 NATURAL LOG OF NOX EI VERSUS COMBUSTOR INLET TEMPERATURE – CFM 56 COMBUSTOR RIG AT CLIMB (PRESSURE AND HUMIDITY FIXED)

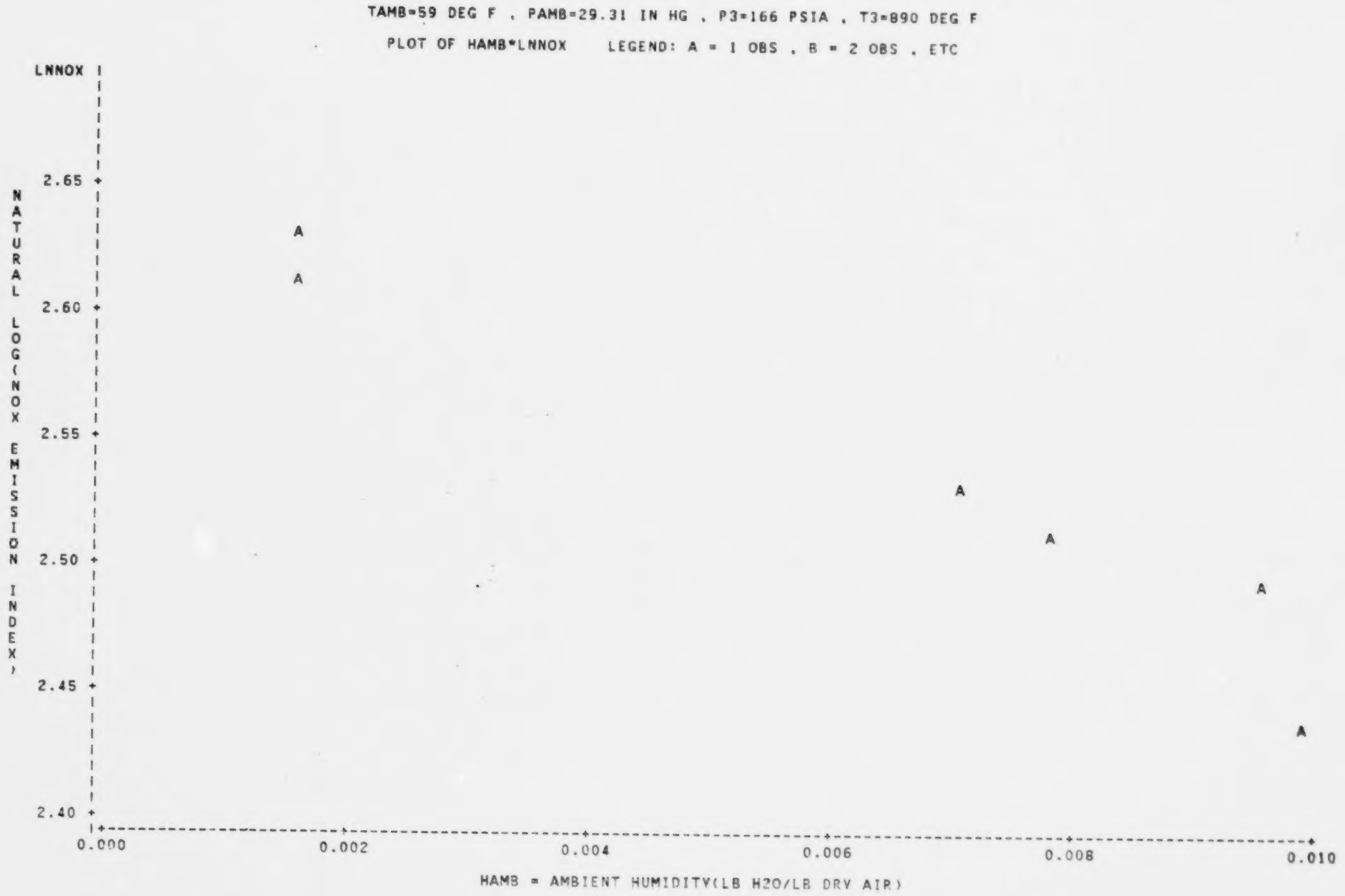

Figure 13 NATURAL LOG OF NOX EI VERSUS AMBIENT HUMIDITY - CFM56 COMBUSTOR RIG AT CLIMB (PRESSURE AND TEMPERATURE FIXED)

LNHC = f(T3)

LNCO = f(T3)

LNNOX = f(T3, HAMB)

LNSMK = f(LNP3)

WHERE:

T3 = COMBUSTOR INLET TEMPERATURE
HAMB = AMBIENT HUMIDITY
LNP3 = NATURAL LOG COMBUSTOR INLET PRESSURE
LNHC = NATURAL LOG HC EI
LNCO = NATURAL LOG CO EI
LNNOX = NATURAL LOG NOX EI
LNSMK = NATURAL LOG SMOKE NUMBER

Figure 14 AMBIENT EFFECTS PROGRAM REGRESSION MODEL SUMMARY

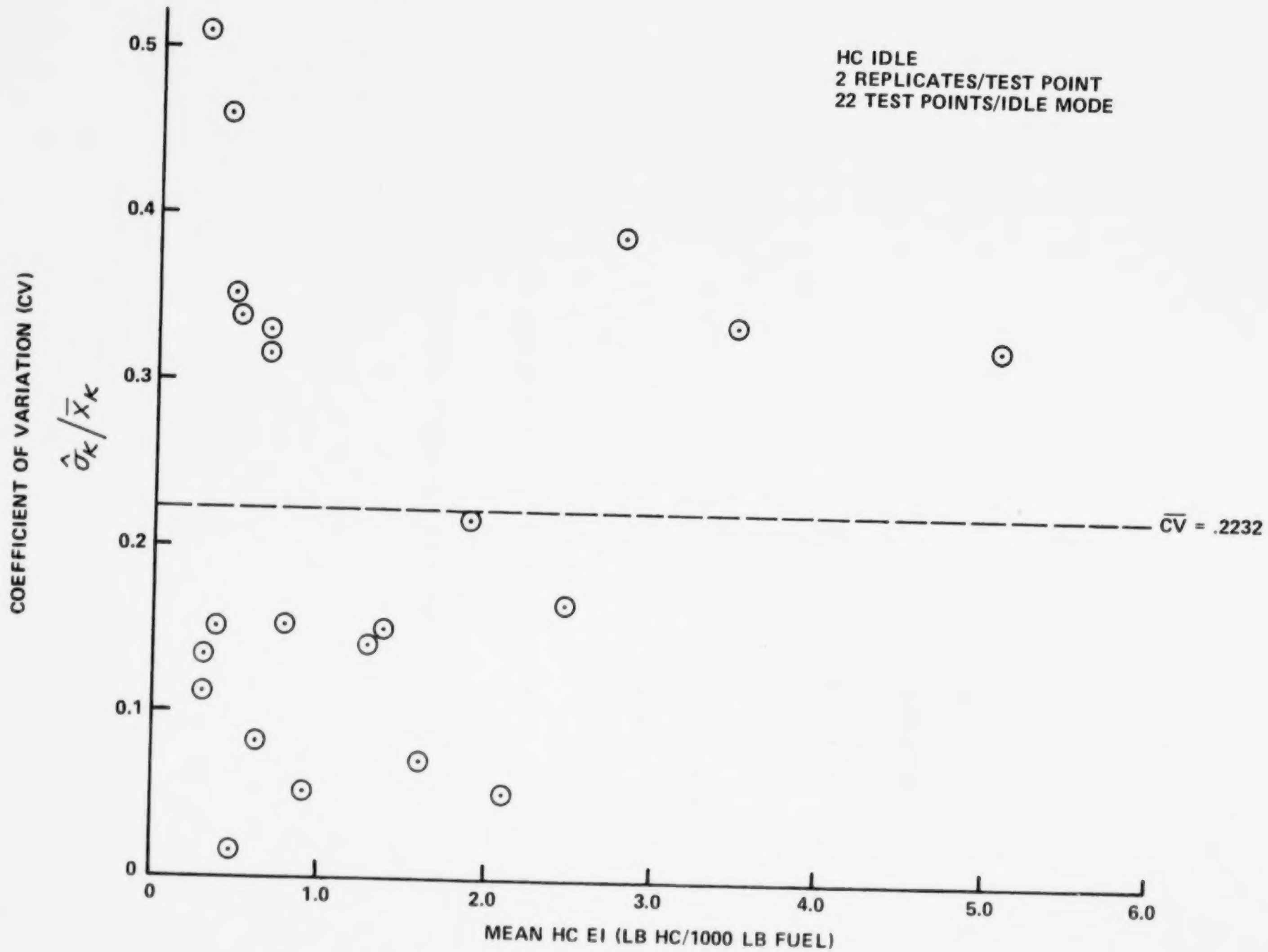

Figure 15 REPLICATE ANALYSIS COEFFICIENT OF VARIATION FOR CFM56 COMBUSTOR RIG, HC IDLE DATA

$$CF = \frac{\text{EMISSIONS AT STANDARD CONDITIONS}}{\text{MEASURED EMISSIONS}}$$

EXAMPLE – CFM 56 COMBUSTOR RIG TEST

$$\text{NOX EI}_{TEST} = 1.5956\, e^{.002503\ T3_{TEST}}\, e^{-20.7\ HAMB_{TEST}}$$

$$\text{NOX EI}_{TEST} = 1.5956\, e^{.002503\ T3_{STD}}\, e^{-20.7\ HAMB_{STD}}$$

$$CF = \frac{\text{NOX EI}_{STD}}{\text{NOX EI}_{TEST}}$$

$$CF = e^{.002503\ (T3_{STD} - T3_{TEST})}\, e^{-20.7\ (HAMB_{TEST} - HAMB_{STD})}$$

Figure 16 CORRECTION FACTOR STRUCTURE

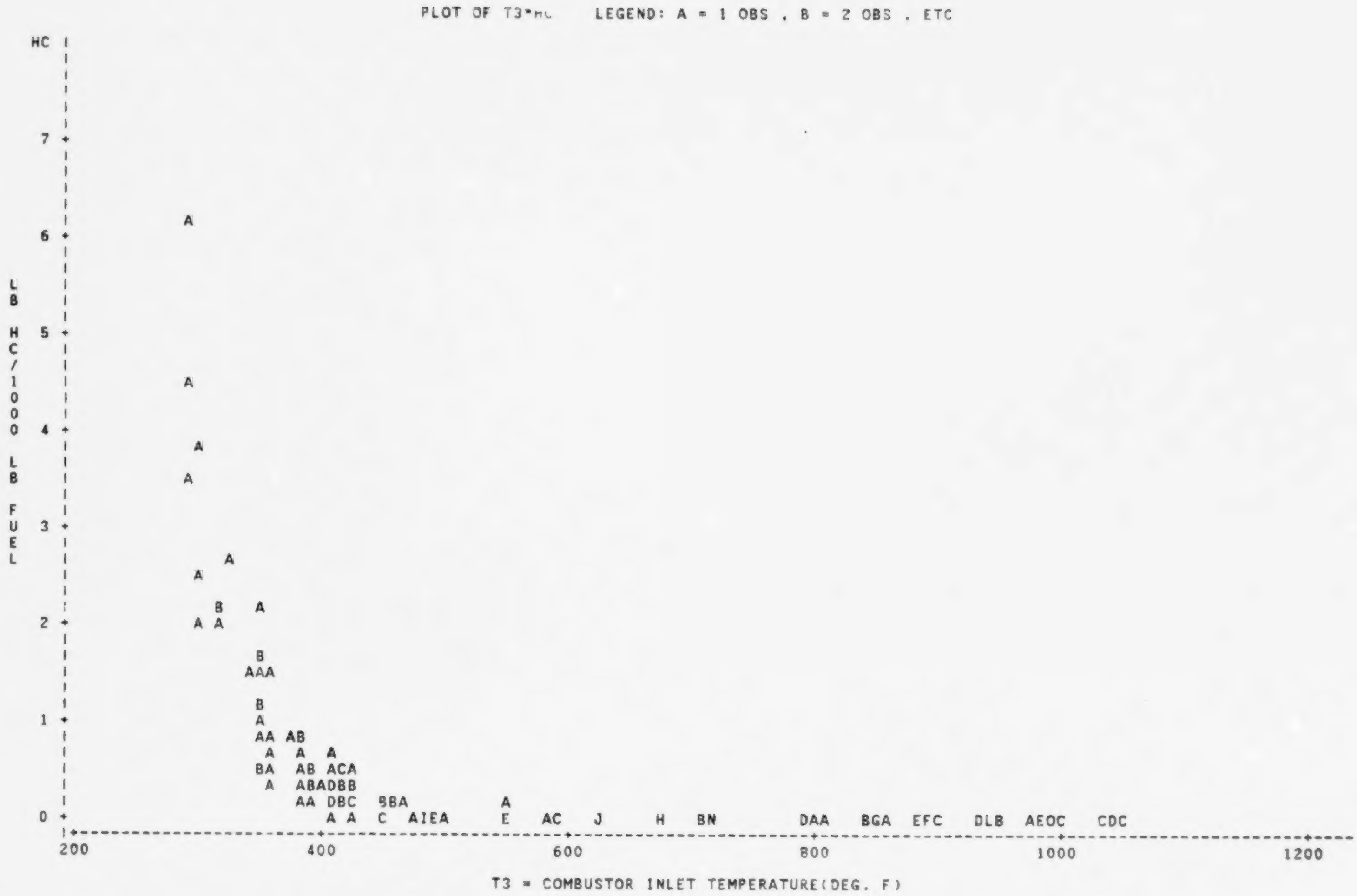

Figure 17 HC EI VERSUS COMBUSTOR INLET TEMPERATURE - CFM56 COMBUSTOR RIG, IDLE TO TAKEOFF

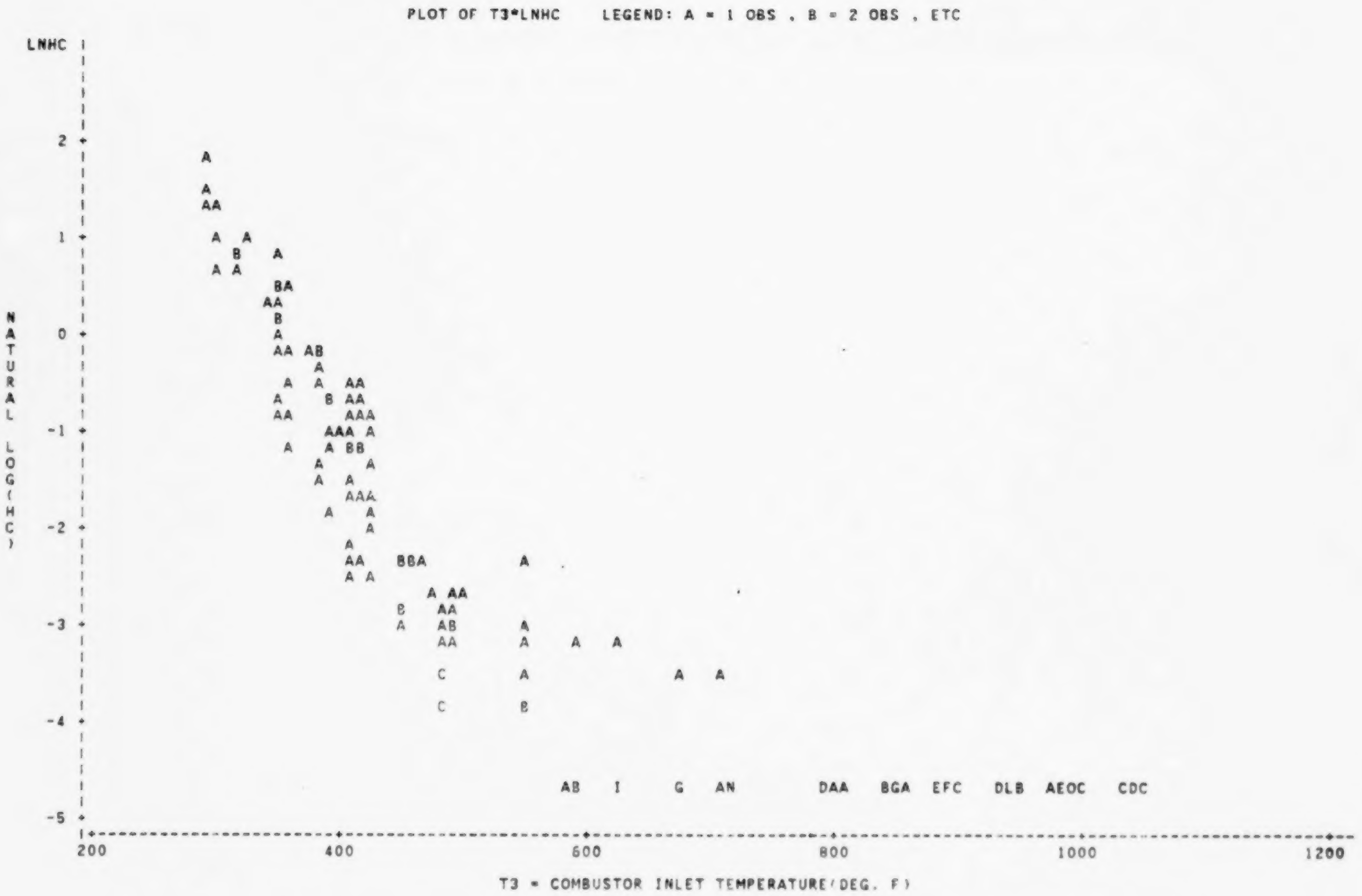

Figure 18 NATURAL LOG HC EI VERSUS COMBUSTOR INLET TEMPERATURE - CFM56 COMBUSTOR RIG, IDLE TO TAKEOFF

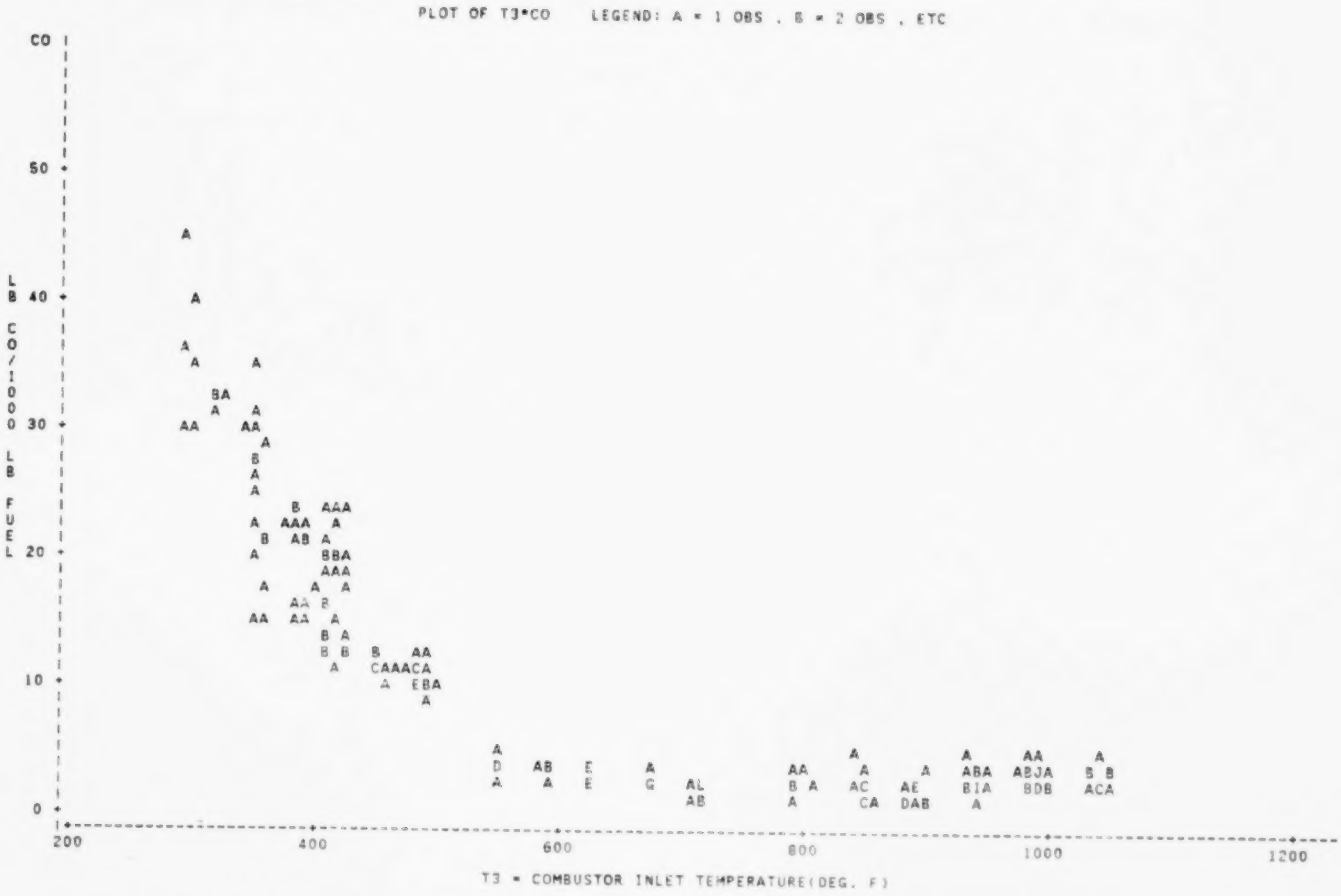

Figure 19 CO EI VERSUS COMBUSTOR INLET TEMPERATURE - CFM56 COMBUSTOR RIG, IDLE TO TAKEOFF

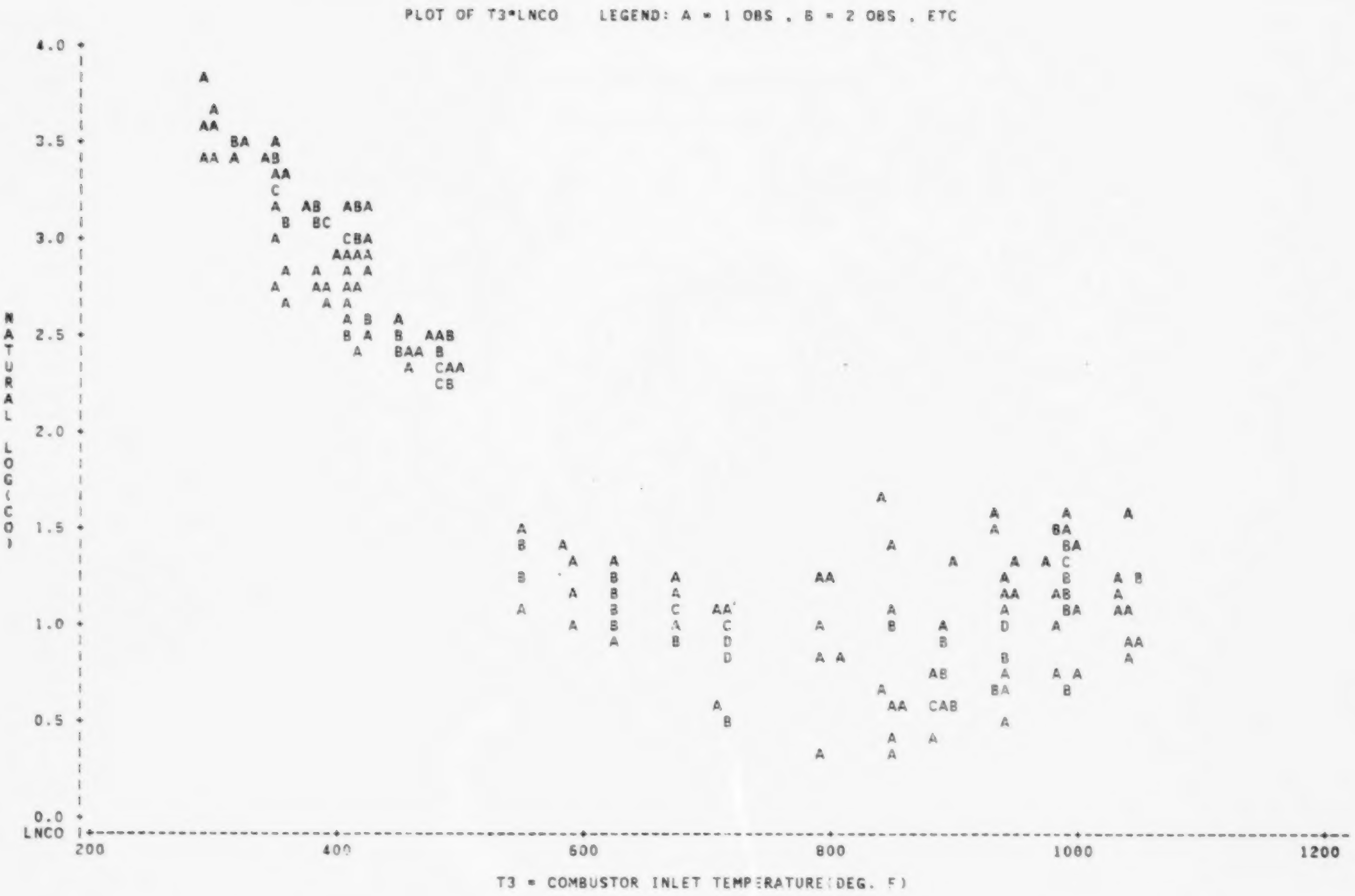

Figure 20 NATURAL LOG CO EI VERSUS COMBUSTOR INLET TEMPERATURE - CFM56 COMBUSTOR RIG, IDLE TO TAKEOFF

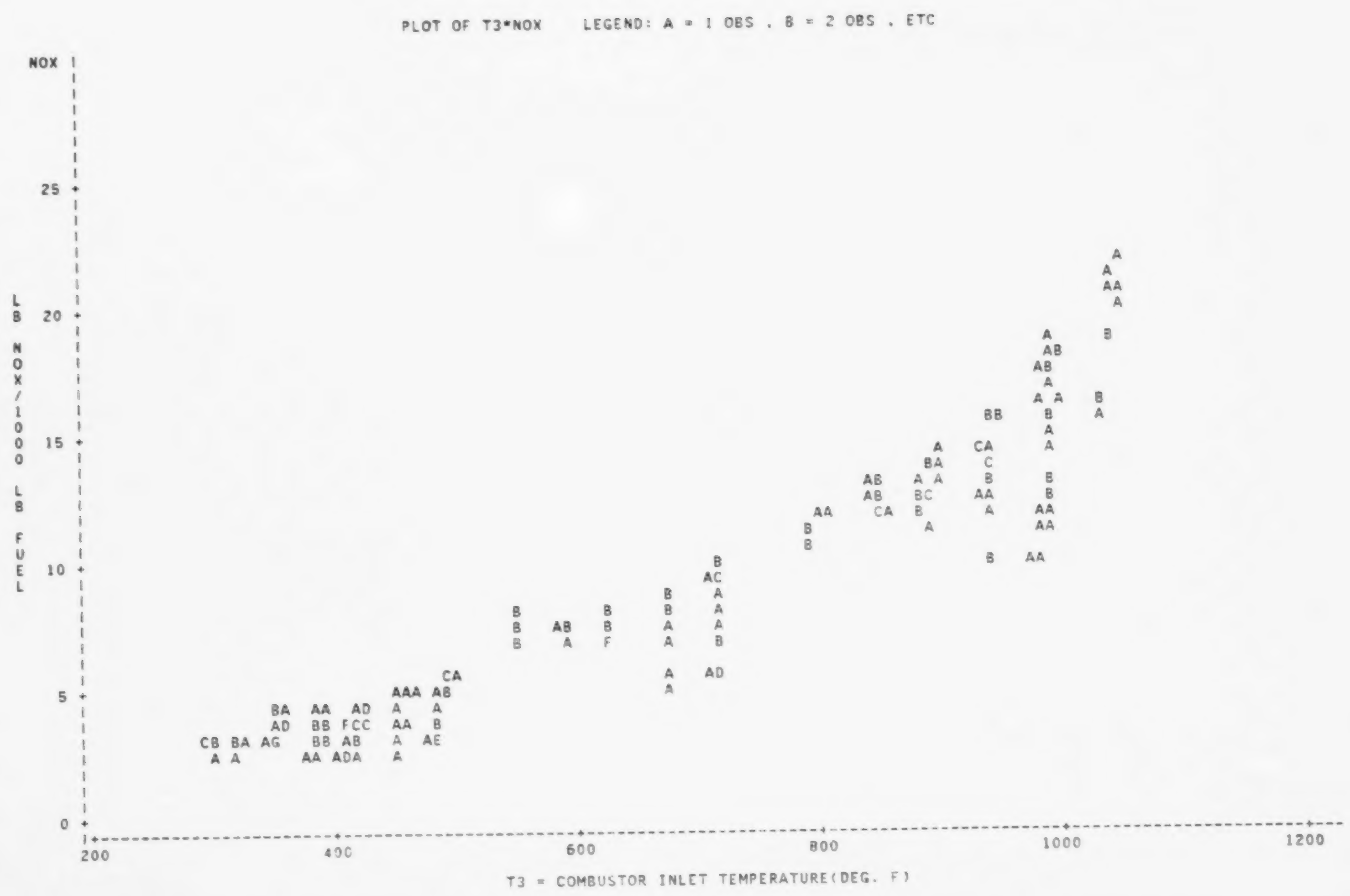

Figure 21 NOX EI VERSUS COMBUSTOR INLET TEMPERATURE - CFM56 COMBUSTOR RIG, IDLE TO TAKEOFF

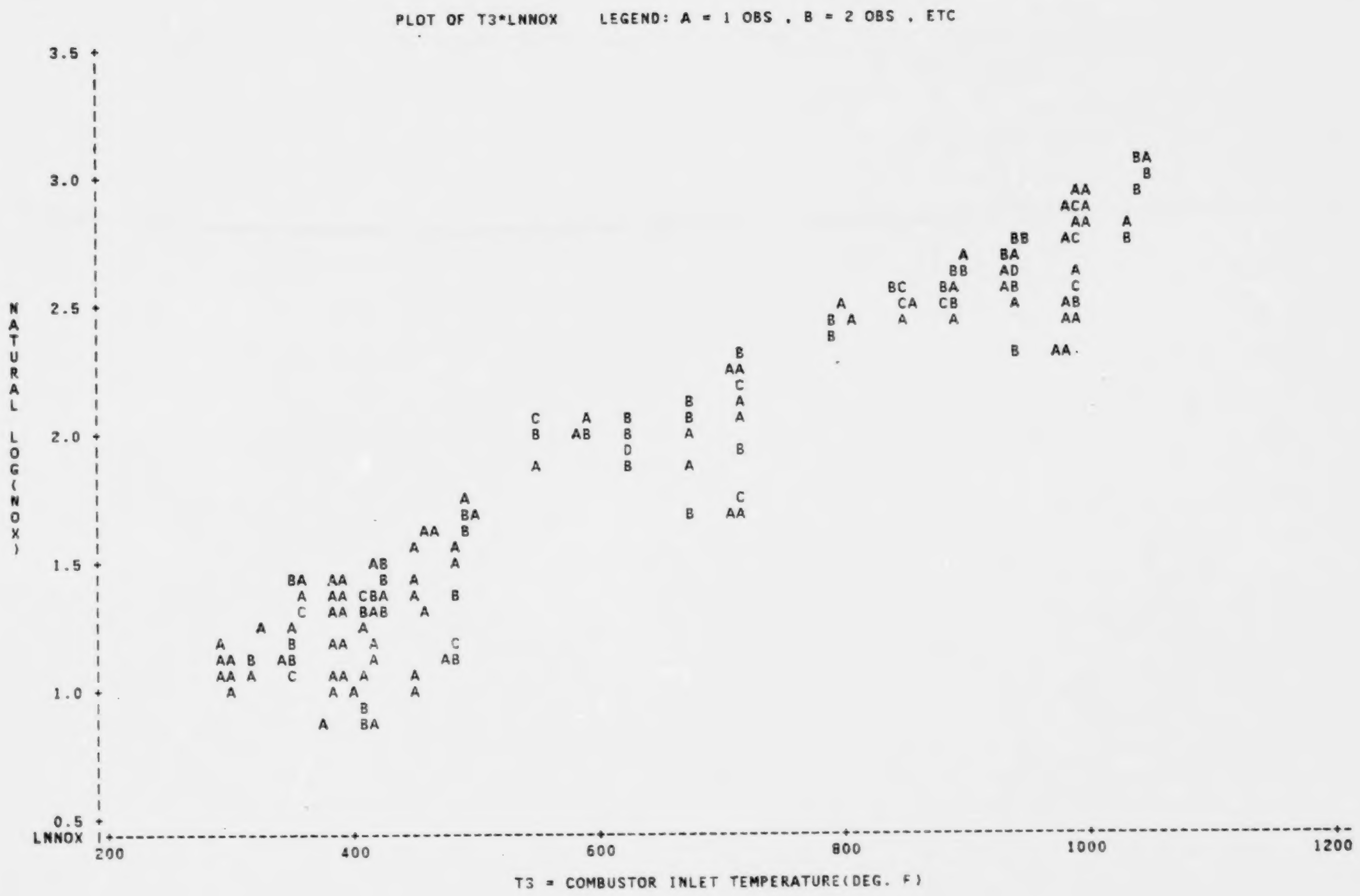

Figure 22 NATURAL LOG OF NOX EI VERSUS COMBUSTOR INLET TEMPERATURE - CFM56 COMBUSTOR RIG, IDLE TO TAKEOFF

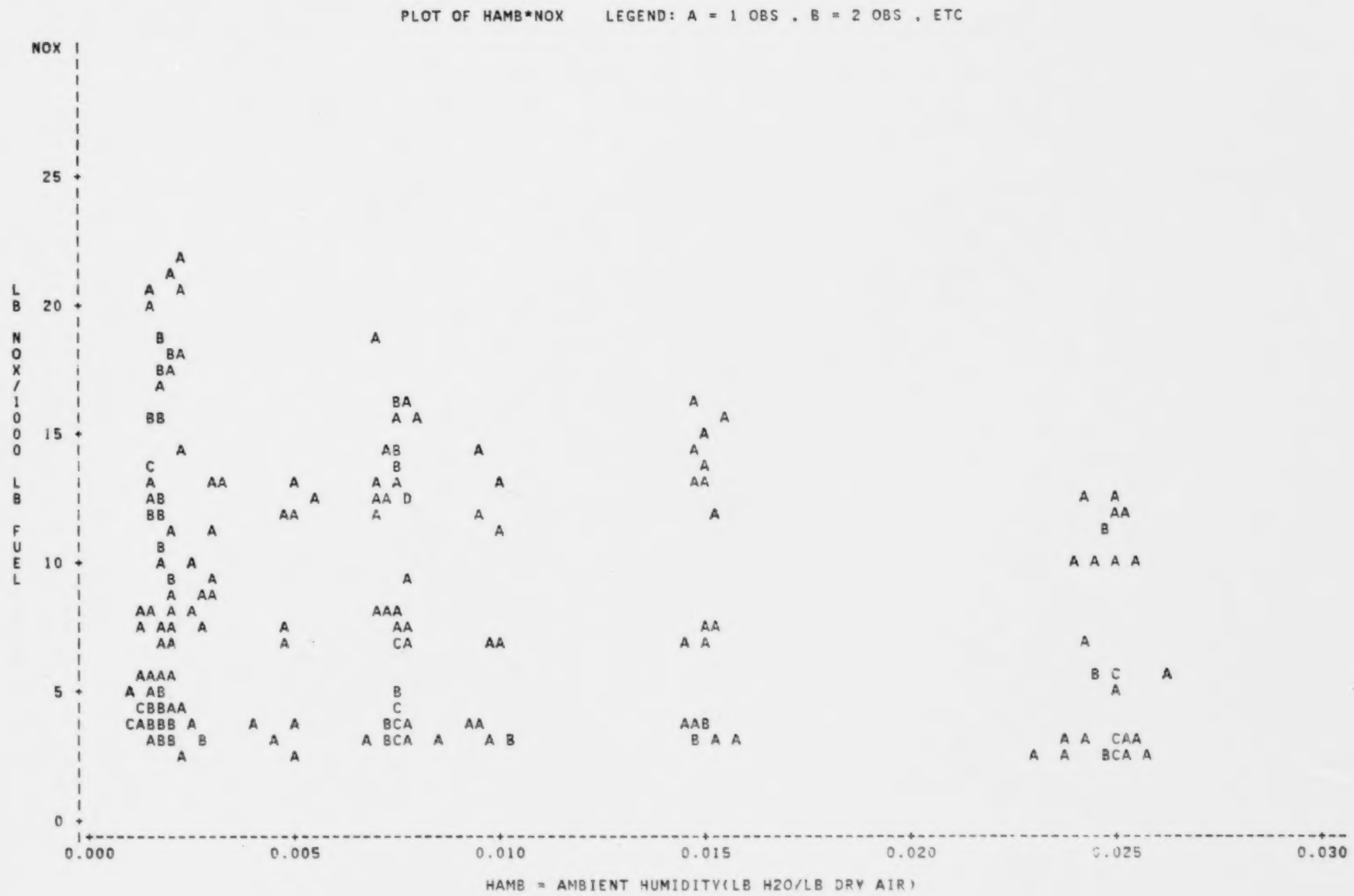

Figure 23 NOX EI VERSUS AMBIENT HUMIDITY - CFM56 COMBUSTOR RIG, IDLE TO TAKEOFF

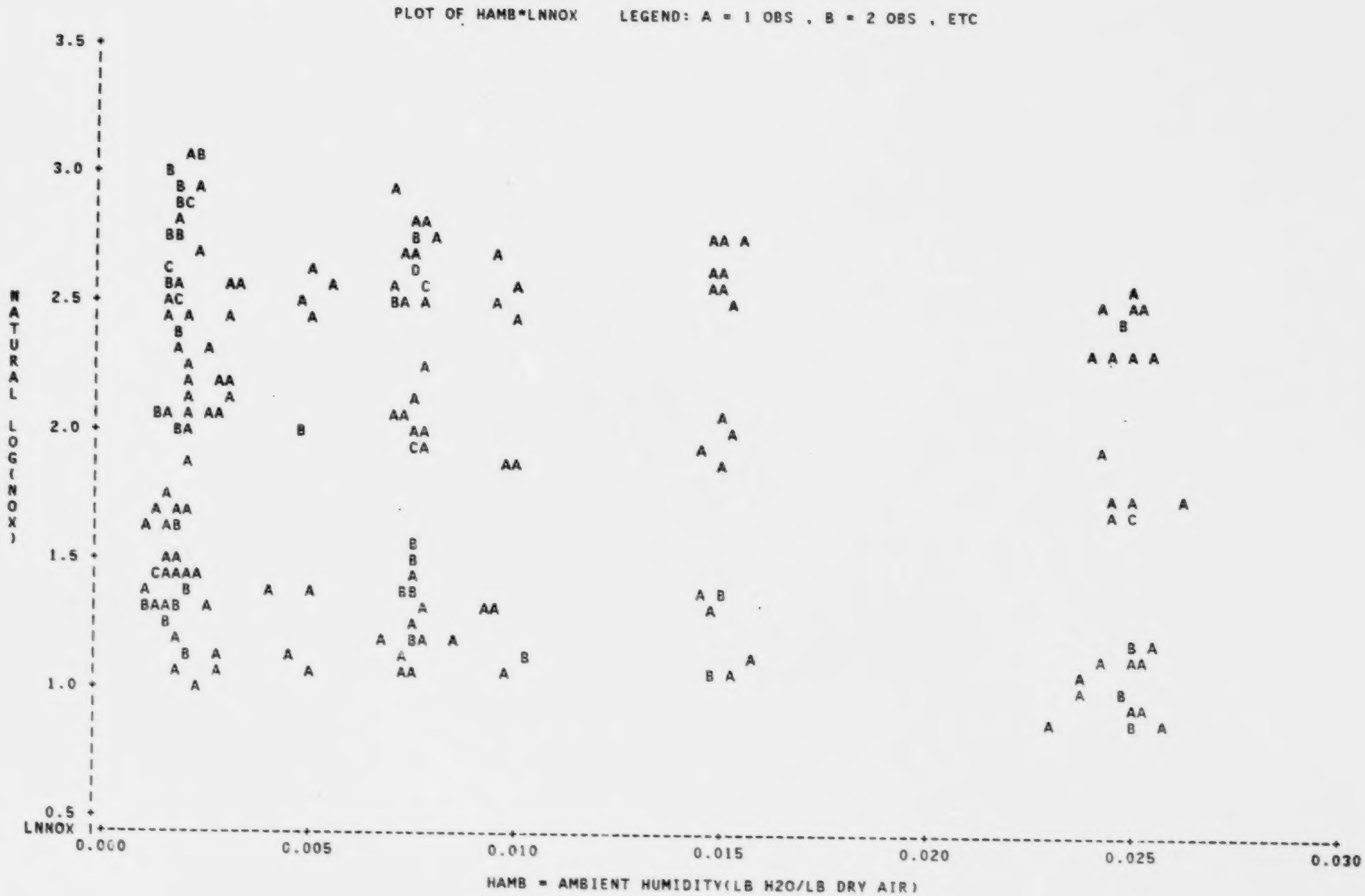

Figure 24 NATURAL LOG OF NOX EI VERSUS AMBIENT HUMIDITY - CFM56 COMBUSTOR RIG, IDLE TO TAKEOFF

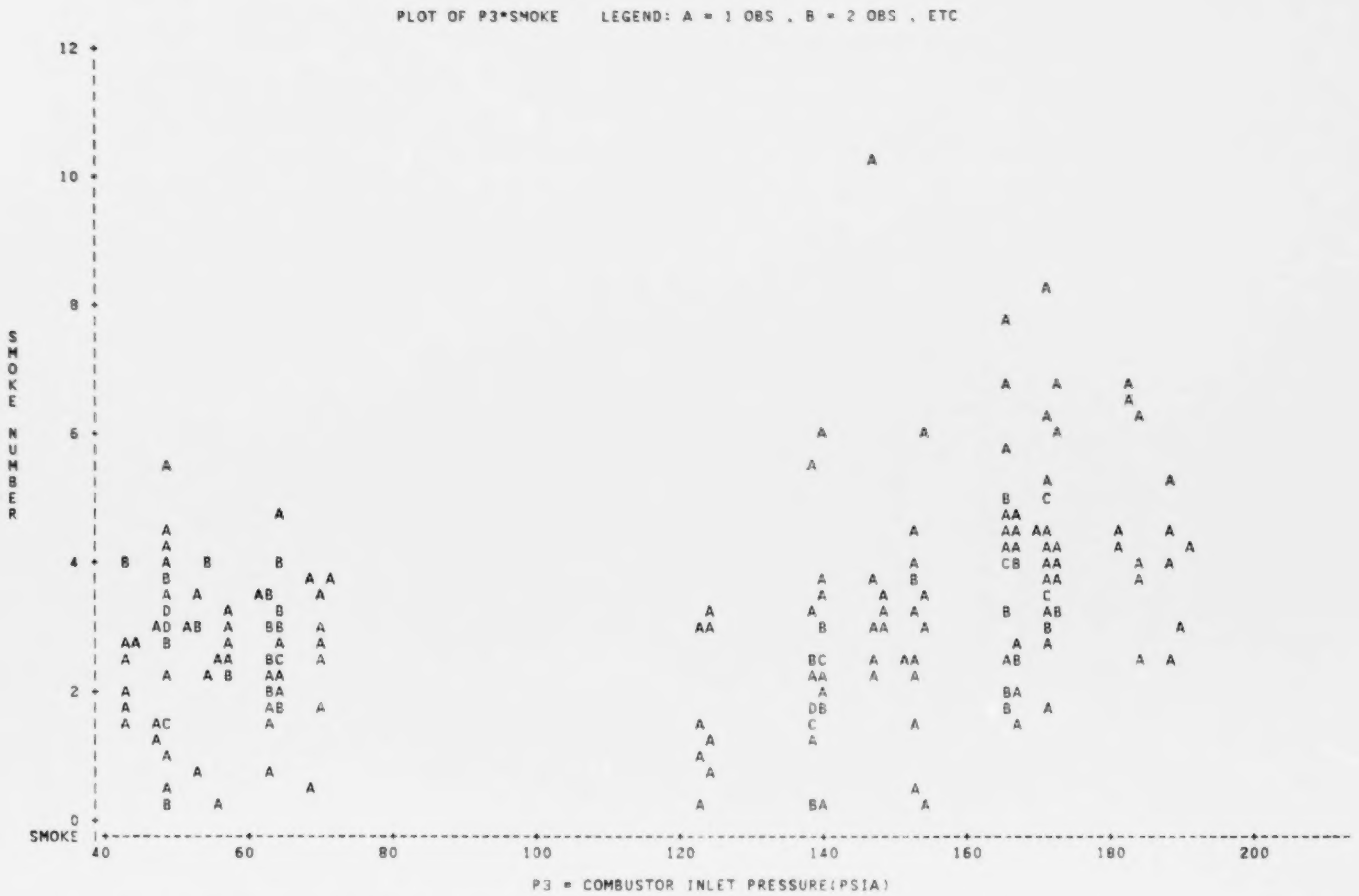

Figure 25 SMOKE NUMBER VERSUS COMBUSTOR INLET PRESSURE - CFM56 COMBUSTOR RIG, IDLE TO TAKEOFF

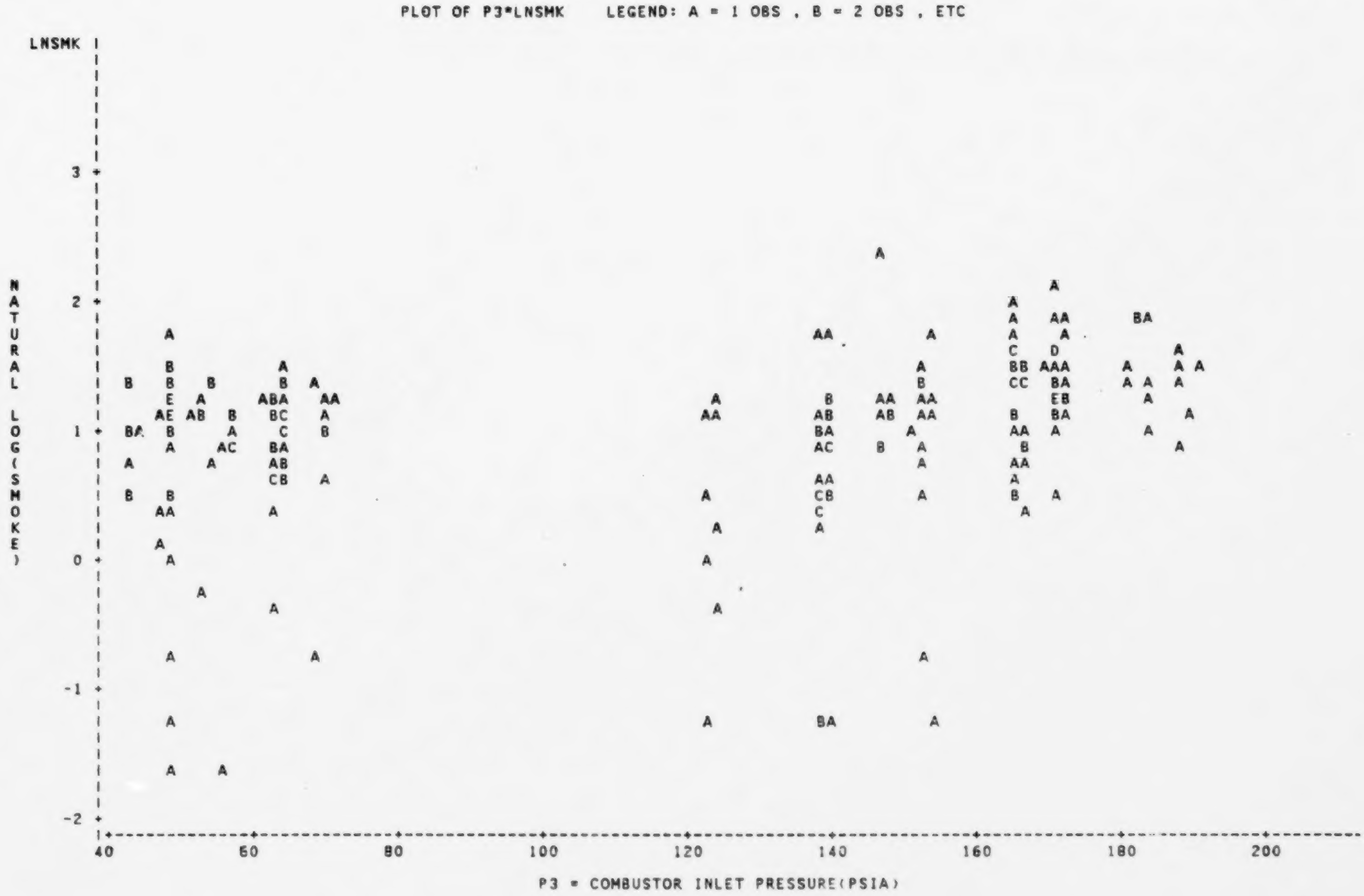

Figure 26 NATURAL LOG OF SMOKE NUMBER VERSUS COMBUSTOR INLET PRESSURE-CFM56 COMBUSTOR RIG, IDLE TO TAKEOFF

$$\text{HC EI} = 3848.5658 * e^{-.023486 * T3}$$

$$\text{CO EI} = 239.1063 * e^{-.006443 * T3}$$

$$\text{NOX EI} = 1.5956 * e^{.002503 * T3} * e^{-20.7 * HAMB}$$

$$\text{SMOKE} = .7318 * P3^{.2775}$$

WHERE

P3 = COMBUSTOR INLET PRESSURE - PSIA
T3 = COMBUSTOR INLET TEMPERATURE - DEG F
HAMB = AMBIENT HUMIDITY - LB H20/LB DRY AIR

Figure 27 REGRESSION COEFFICIENT SUMMARY CFM56 COMBUSTOR RIG

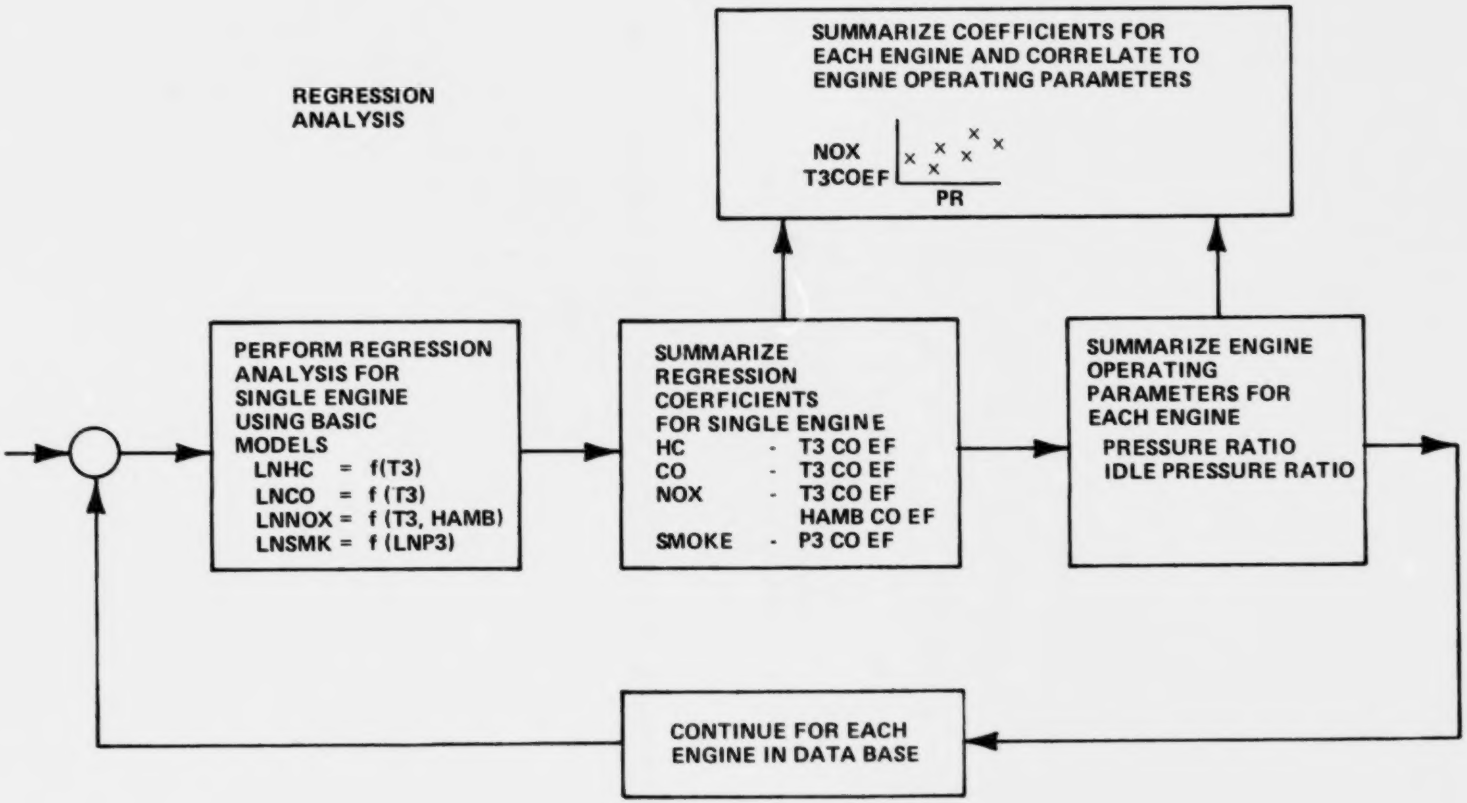
REGRESSION ANALYSIS
PERFORM REGRESSION ANALYSIS FOR SINGLE ENGINE USING BASIC MODELS
LNHC = f(T3)
LNCO = f (T3)
LNNOX = f (T3, HAMB)
LNSMK = f (LNP3)
SUMMARIZE REGRESSION COERFICIENTS FOR SINGLE ENGINE
HC - T3 CO EF
CO - T3 CO EF
NOX - T3 CO EF
HAMB CO EF
SMOKE - P3 CO EF
SUMMARIZE ENGINE OPERATING PARAMETERS FOR EACH ENGINE
PRESSURE RATIO
IDLE PRESSURE RATIO
SUMMARIZE COEFFICIENTS FOR EACH ENGINE AND CORRELATE TO ENGINE OPERATING PARAMETERS
NOX
T3COEF
PR
CONTINUE FOR EACH ENGINE IN DATA BASE

Figure 28 CORRECTION FACTOR COEFFICIENT VERSUS ENGINE OPERATING PARAMETER - DEVELOPMENT APPROACH

ENGINE = Engine or Rig used to develop regression equation.

MODES = Power modes included in analysis.

SAMPLES = Number of test points in analysis.

CONSTANT = Constant term in regression equation (based on T3 data in Deg. F of P3 data in PSIA)

T3COEF = Combustor Inlet Temperature Regression Coefficient (input T3 data in Deg. F)

T3STD = Standard Error of T3COEF

HAMBCOEF = Ambient Specific Humidity Regression Coefficient (input HAMB data in lb H_2O/lb dry air)

HAMBSTD = Standard Error of HAMBCOEF

P3COEF = Combustor Inlet Pressure Regression Coefficient (input P3 data in PSIA)

P3STD = Standard Error of P3COEF

RSQ = Coefficient of Determination for Regression, $0 \leq R^2 \leq 1$.

T3MEAN = Mean Combustor Inlet Temperature (T3) in Deg. F of test data and defined as follows:
- HC: Mean Idle T3
- CO: Mean Idle T3
- NOX: Mean Takeoff T3

Note: Where NOX takeoff data was not available, T3MEAN corresponds to mean T3 at highest thrust level (e.g., approach, climb, or cruise) for which data was available.

P3MEAN = Mean Combustor Inlet Pressure (P3) in PSIA of test data and defined as follows:
- HC: Mean Idle P3
- CO: Mean Idle P3
- NOX: Mean Takeoff P3
- SMOKE: Mean Takeoff P3

Note: Where Takeoff data was not available, P3MEAN corresponds to mean P3 at highest thrust level (e.g. approach, climb, or cruise) for which data was available.

HCMEAN = Mean Idle HC EI.

COMEAN = Mean Idle CO EI

NOXMEAN = Mean Takeoff NOX EI -- Note: If Takeoff data unavailable NOXMEAN corresponds to mean NOX EI at highest power setting measured.

SMKMEAN = Mean Takeoff EPA Smoke Number -- Note: If Takeoff data unavailable SMKMEAN corresponds to mean EPA Smoke Number at highest power setting measured.

PR = Rated Pressure Ratio -- Note: If Takeoff data unavailable, PR corresponds to P3MEAN/14.7 PSIA

IPR = Idle Pressure Ratio (computed from engine test data)

CLASS = EPA Engine Class Designation

Figure 29 CORRECTION FACTOR NOMENCLATURE

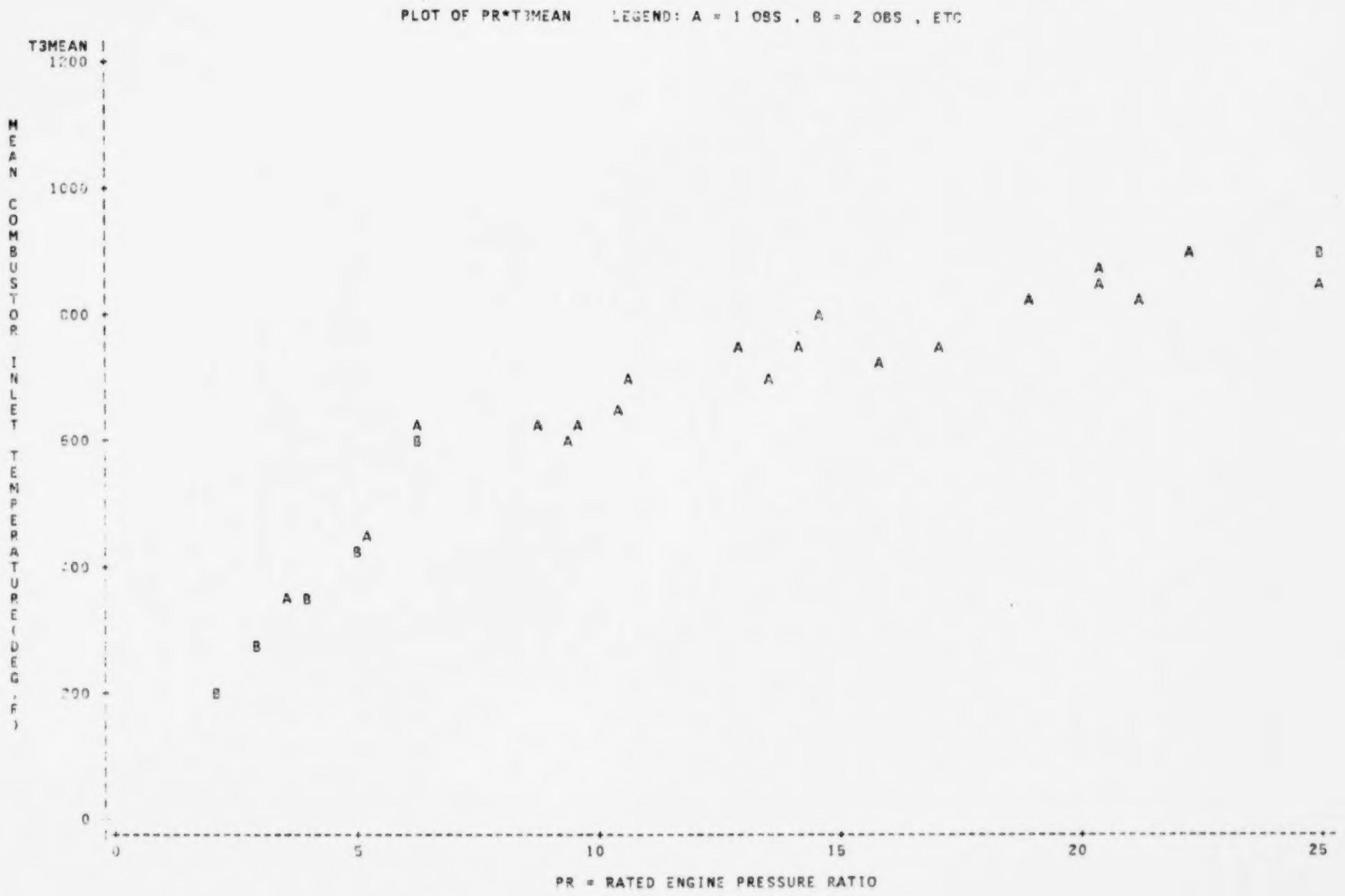

Figure 30 T3MEAN VERSUS RATED PRESSURE RATIO PR, AMBIENT EFFECTS DATA BASE

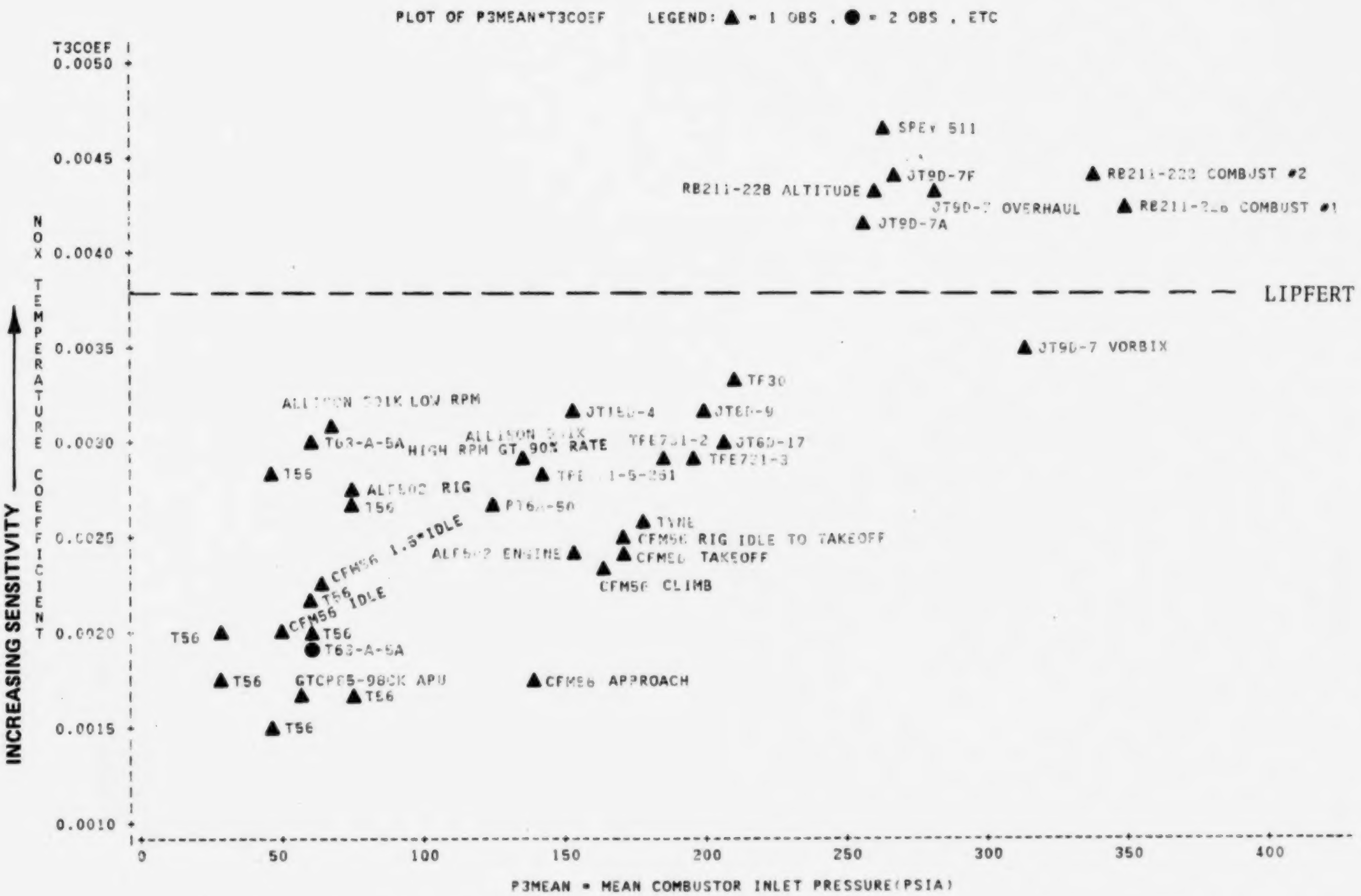

Figure 31 NOX COMBUSTOR INLET TEMPERATURE COEFFICIENT T3COEF VERSUS COMBUSTOR INLET PRESSURE P3MEAN

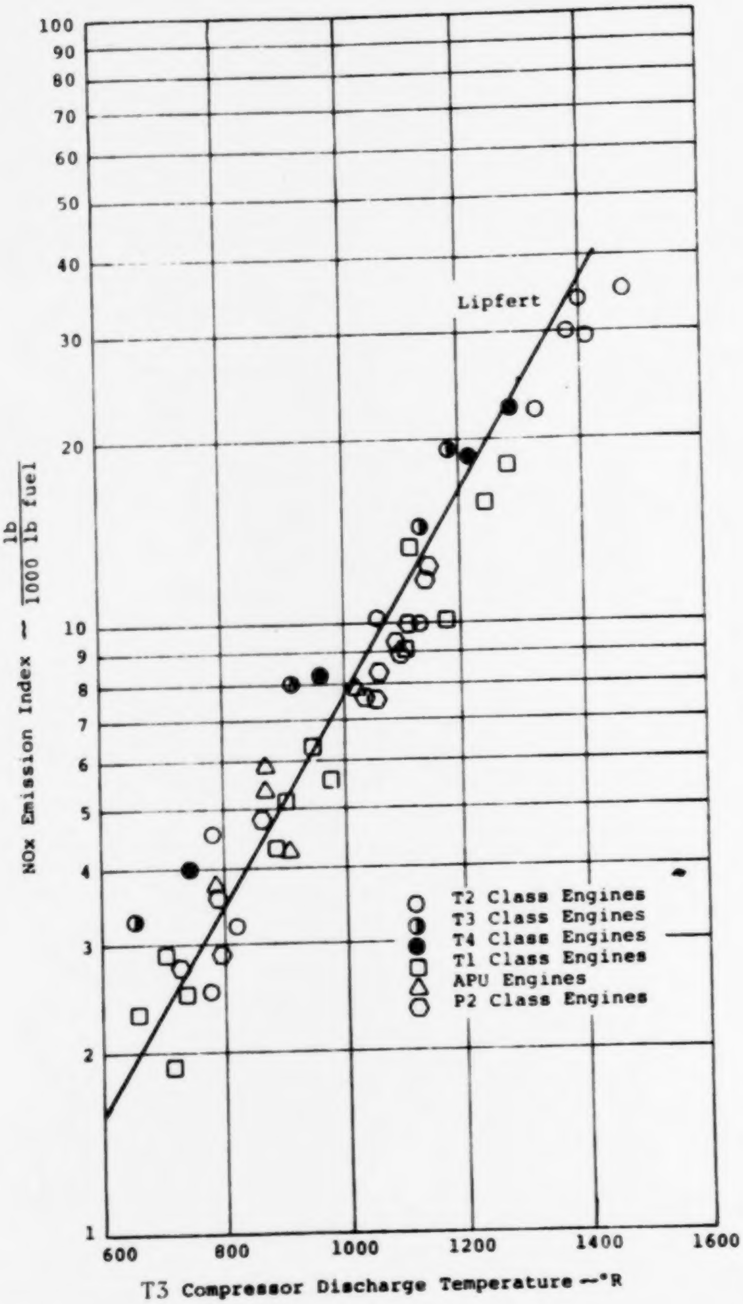

Figure 32 NOX EMISSIONS INDEX AS A FUNCTION OF COMPRESSOR DISCHARGE TEMPERATURE PRODUCTION ENGINES (REFERENCE 13)

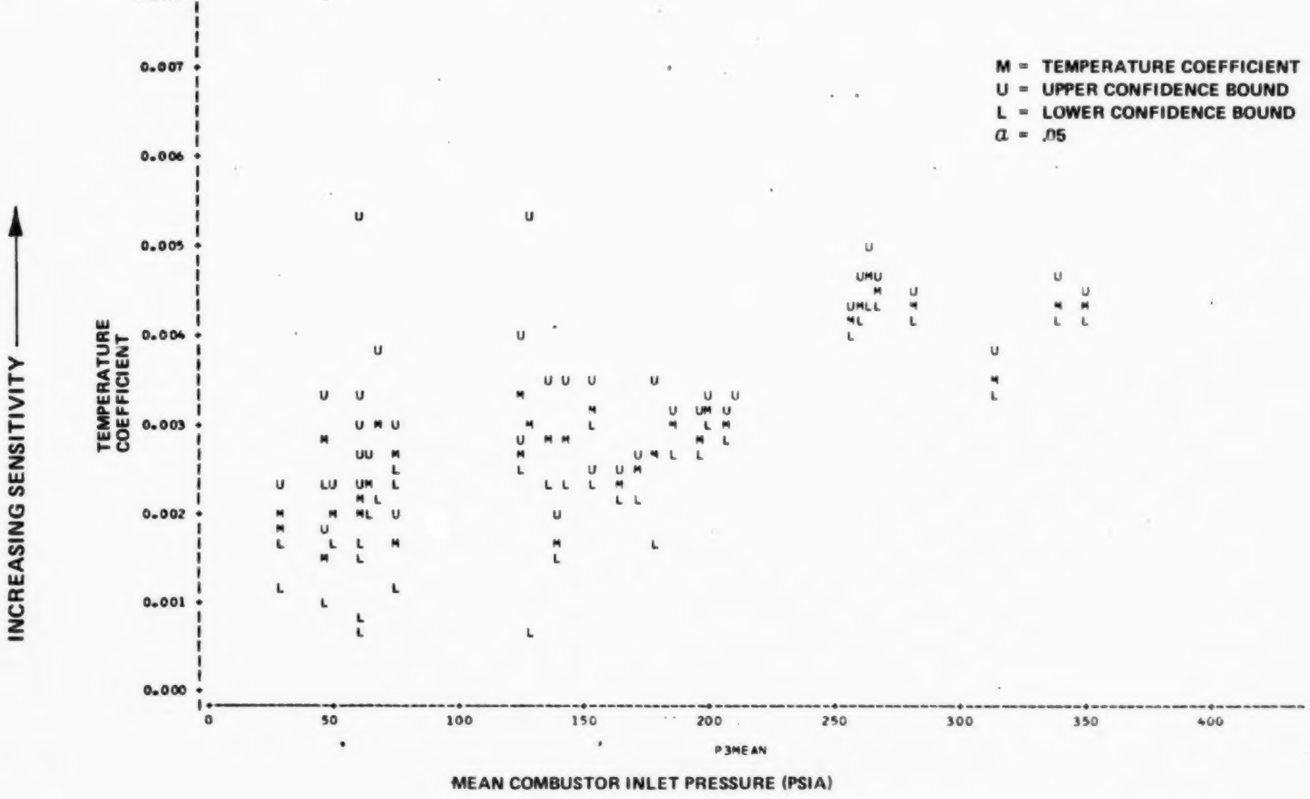

Figure 33 NOX TEMPERATURE COEFFICIENT VERSUS COMBUSTOR INLET PRESSURE P3MEAN - CONFIDENCE BOUNDS

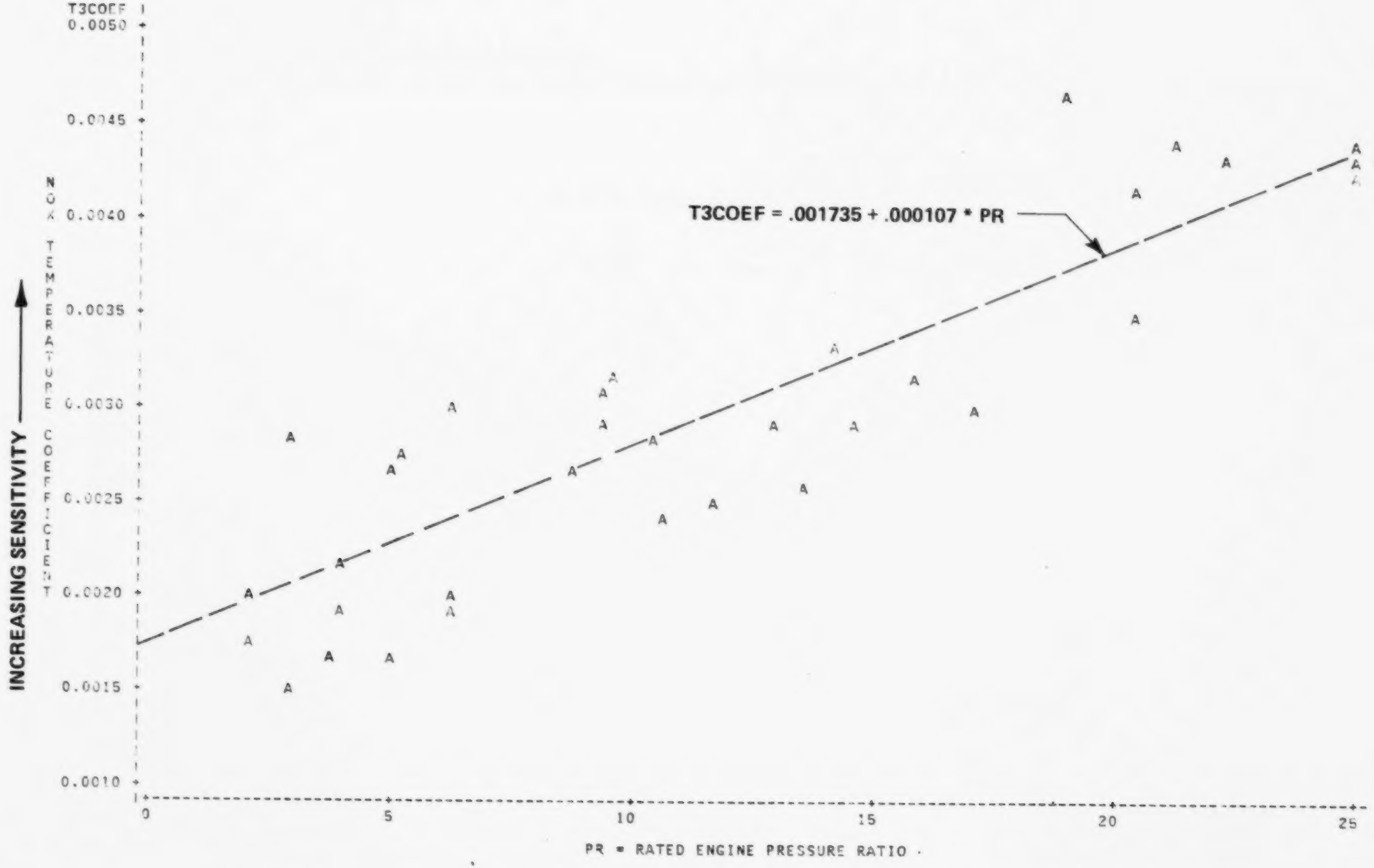

Figure 34 NOX COMBUSTOR INLET TEMPERATURE COEFFICIENT T3COEF VERSUS RATED ENGINE PRESSURE RATIO PR

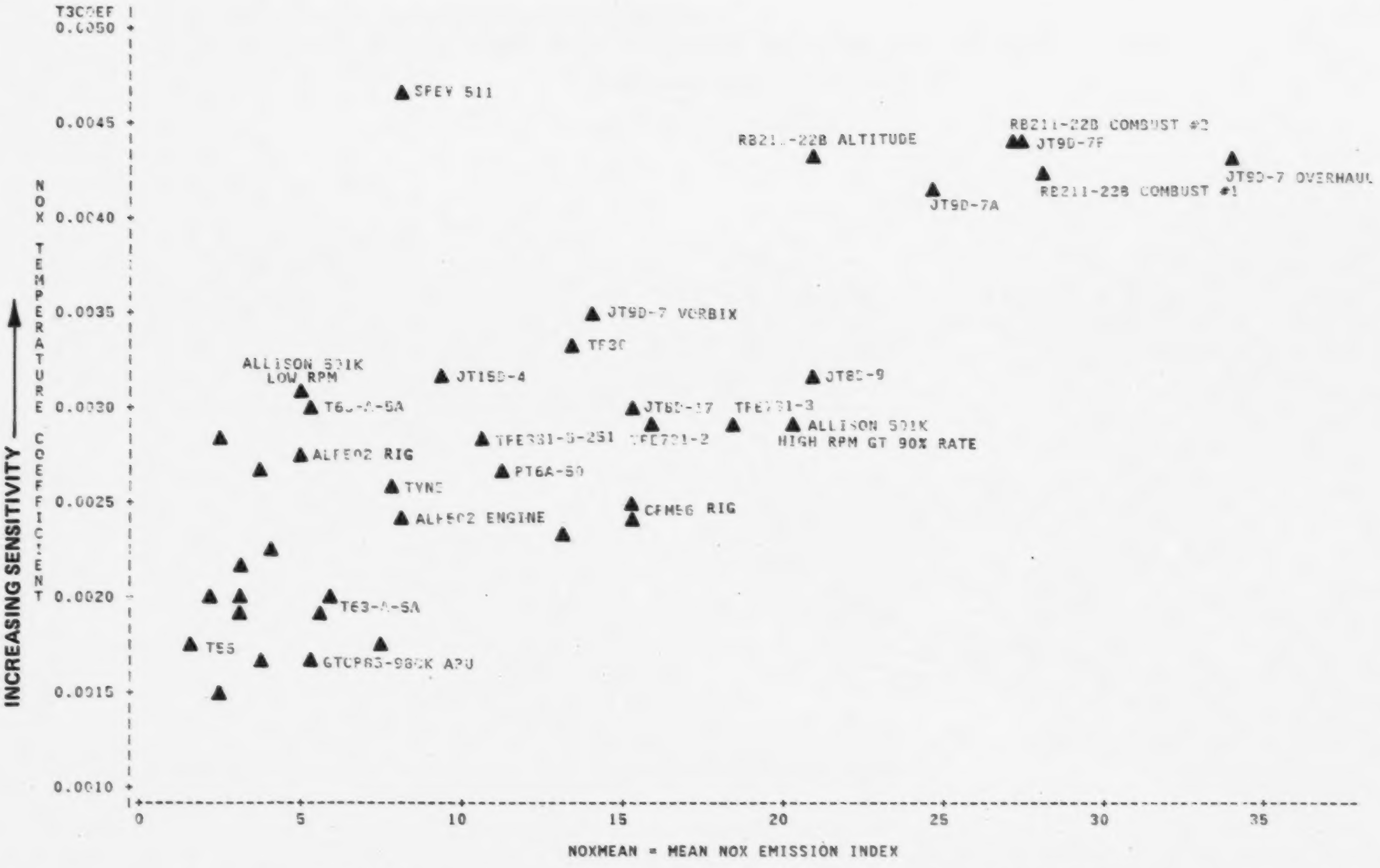

Figure 35 NOX COMBUSTOR INLET TEMPERATURE COEFFICIENT T3COEF VERSUS MEAN NOX EMISSION INDEX NOXMEAN

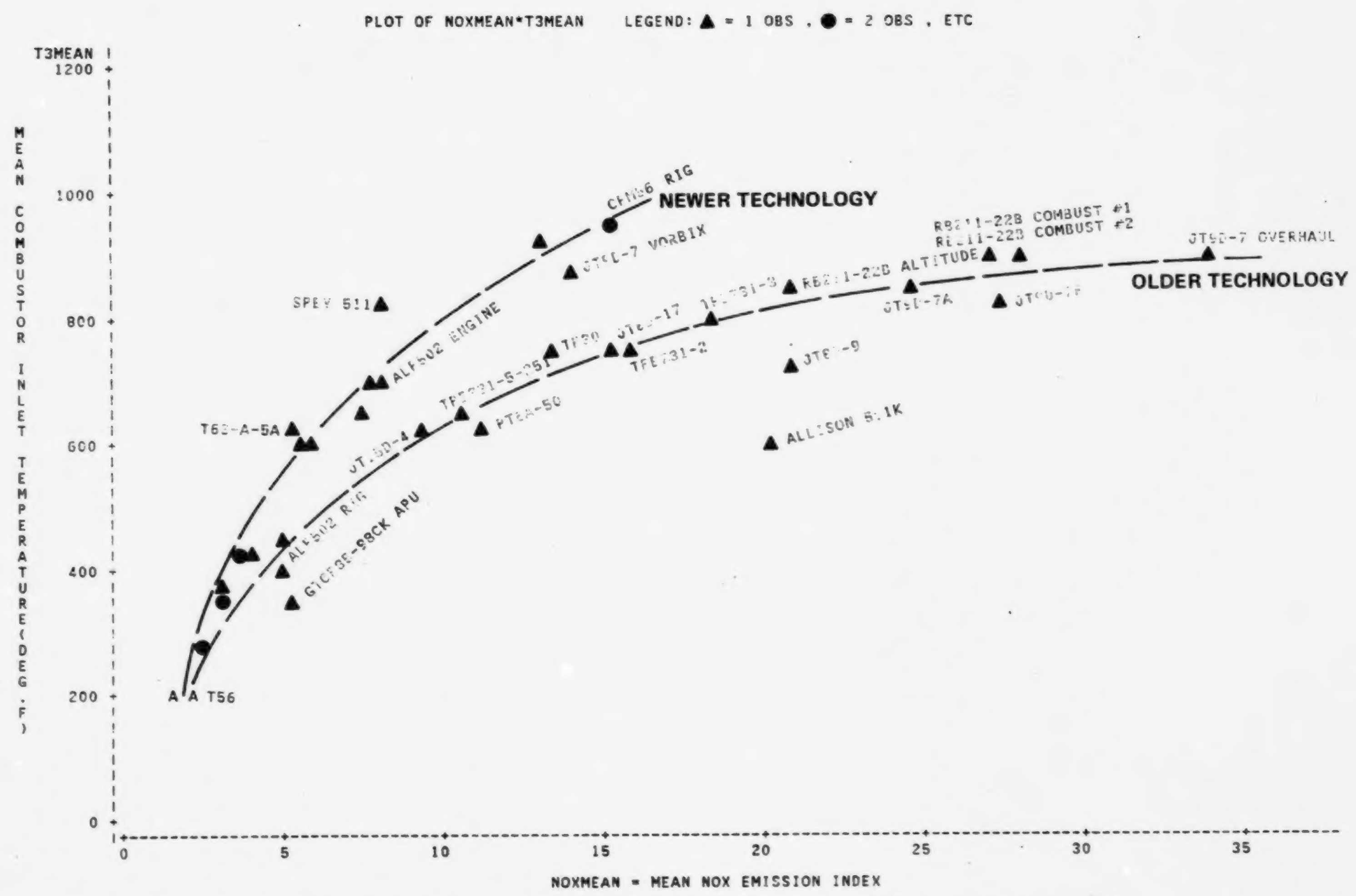

Figure 36 MEAN NOX COMBUSTOR INLET TEMPERATURE T3MEAN VERSUS MEAN NOX EMISSION INDEX NOXMEAN

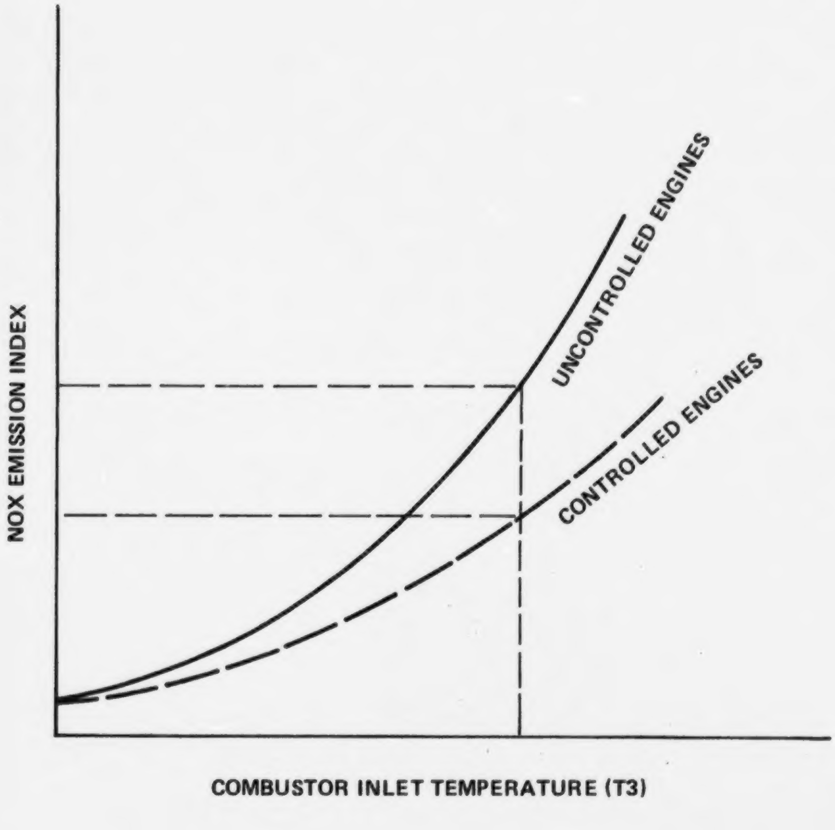

Figure 37 NOX EMISSION INDEX VERSUS COMBUSTOR INLET TEMPERATURE - UNCONTROLLED AND CONTROLLED ENGINES

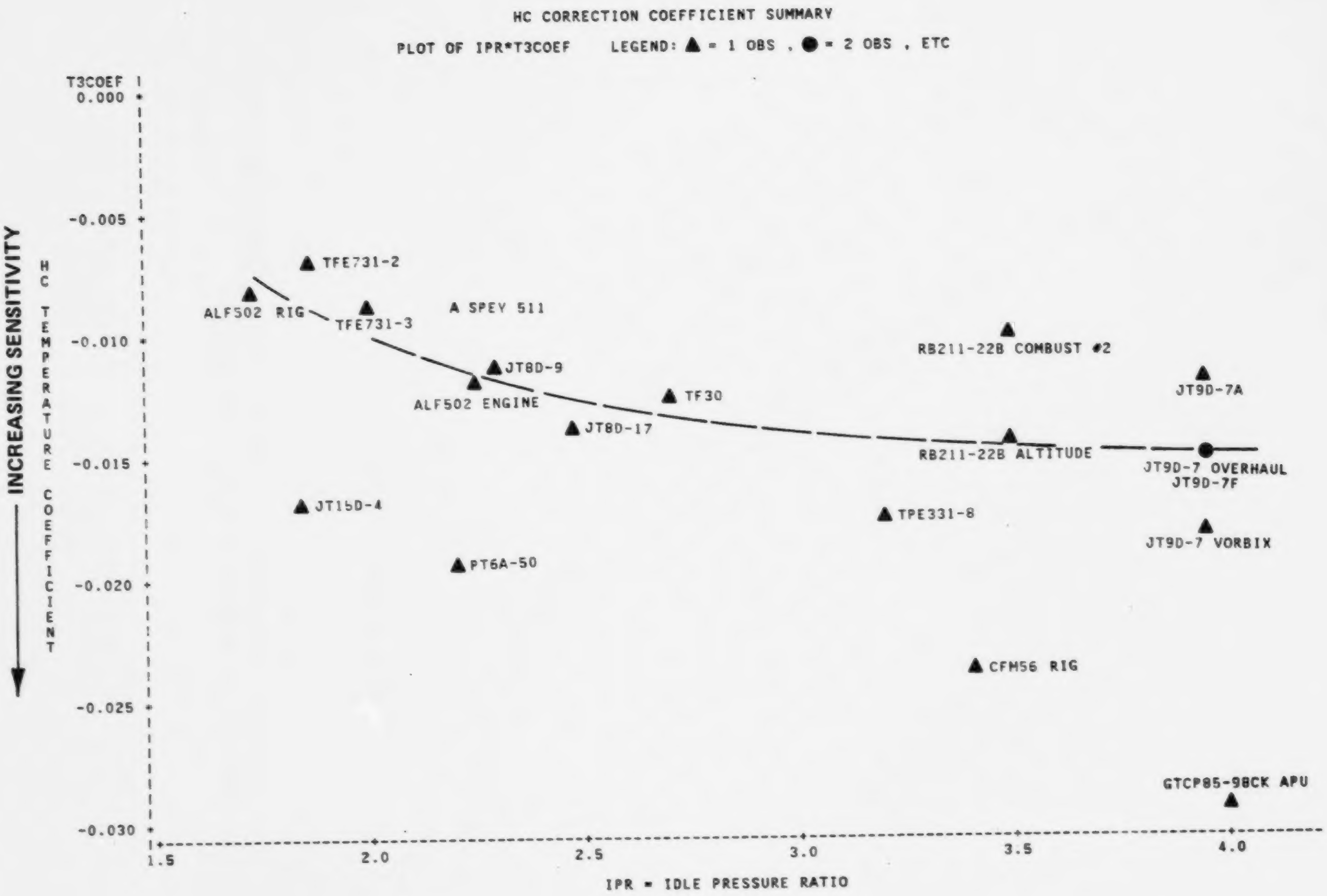

Figure 38 HC COMBUSTOR INLET TEMPERATURE COEFFICIENT T3COEF VERSUS ENGINE IDLE PRESSURE RATIO IPR

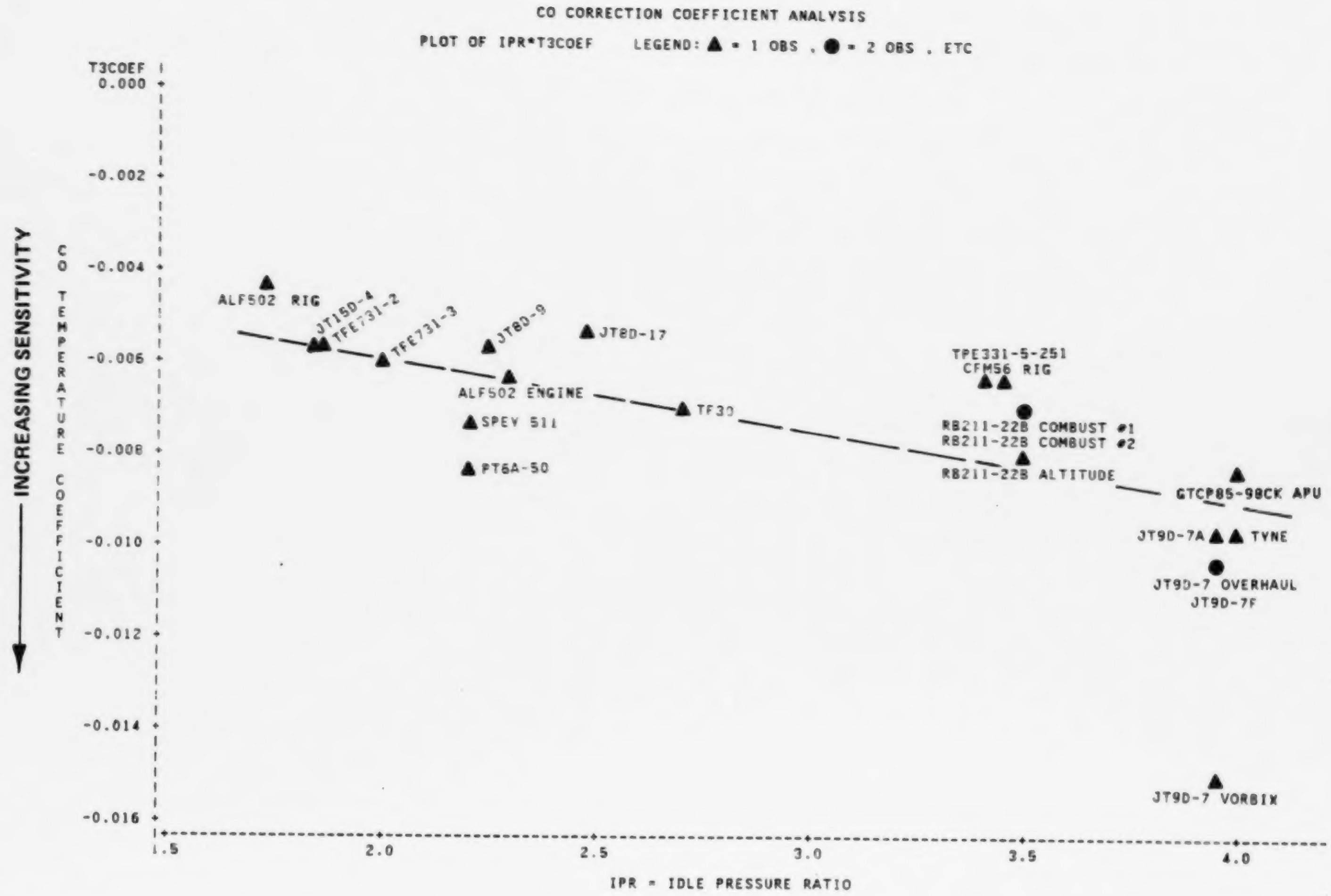

Figure 39 CO COMBUSTOR INLET TEMPERATURE COEFFICIENT T3COEF VERSUS ENGINE IDLE PRESSURE RATIO IPR

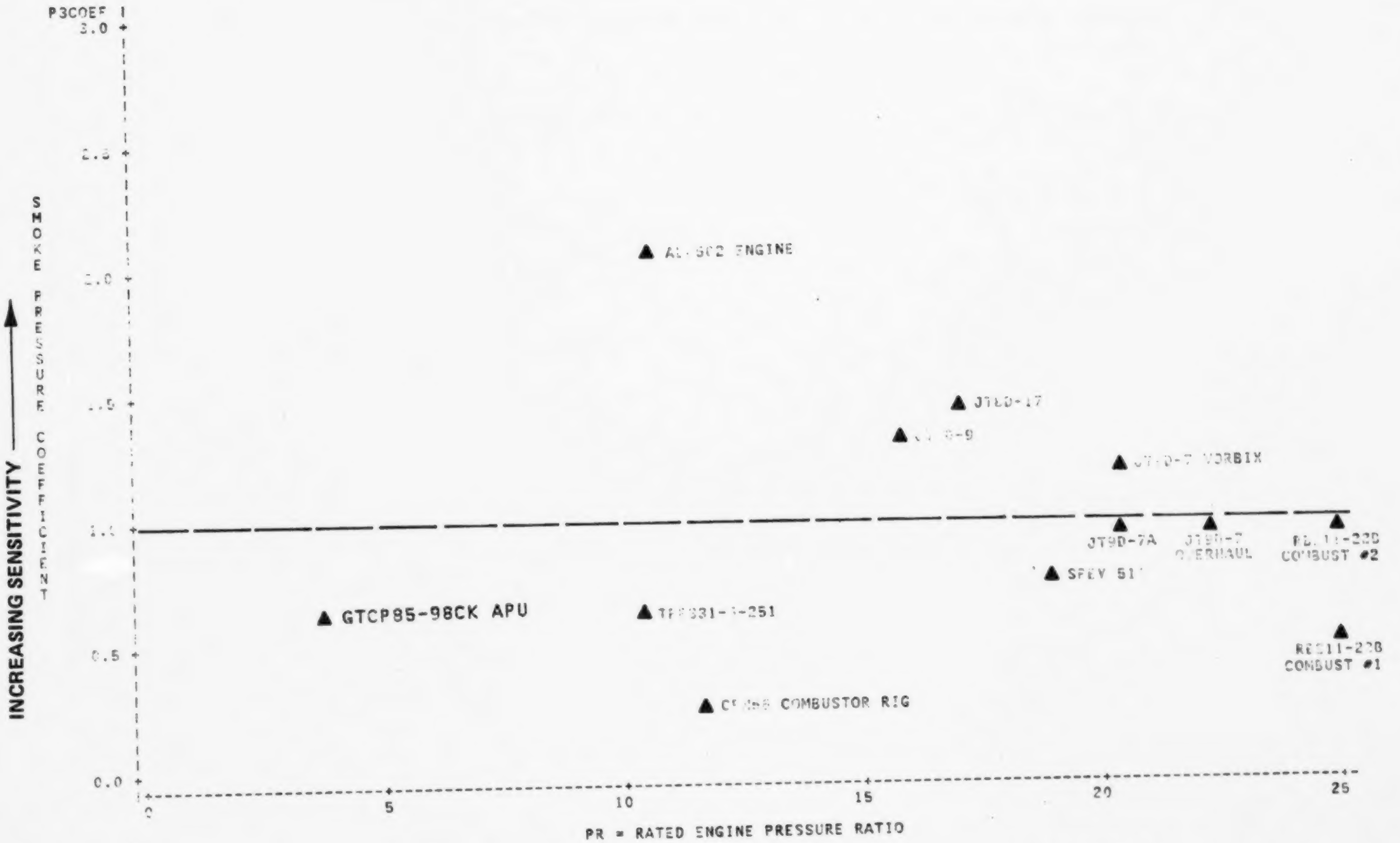

Figure 40 SMOKE NUMBER COMBUSTOR INLET PRESSURE COEFFICIENT P3COEF VERSUS RATED ENGINE PRESSURE RATIO PR

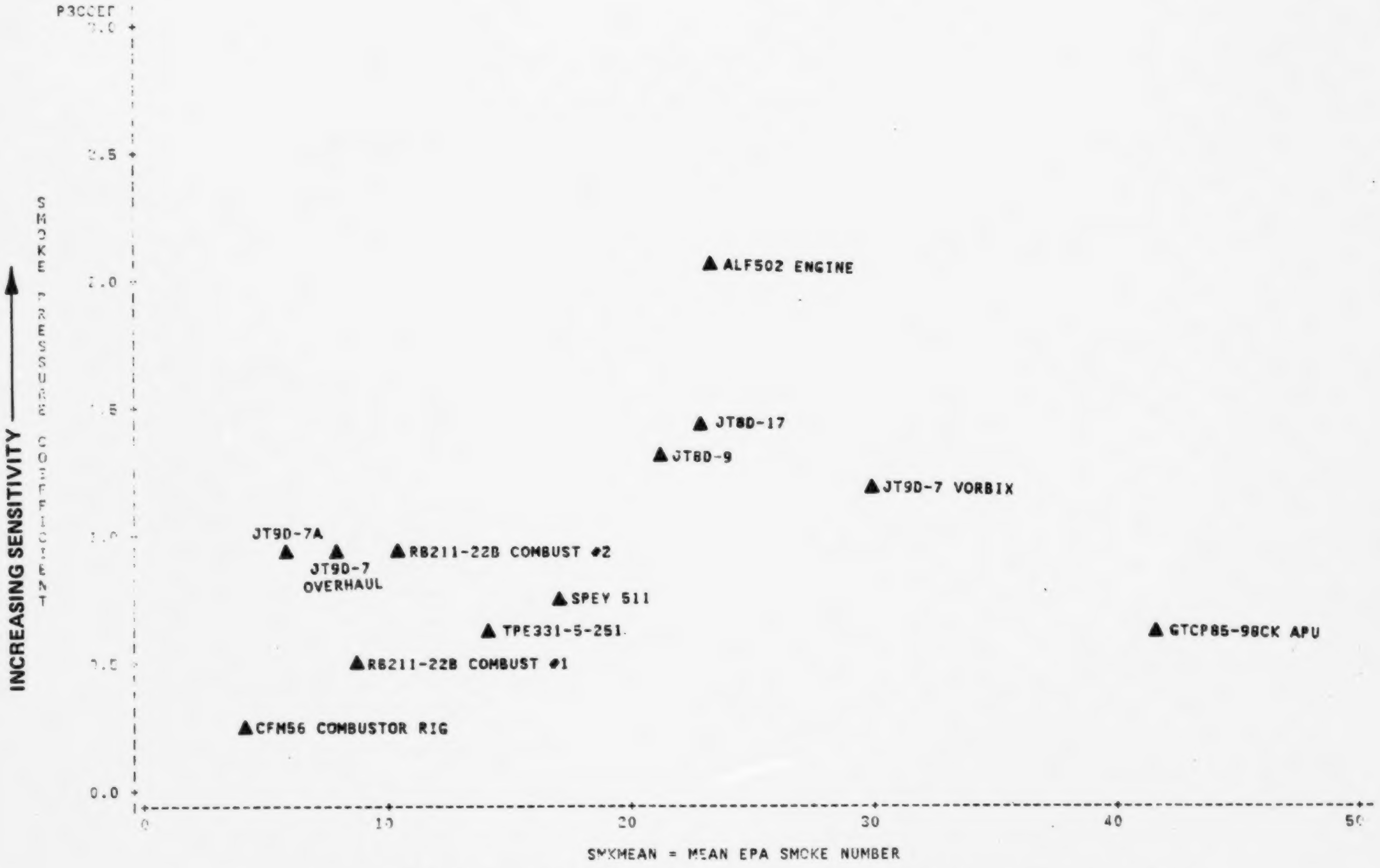

Figure 41 SMOKE NUMBER COMBUSTOR INLET PRESSURE COEFFICIENT P3COEF VERSUS MEAN SMOKE NUMBER SMKMEAN

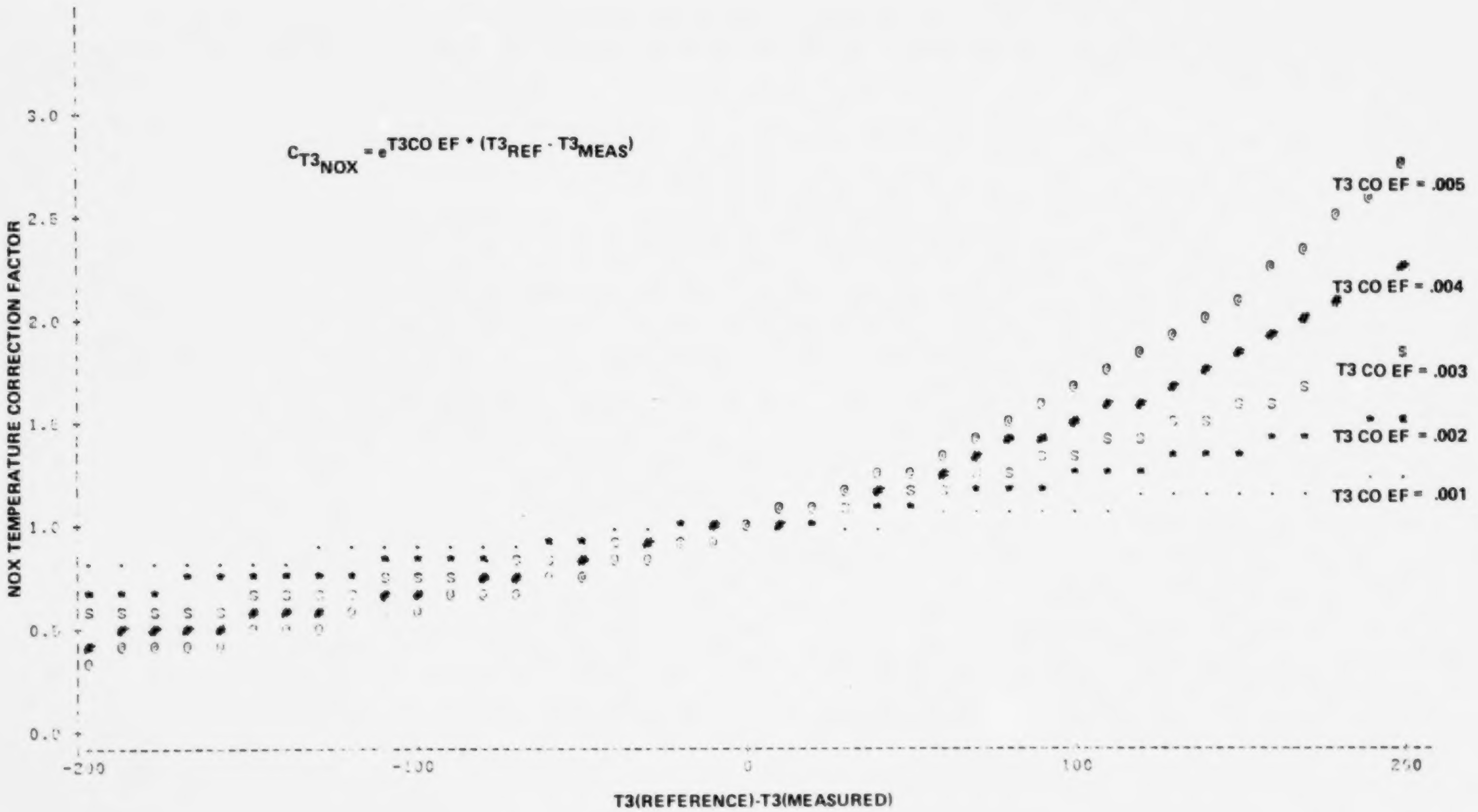

Figure 42 NOX TEMPERATURE CORRECTION FACTORS

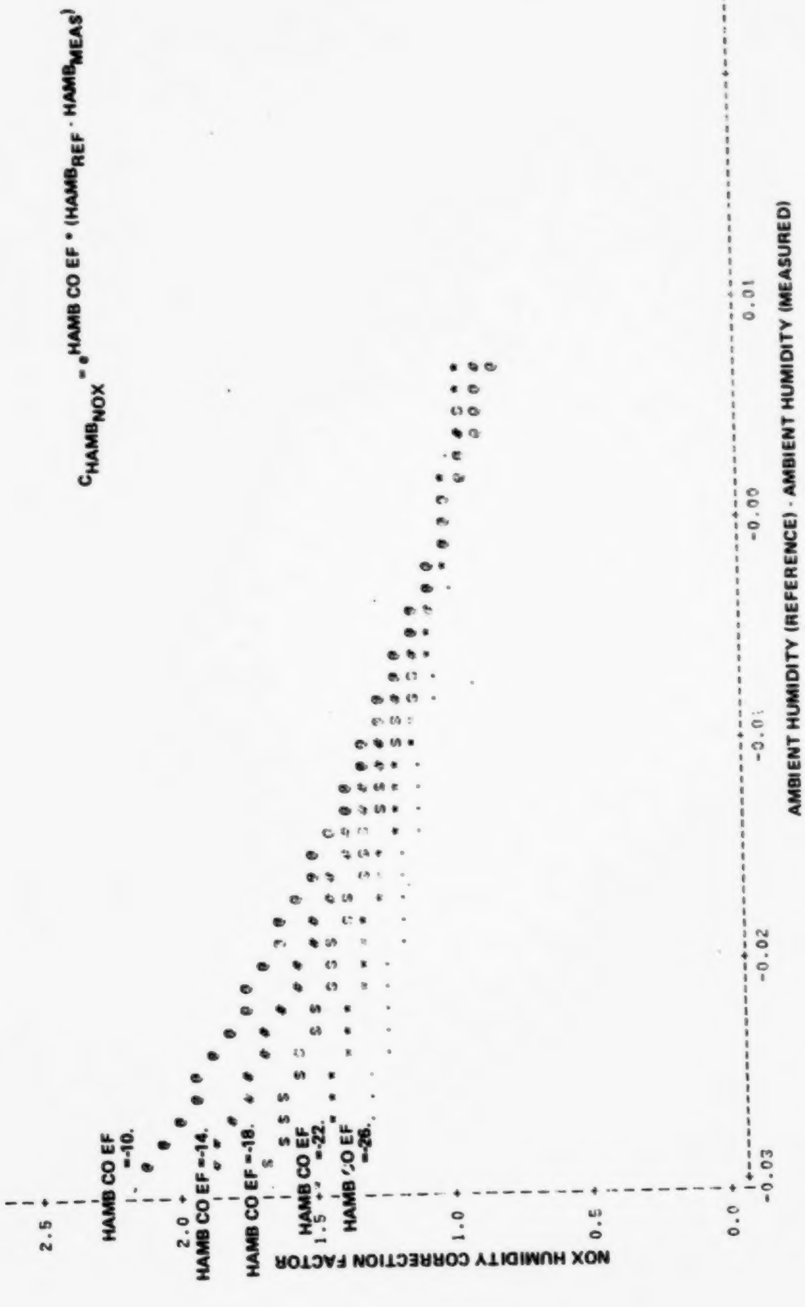

Figure 43 NOX HUMIDITY CORRECTION FACTORS

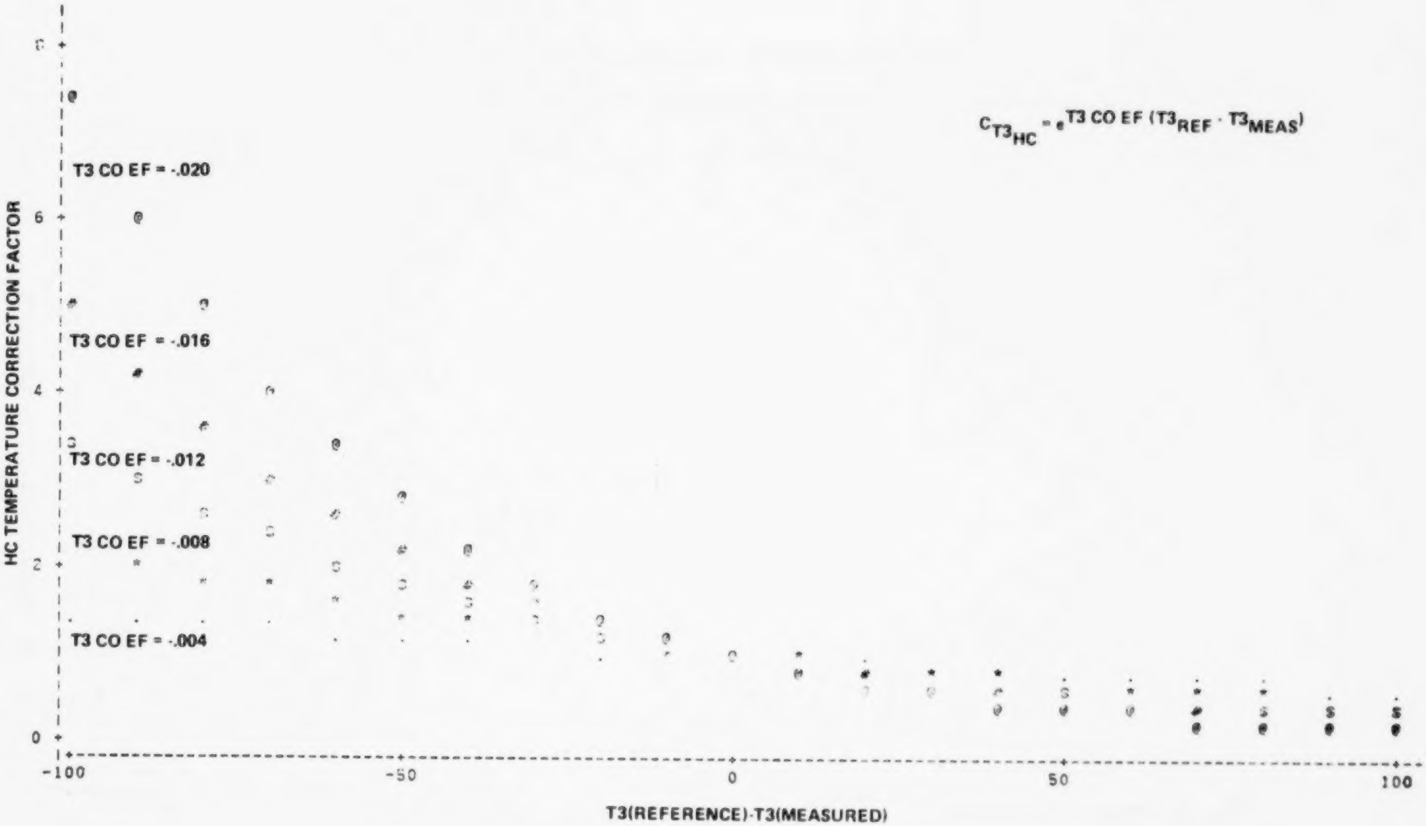

$C_{T3_{HC}} = e^{T3\,CO\,EF\,(T3_{REF} - T3_{MEAS})}$

Figure 44 HC TEMPERATURE CORRECTION FACTORS

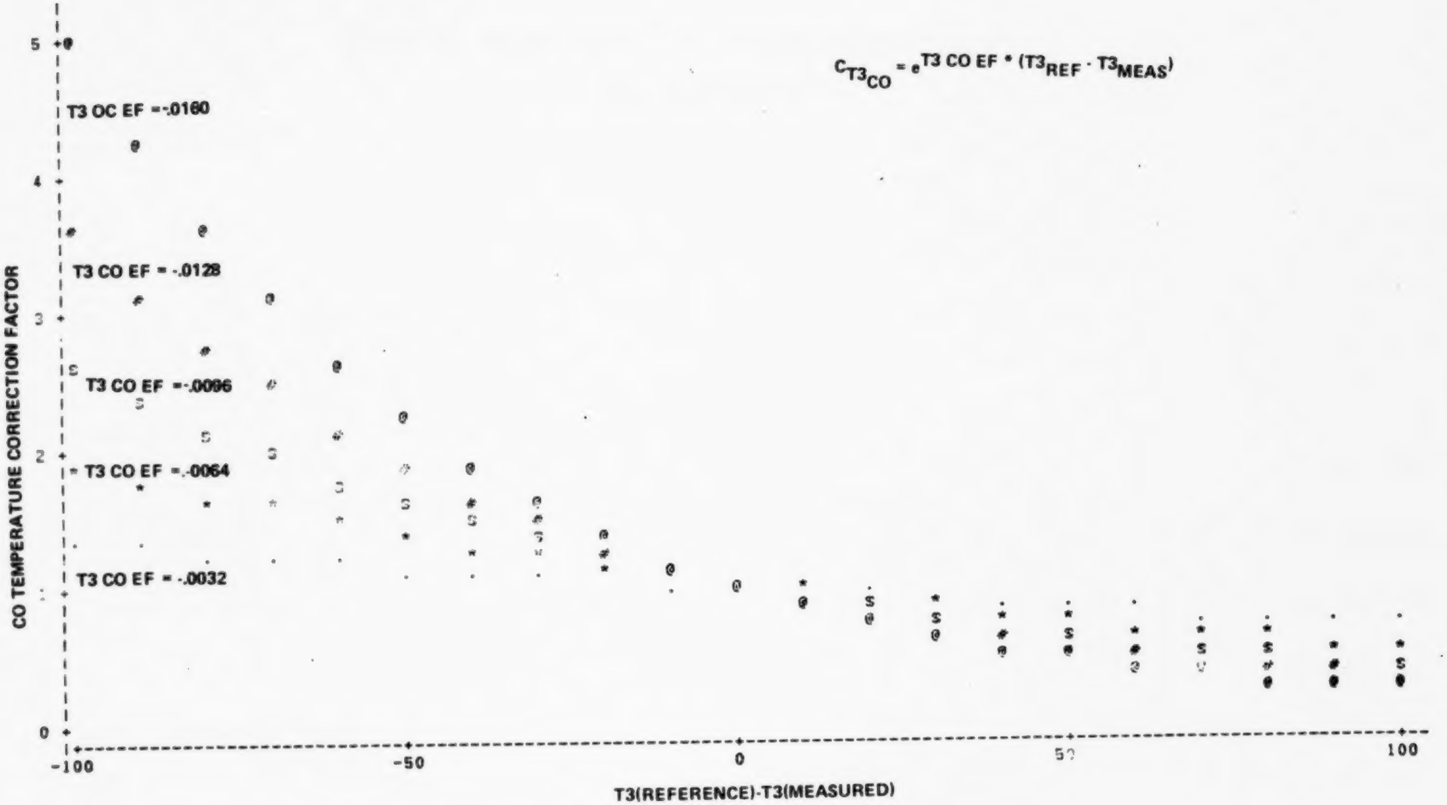

Figure 45 CO TEMPERATURE CORRECTION FACTORS

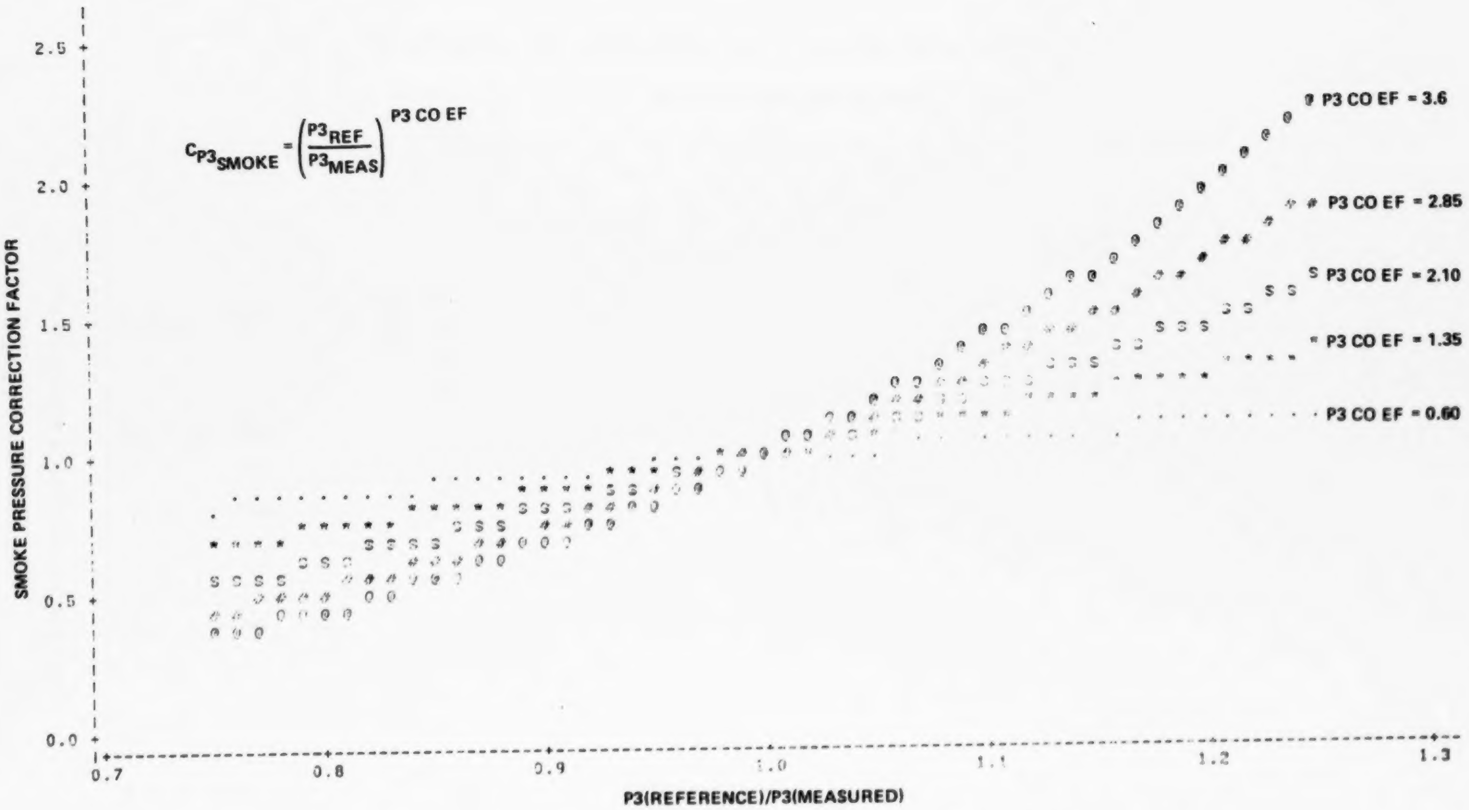

Figure 46 SMOKE PRESSURE CORRECTION FACTORS

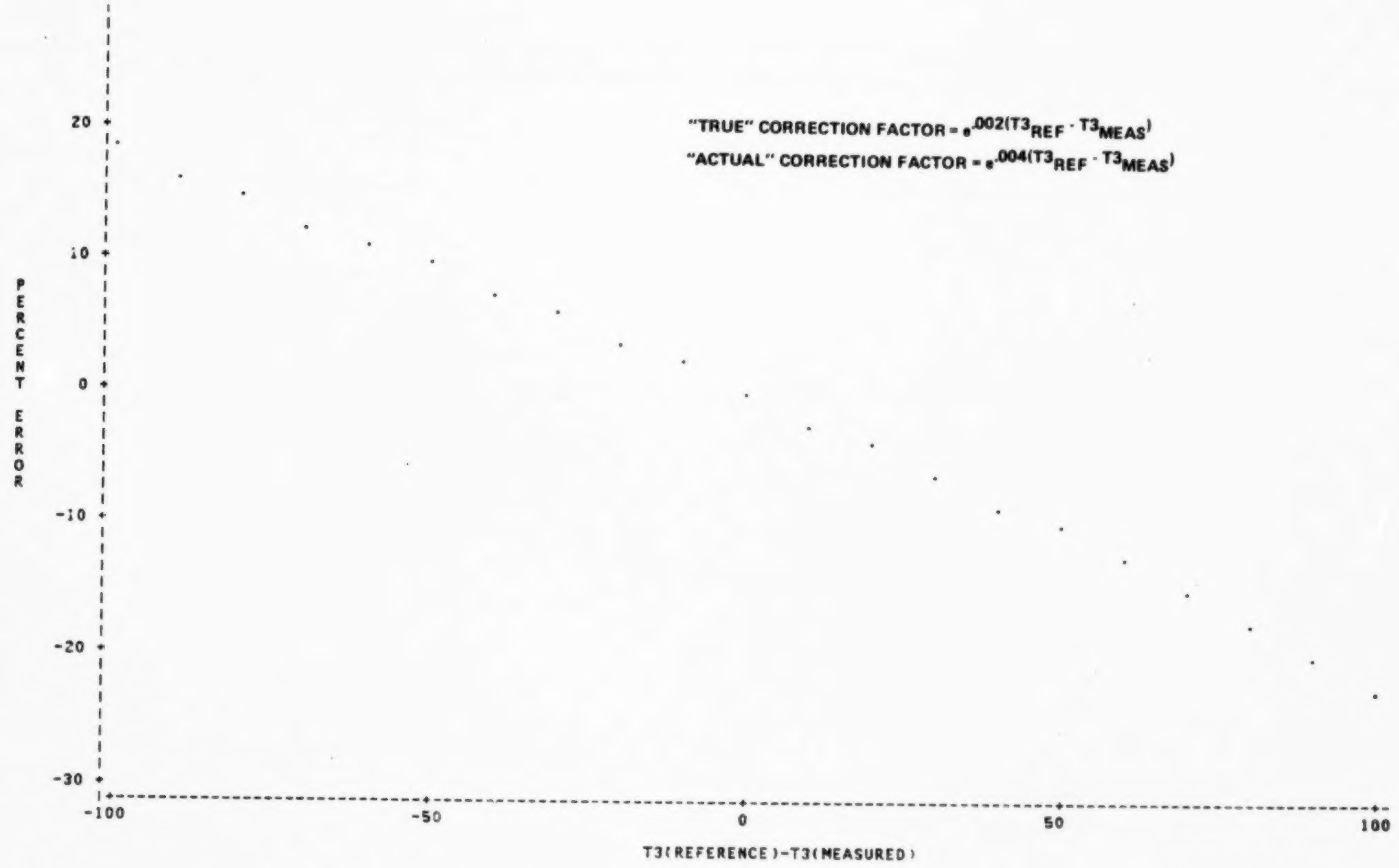

Figure 47 CORRECTION FACTOR SENSITIVITY ANALYSIS NOX TEMPERATURE CORRECTION PERCENT ERROR = ((TRUE CORRECTION - ACTUAL CORRECTION)/TRUE CORRECTION)*100

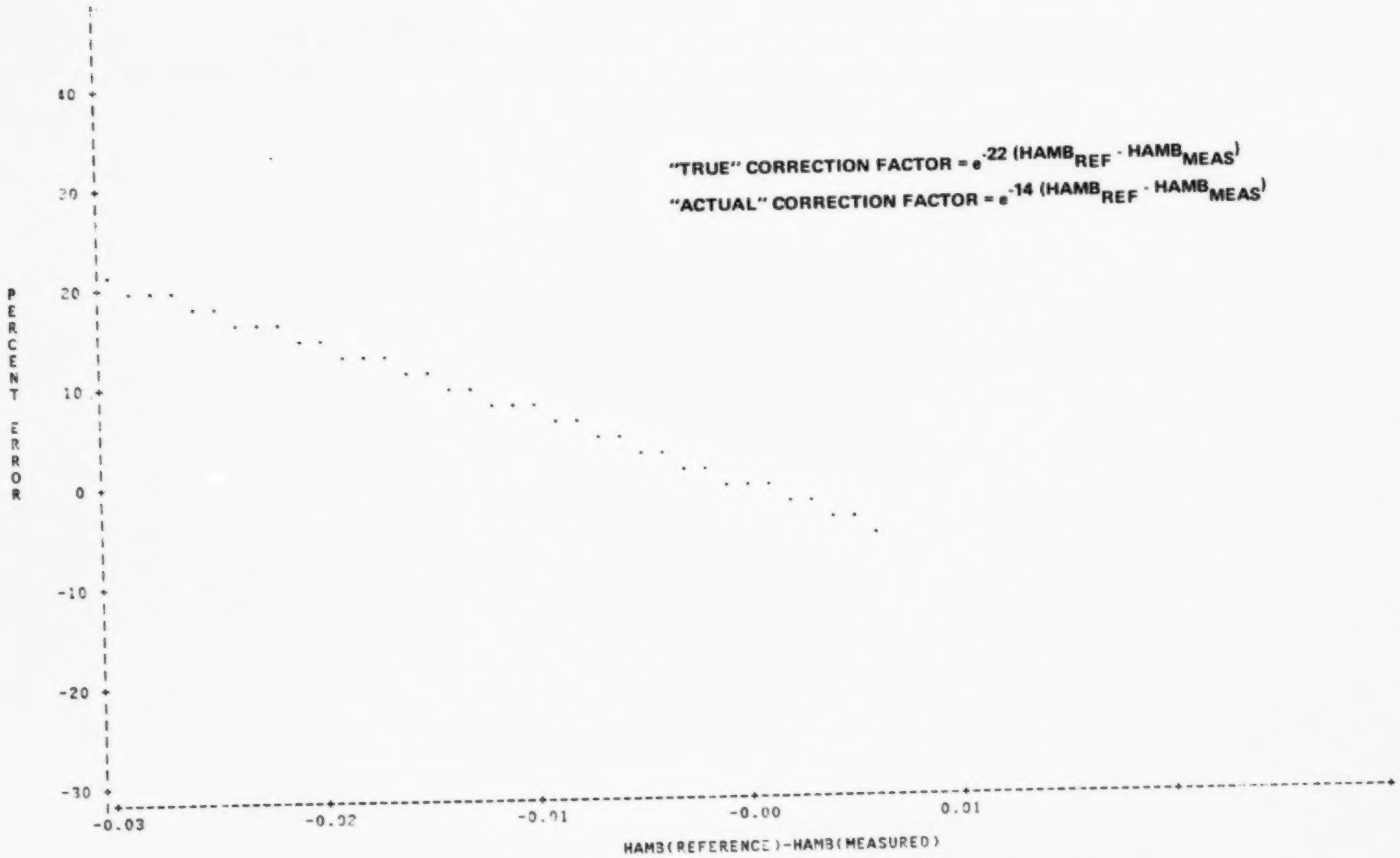

"TRUE" CORRECTION FACTOR = $e^{-22\,(HAMB_{REF}\,-\,HAMB_{MEAS})}$

"ACTUAL" CORRECTION FACTOR = $e^{-14\,(HAMB_{REF}\,-\,HAMB_{MEAS})}$

Figure 48 CORRECTION FACTOR SENSITIVITY ANALYSIS NOX HUMIDITY CORRECTION PERCENT ERROR = ((TRUE CORRECTION-ACTUAL CORRECTION)/TRUE CORRECTION)*100

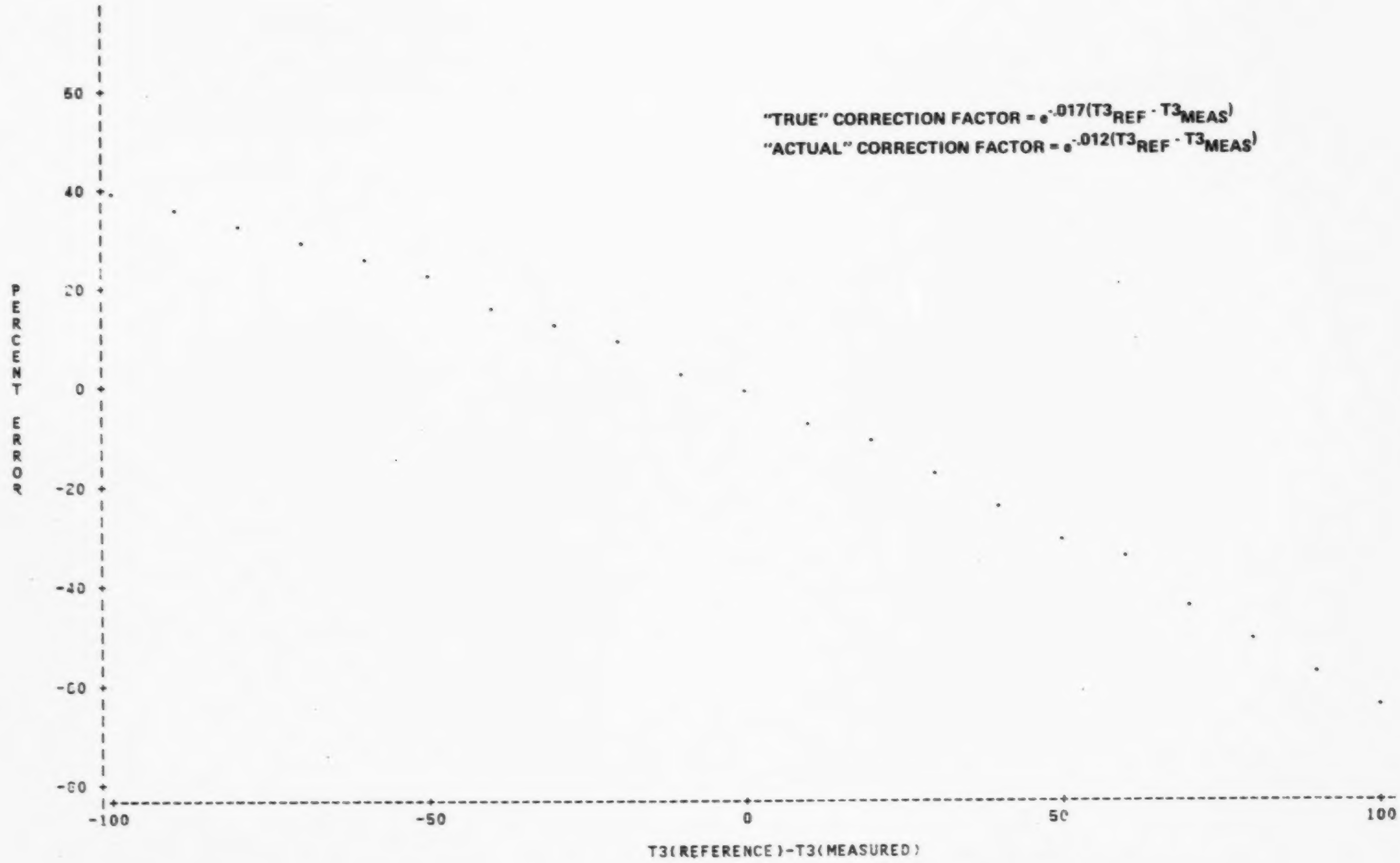

Figure 49 CORRECTION FACTOR SENSITIVITY ANALYSIS HC TEMPERATURE CORRECTION PERCENT ERROR = ((TRUE CORRECTION-ACTUAL CORRECTION)/TRUE CORRECTION)*100

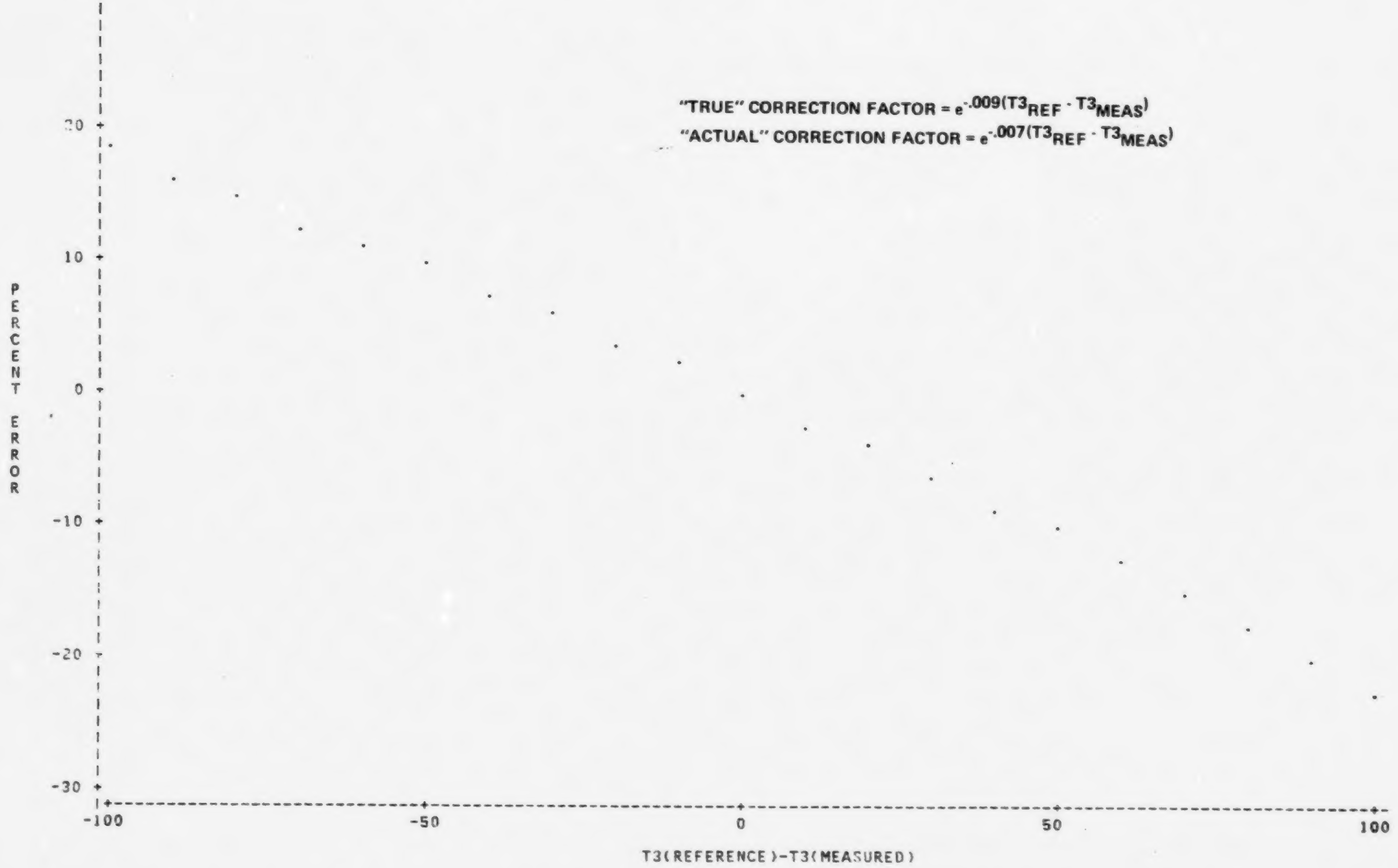

Figure 50 CORRECTION FACTOR SENSITIVITY ANALYSIS CO TEMPERATURE CORRECTION PERCENT ERROR = ((TRUE CORRECTION-ACTUAL CORRECTION)/TRUE CORRECTION)*100

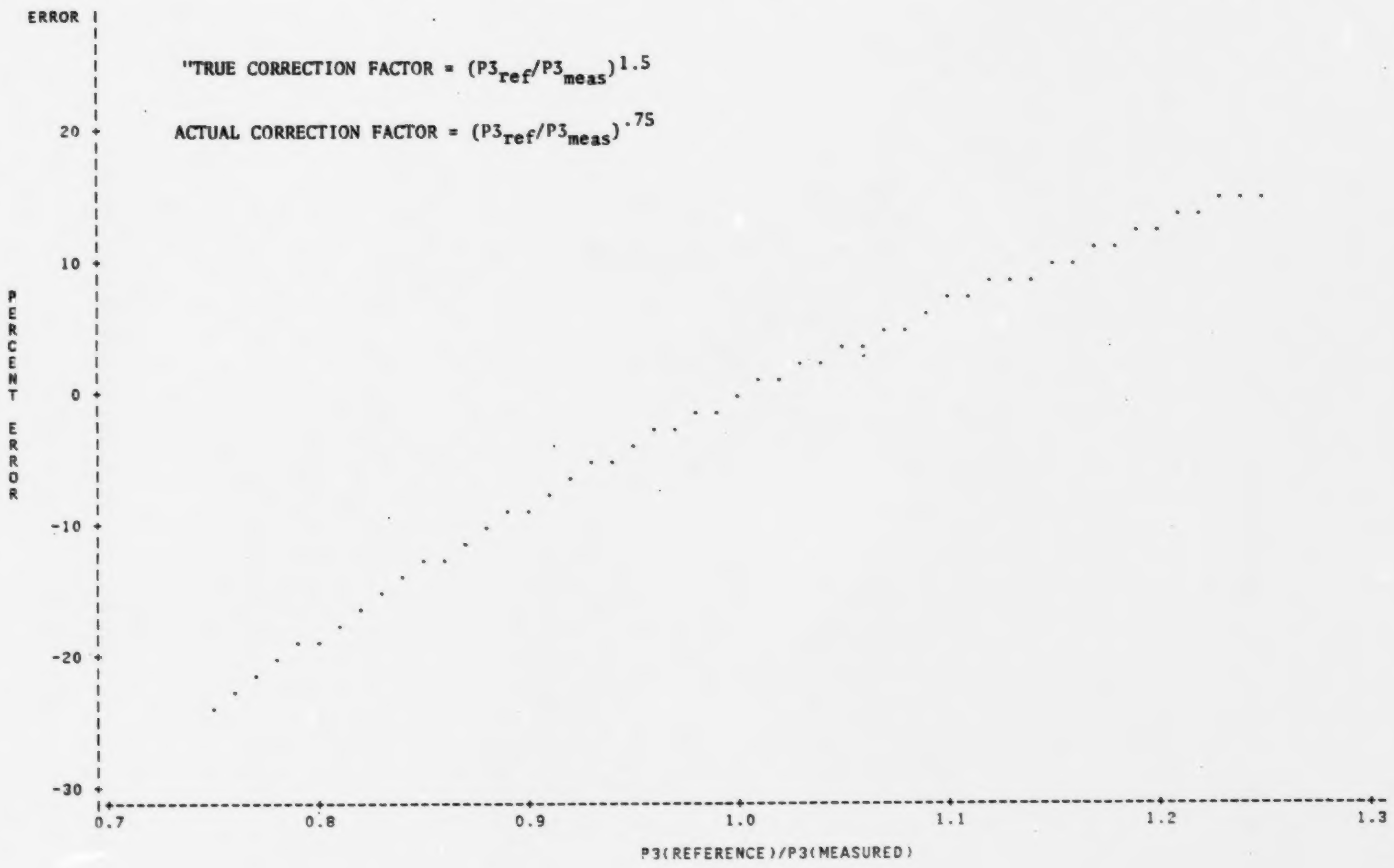

Figure 51 CORRECTION FACTOR SENSITIVITY ANALYSIS SMOKE PRESSURE CORRECTION PERCENT ERROR = ((TRUE CORRECTION-ACTUAL CORRECTION)/TRUE CORRECTION)*100

ENGINE	MODE	UNCORRECTED CV (%)	CORRECTED CV (%)			
			Specific Engine Coefficient		General Coefficient	
				% Reduction		% Reduction
CFM56 RIG	IDLE	15	6	60	6	60
	1.5 IDLE	18	5	72	7	61
	APPROACH	16	7	56	10	35
	CLIMB	18	5	72	6	67
	TAKEOFF	19	5	74	6	68
ALF502 RIG	IDLE	13	4	69	3	77
	1.5 IDLE	13	3	77	3	77
	APPROACH	11	4	64	3	73
		15	5	68	6	65

CV = Coefficient of Variation = $\frac{\sigma}{\mu}$

where σ = standard deviation

μ = mean value

Figure 52 NOX AMBIENT EFFECTS CORRECTION SUMMARY

ENGINE	MODE	UNCORRECTED CV (%)	CORRECTED CV (%)			
			Specific Engine Coefficient		General Coefficient	
				% Reduction		% Reduction
CFM56 RIG	IDLE	98	34	65	31	68
ALF502 RIG	IDLE	48	18	62	20	58
	1.5 IDLE	36	23	36	24	33
		61	25	54	25	53

$$CV = \text{Coefficient of Variation} = \frac{\sigma}{\mu}$$

where σ = standard deviation

μ = mean value

Figure 53 HC AMBIENT EFFECTS CORRECTION SUMMARY

ENGINE	MODE	UNCORRECTED CV (%)	CORRECTED CV (%)			
			Specific Engine Coefficient		General Coefficient	
				% Reduction		% Reduction
CFM56 RIG	IDLE	25	12	52	19	24
	1.5 IDLE	23	15	35	24	-4
ALF502 RIG	IDLE	23	6	74	7	70
	1.5 IDLE	15	6	60	8	47
	APPROACH	20	10	50	11	45
		21	10	54	14	36

CV = Coefficient of Variation = $\frac{\sigma}{\mu}$

where σ = standard deviation

μ = mean value

Figure 54 CO AMBIENT EFFECTS CORRECTION SUMMARY

ENGINE	MODE	UNCORRECTED CV (%)	CORRECTED CV (%)			
			Specific Engine Coefficient		General Coefficient	
				% Reduction		% Reduction
ALF502	IDLE	79	76	4	78	1
	1.5 IDLE	90	83	8	87	3
	APPROACH	31	26	16	28	10
		67	62	9	64	5

$$CV = \text{Coefficient of Variation} = \frac{\sigma}{\mu}$$

where σ = standard deviation

μ = mean value

Figure 55 **SMOKE AMBIENT EFFECTS CORRECTION SUMMARY**

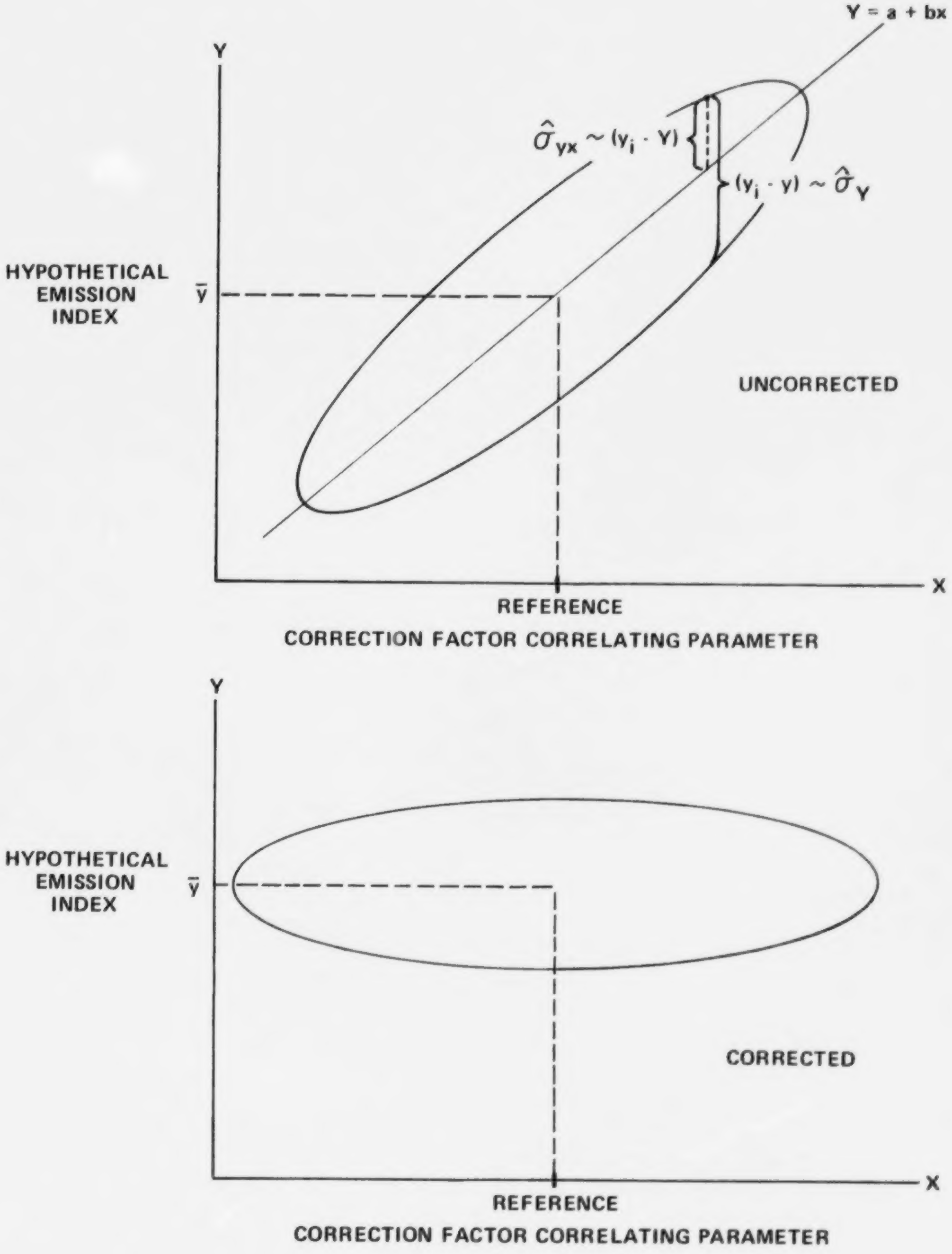
Y = a + bx
Y
$\hat{\sigma}_{yx} \sim (y_i - Y)$
$(y_i - y) \sim \hat{\sigma}_Y$
HYPOTHETICAL EMISSION INDEX
$\bar{y}$
UNCORRECTED
X
REFERENCE
CORRECTION FACTOR CORRELATING PARAMETER
Y
HYPOTHETICAL EMISSION INDEX
$\bar{y}$
CORRECTED
X
REFERENCE
CORRECTION FACTOR CORRELATING PARAMETER

Figure 56 HYPOTHETICAL EMISSION INDEX CORRECTION

APPENDICES

APPENDIX A

DATA BASE SUMMARY

ENGINE SUMMARY BY CLASS

ENGINE	CLASS	TESTS	SOURCE	SMOKE	MODES	COMMENTS
ALF502	T1	56	AVCO (EPA SPONSORED DATA)	Y	IDLE TO TAKEOFF	LIMITED HUMIDITY VARIATION
ALF502 RIG	T1	66	AVCO (EPA SPONSORED DATA)	Y	IDLE TO APPROACH	NONSTANDARD AIR FLOW AT IDLE & 1.5 IDLE
JT15D-4	T1	12	PRATT & WHITNEY CANADA	N	IDLE TO TAKEOFF	.
TFE731-2	T1	53	GARRETT	N	IDLE TO TAKEOFF	.
TFE731-3	T1	28	GARRETT	N	IDLE TO TAKEOFF	.
CFM56 RIG	T2	214	GE (EPA SPONSORED DATA)	Y	IDLE TO TAKEOFF	REDUCED P3 AT TAKEOFF
JT9D-7A	T2	181	PRATT & WHITNEY	Y	IDLE TO TAKEOFF	PILOT LOT DATA
JT9D-7F	T2	94	PRATT & WHITNEY	Y	IDLE TO TAKEOFF	PILOT LOT DATA
JT9D-7 OVERHAUL	T2	114	BRITISH MINISTRY OF DEFENCE	Y	IDLE TO TAKEOFF	BRITISH ENGINE OVERHAUL LTD.
JT9D-7 VORBIX	T2	86	NASA CLEAN COMBUSTOR PROGRAM	Y	IDLE TO TAKEOFF	MODEL 27E, PILOT FA ABOVE/BELOW 0.009
RB211-22B COMBUST #1	T2	52	ROLLS-ROYCE (SEA LEVEL DATA)	Y	IDLE TO TAKEOFF	LIMITED HUMIDITY RANGE
RB211-22B COMBUST #2	T2	16	ROLLS-ROYCE (SEA LEVEL DATA)	Y	IDLE TO TAKEOFF	LIMITED HUMIDITY RANGE
RB211-22B	T2	21	ROLLS-ROYCE (ALTITUDE DATA)	N	IDLE TO TAKEOFF	10700 METER SIMULATED ALTITUDE
SPEY 511	T2	152	ROLLS-ROYCE	Y	IDLE TO TAKEOFF	.
TF30	T2	194	ALLEN-SLUSHER FAA DATA	N	IDLE TO TAKEOFF	FIXED AREA EXHAUST REPLACES AFTERBURNER
JT8D-9	T4	137	PRATT & WHITNEY	Y	IDLE TO TAKEOFF	PILOT LOT DATA
JT8D-17	T4	85	PRATT & WHITNEY	Y	IDLE TO TAKEOFF	PILOT LOT DATA
ALLISON 501K	P2	81	DETROIT DIESEL ALLISON	Y	10500 RPM,13800 RPM	STATIONARY GAS TURBINE
PT6A-50	P2	15	PRATT & WHITNEY CANADA	N	IDLE TO TAKEOFF	.
TPE331-5-251	P2	336	GARRETT (EPA SPONSORED DATA)	Y	IDLE TO TAKEOFF	WATER(HUMIDITY) NOT FULLY VAPORIZED
TPE331-8	P2	31	GARRETT	N	IDLE TO TAKEOFF	.
TYNE	P2	28	ROLLS ROYCE	Y	IDLE TO CLIMB	.
T56 RIG STANDARD	P2	110	USAF AFAPL (JP4 ,TEMPERATURE)	N	IDLE	PARAMETRIC RIG TEST
T56 RIG LEAN	P2	64	USAF AFAPL (JP4 ,TEMPERATURE)	N	IDLE	PARAMETRIC RIG TEST
T56 RIG RICH	P2	16	USAF AFAPL (JP4 ,TEMPERATURE)	N	IDLE	PARAMETRIC RIG TEST
T56 RIG STANDARD	P2	64	USAF AFAPL (JETA,TEMPERATURE)	N	IDLE	PARAMETRIC RIG TEST
T56 RIG LEAN	P2	64	USAF AFAPL (JETA,TEMPERATURE)	N	IDLE	PARAMETRIC RIG TEST
T56 RIG STANDARD	P2	84	USAF AFAPL (JP4 ,PRESSURE)	N	IDLE	PARAMETRIC RIG TEST
T56 RIG RICH	P2	24	USAF AFAPL (JP4 ,PRESSURE)	N	IDLE	PARAMETRIC RIG TEST
T56 RIG STANDARD	P2	60	USAF AFAPL (JETA,PRESSURE)	N	IDLE	PARAMETRIC RIG TEST
T63-A-5A WALL FILM	P2	9	DETROIT DIESEL ALLISON	Y	N/A	PARAMETRIC RIG TEST
T63-A-5A PRES ATOM	P2	9	DETROIT DIESEL ALLISON	Y	N/A	PARAMETRIC RIG TEST
T63-A-5A AIR BLAST	P2	9	DETROIT DIESEL ALLISON	Y	N/A	PARAMETRIC RIG TEST
GTCP85-98CK	APU	240	GARRETT (EPA SPONSORED DATA)	Y	BLEED+SHAFT,OTHER	WATER(HUMIDITY) NOT FULLY VAPORIZED
GTCP85-98CK	APU	10	GARRETT	N	BLEED+SHAFT	MAXIMUM POWER
GTCP85-98D	APU	8	GARRETT	N	BLEED+SHAFT	MAXIMUM POWER
GTCP85-129	APU	6	GARRETT	N	BLEED+SHAFT	MAXIMUM POWER
GTCP660-4	APU	6	GARRETT	N	BLEED+SHAFT	MAXIMUM POWER
TSCP700-4	APU	6	GARRETT	N	BLEED+SHAFT	MAXIMUM POWER

APPENDIX B

COMBUSTOR INLET CONDITIONS RELATED TO AMBIENT CONDITIONS

The compressor discharge temperature (or the combustor inlet temperature) of a jet engine that corresponds to a particular discharge pressure or pressure ratio depends also upon overall compressor efficiency and inlet temperature to the compressor. Its computation is based upon the definition of overall compressor efficiency, which is the ratio of ideal isentropic change of enthalpy (energy) of the air as it passes through the compressor to its actual change.

Gas tables[1] have been prepared that aid in the computation of discharge enthalpy and the related discharge temperature. Their use for this purpose can be explained best by example using typical values for compressor characteristics:

Given: Pressure ratio = 20

T2 inlet temperature = 580°R

η_c efficiency = 0.85

Procedure: Look up 580°R in the table for air and note the corresponding value for h, enthalpy, and P_r, relative pressure, a computation parameter:

h_2 = 138.66 Btu/lb and P_{r_2} = 1.78

Compute $P_{r_3} = P_{r_2}$ x pressure ratio = 35.6

Look up T3 and h_3 corresponding to P_{r_3},

T3 = 1333°R h_3 = 325.47 Btu/lb.

These are the ideal values for state 3. To find the actual values, use the definition of η_c.

$$\Delta h_{actual} = \frac{\Delta h_{ideal}}{\eta_c}$$

$$= \frac{325.47 - 138.66}{85} = 219.78 \text{ Btu/lb}$$

Then $h_{3_{actual}} = 219.78 + 138.66 = 358.44$ Btu/lb

Look up $T3_{actual}$ that corresponds to the value of $h_{3_{actual}}$

$T3_{actual} = 1459$ °R.

The computation of accurate values for actual T3, such as is done for performance analysis, requires this kind of procedure. However, a simpler method exists, which may suffice for some purposes. In fact, evidence of its use can be found in the literature[2] of the gas turbine industry. This is manifested by a simple formula for T3, which is based upon the definition for η_c, and the assumption of a constant specific heat for air. Its derivation follows:

$$\eta_c = \frac{\Delta h_{ideal}}{\Delta h_{actual}} = \frac{C_p\,(T3_{ideal} - T2)}{C_p\,(T3_{actual} - T2)} \qquad (1)$$

and

$$T3_{ideal} = T2 \left(\frac{P3}{P2}\right)^{\frac{k-1}{k}} \qquad (2)$$

where P3/P2 is simply the compressor pressure ratio, k is the ratio of specific heats for air, and C_p is the specific heat at constant pressure.

Substituting Eq. (2) into Eq. (1) and solving for $T3_{actual}$, we get:

$$T3_{actual} = \frac{T2}{\eta_c}\left[\left(\frac{P3}{P2}\right)^{\frac{k-1}{k}} - 1\right] + T2$$

The error incurred by using this formula increases with temperature, i.e., pressure ratio. In order to evaluate this effect, discharge temperature was computed using both methods over a range of pressure ratios and the results are presented in a table below.

ERROR DUE TO FORMULA FOR DISCHARGE
TEMPERATURE $T2 = 580°R, \eta_c = 0.85$

Pressure Ratio	$T3_{actual}$ by formula, °R	$T3_{actual}$ by table, °R	Percent Error
10	1215.0	1196.7	1.51
15	1376.8	1345.5	2.27
20	1503.6	1459	2.97

Note that the purposes of this report, T2 is equivalent to TAMB, the ambient temperature of the testing chamber.

---

[1] Keenan, J.H. and Kaye, J., Gas Tables, J. Wiley & Sons, Inc., 1963.

[2] For example, see Shaw, H., "The Effects of Water, Pressure, and Equivalence Ratio on Nitric Oxide Production in Gas Turbines," Trans. of the ASME, J. of Eng. for Power, July 1974.

APPENDIX C

MULTICOLLINEARITY AND AIRCRAFT EMISSIONS DATA

One problem which can arise in the development of regression models to predict the effect of changing combustor inlet conditions on emission levels is that of multicollinearity. Multicollinearity arises whenever, either in the population or in the sample, various of the explanatory variables stand in an exact or almost-exact linear relation to each other. When multicollinearity occurs, it is as if members of a subset of explanatory variables always act in unison. As a result, the data lack sufficient independent variation to allow one to sort out the separate effect of each independent variable. The greater the degree of multicollinearity that exists, the more arbitrarily and unreliably does least squares regression allocate the sum of the unexplained variation among the individual explanatory variables. This phenomenon therefore can result in coefficient estimates which are particularly sensitive to changes both in the model specification and data used to develop the model.

Table C1 has been constructed to analyze the impact of multicollinearity on a subset of the ambient effects program test data. Presented in this table are the correlation coefficients for LN(NOX), T3, LN(P3) and HAMB (ambient humidity), and the regression coefficients and their standard errors for a variety of NOX model formulations. The data used to develop this table is the CFM56 combustor rig, all thrust levels.

The first point of note in this table is the high degree of correlation (.91507) between combustor inlet temperature T3 and the logarithm of combustor inlet pressure LNP3. This situation suggests that a model using both these terms may be subject to multicollinearity problems. In order to analyze the impact of this potential problem, five regression models were developed and are summarized in Table C1. In the first model (LNNOX=f(T3)), a T3 coefficient of .002481 was determined. Similarly, the model LNNOX=f(LNP3) yielded a LNP3 coefficient of 1.1177. When both T3 and LNP3 are used together to predict LNNOX as in regression #3, a substantial change in the estimated coefficients occurs. The T3 goes from .002481 to .001670, a change of -32.7%, and the LNP3 coefficient changes from 1.1177 to 0.4101, a change of -63.3%. This volatility in the estimated T3, LNP3 coefficients and the high correlation between these two variables suggests that multicollinearity is present to a considerable degree.

On the other hand, the addition of the HAMB to the equation represents a substantial "real" improvement in the estimation process. As shown in Table C1 the correlation between T3 and HAMB is only 0.03248 and the correlation between LNNOX and HAMB is -0.23270. Ambient humidity therefore represents a reasonable predictor of NOX emission levels that is not as highly related to T3 as is P3. The inclusion of the HAMB term results in a substantial reduction in the residual sum of squares (SS_{error}) and only changes the T3 coefficient from .002481 to .002503 (0.9%). In this case, multicollinearity does not pose a serious problem.

The trends illustrated by the above example were also demonstrated by the contributed data analyzed during the program. In fact, since much of the contributed data had relatively small sample sizes and was collected for the most part in undesigned experiments, the degradation in the coefficient standard errors was more pronounced than in the CFM56 data. Table C2 presents a summary of NOX regression coefficients and standard errors for the Pratt & Whitney JT9D-7A Pilot Lot data. As shown in this table, the addition of combustor inlet pressure adds little to the predictive ability of the equations (same R^2) and the LNP3 standard error (.1075) indicates that the LNP3 coefficient (.0109) is not significantly different from zero.

While the above examples illustrate the instability which can be introduced in the estimation of T3 and LNP3 regression coefficients, they do not necessarily imply that independent combustor inlet temperature and pressure correction factors can never exist. Had sufficient test data existed in the data base for a variety of engines whose engine control strategies result in independent T3 and P3 variation, separate correction coefficients for both T3 and P3 could have been developed and P3 coefficient trends established.

However, only a limited number of engine tests were available in which both temperature and humidity were held constant while pressure was allowed to vary independently.

In order to establish representative values for potential HC, CO and NOX combustor inlet pressure correction coefficients, small subsets of the CFM56 combustor rig data were analyzed in which both ambient temperature and humidity were held constant and ambient pressure permitted to vary from 26.0 in Hg to 32.3 in Hg. Each of these data sets contained six observations. Regressions were performed using the functional models:

$$\begin{aligned} \text{LNHC} &= f(\text{LNP3}) \\ \text{LNCO} &= f(\text{LNP3}) \\ \text{LNNOX} &= f(\text{LNP3}) \end{aligned}$$

with TAMB, HAMB constant.

These models imply a P3 correction factor of the form

$$\text{P3 Correction Factor} = \left(\frac{\text{P3}_{\text{meas}}}{\text{P3}_{\text{ref}}}\right)^{\text{P3 COEF}}$$

where P3COEF is the LNP3 regression coefficient determined above.

For HC, a statistically significant P3 effect could not be established. For CO, on the other hand, a combustor inlet pressure coefficient of -1.46 was found. For ambient pressures in the range 26.0 to 32.3 in Hg, the magnitude of this coefficient implies a CO pressure correction factor ranging from 1.24 to 0.89. For the range of ambient pressures typically experienced during emission testing (e.g., 29.92 ±1 in Hg), this CO pressure correction coefficient provides correction factors from 1.05 to 0.95 or a maximum correction of 5 percent. Similar analyses were performed on the NOX data and a combustor inlet pressure coefficient equal to 0.34 was determined. A correction coefficient of this magnitude will provide NOX pressure correction factors ranging from 0.95 at 26.0 in Hg to 1.03 at 32.3 in Hg or a 5 percent maximum correction.

While the above analysis of small subsets of the CFM56 combustor rig data suggests that independent T3 and P3 correction factors for CO and NOX may be applicable to this particular engine, an independent P3 correction factor could not be established for other engines in the data base which for the most part were subjected to less extensive testing than the CFM56 rig. Since the magnitude of the CFM56 pressure correction factors for CO and NOX cited above were less than 5 percent for normal pressure excursions from reference day conditions, only a combustor inlet temperature coefficient was employed in the development of correction factors presented in this report.

Still another effect of multicollinearity problems can be demonstrated by examining variance maps for the data in question. A brief discussion of variance mapping is given below.

In general, the linear model which gives the true emission level, y, of a particular engine is given by:

$$y = \beta_1 f_1 + \beta_2 f_2 + \beta_3 f_3 + --- + e \qquad (1)$$

where β_i, i = 1,2,3.. are constants, f_1, f_2, f_3 ... are basis functions of combustor inlet temperature (T3), combustor inlet pressure (P3), ambient humidity (HAMB), and e is the random error.

Since e is a random variable, the responses observed at each (T3, P3, HAMB...) point also constitute a random variable. As a result it is only possible to obtain from the observations an equation of the form:

$$\hat{y} = b_1 f_1 + b_2 f_2 + b_3 f_3 * \ldots \qquad (2)$$

where $\hat{y}$ is an estimate of y and b_i, i = 1,2,3 ... is an estimate of β_i.

The variance function is controlled by three considerations:

1) The type of basis functions employed in the regression model.

2) The positions in T3, P3, HAMB space, called design points, at which emission measurements are taken, and

3) The magnitude of the error variance σ^2 at each design point.

Var $(\hat{y})$ varies at different coordinates in T3, P3, HAMB space. At some points the response can be estimated with relatively little error; at other positions the error can be quite large. The variance in the estimated response at a point P in T3, P3, HAMB space is given by

$$\text{Var}\ (\hat{y}) = \underline{x}\ (X'X)^{-1}\ \underline{x}'\ \sigma^2 \qquad (3)$$

where $\underline{x}$ is a vector obtained by evaluating each of the basis functions at the particular point P and X'X is matrix of the least squares normal equations. Therefore, for every point P, Var $(\hat{y})$ is actually a variance function. By dividing both sides by σ^2, one can obtain the function in normalized form:

$$\text{Var}\ (y)/\sigma^2 = \underline{x}\ (X'X)^{-1}\ \underline{x}' \qquad (4)$$

This emission index variance function can be viewed as a response surface generated by evaluating the function at given increments over any region of interest. The propagation of error over T3, P3, HAMB space can be considered relative to the basis functions used and the design points chosen by examination of Var $(y)/\sigma^2$, the variance function in normalized form. The actual magnitude of the variance at any point can be examined by evaluating Var $(\hat{y})$, which includes a scalar multiplication by the error variance σ^2.

One should observe that the normalized variance (equation 4) is a function of the inverse of the X'X matrix. The effect of multicollinearity presents itself by noting that, as the dependence between explanatory variables increases, the diagonal terms in $(X'X)^{-1}$ matrix corresponding to these variables tend toward infinity. In more practical terms, this means that the variance function itself increases with the degree of multicollinearity. In addition, the variance (standard errors) of the regression coefficients are directly related to the $(X'X)^{-1}$ matrix. As terms in this matrix increase, due to multicollinearity problems, the magnitude of the coefficient standard error also increases.

The increase in the variance function due to multicollinearity in the explanatory variables T3 and P3 is demonstrated as follows. Figures C1 and C2 are variance contour maps for the CFM56 data as a function of (1) T3 and (2) T3 and P3. (Note that in Figure C1 the contours are constant with respect to P3 because it was not included in the basis function for this map. The variance contours are plotted vs T3 and P3 in this figure for consistency only.) The contour lines trace a constant value (as indicated on each line) of $\mathrm{Var}(\hat{y})/\sigma^2$ in the T3, P3 space. It can be shown that the value of the function $\mathrm{Var}(\hat{y})/\sigma^2$ always has its minimum value at the mean values of the explanatory variables. In Figure C1, the minimum value of $\mathrm{Var}(\hat{y})/\sigma^2$ is approximately .005 and it occurs at the mean value of T3 (650 deg), while in Figure C2 the minimum value is approximately .005 and it occurs at the mean values of P3, T3. The effect of the multicollinearity between P3 and T3 upon $\mathrm{Var}(\hat{y})/\sigma^2$ is seen by examining the contours as one moves away from the minimum. For example, in Figure C1, the value of the variance function at T3 = 1250 deg ranges from .05 to .5 while in Figure C2 it is between .03 and .04.

TABLE C1

NOX REGRESSION COEFFICIENTS VS. MODEL FORMULATION
GE CFM56 COMBUSTOR RIG - IDLE TO TAKEOFF
(214 Observations)

MODEL	COEFFICIENT/STD ERROR					
	CONSTANT	LNP3	T3	HAMB	SS_{ERROR}	R^2
(1) LNNOX=f(T3)	.3049	-	.002481	-	7.22	.9168
	(.0361)		(.000051)			
(2) LNNOX=f(LNP3)	-3.2315	1.1177	-	-	11.43	.8682
	(0.1393)	(0.0299)				
(3) LNNOX=f(T3,LNP3)	-1.0584	.4101	.001670	-	5.57	.9358
	(0.1754)	(.0519)	(.000112)			
(4) LNNOX=f(T3,LNP3,HAMB)	-.3971	.2567	.001994	-19.28	0.56	.9936
	(.0578)	(.0169)	(.000036)	(0.44)		
(5) LNNOX=f(T3, HAMB)	.4674	-	.002503	-20.70	1.18	.9864
	(.0154)		(.000021)	(0.63)		

CORRELATION COEFFICIENTS

	LNNOX	T3	LNP3	HAMB
LNNOX	1.00000	0.95748	0.93176	-0.23270*
T3		1.00000	0.91507	0.03248
LNP3			1.00000	-0.05482
HAMB				1.00000

*When effect of varying thrust levels is removed by fitting LNNOX=f(T3), the HAMB-LNNOX correlation is -0.91437.

( ) = Coefficient Standard Error

TABLE C2 NOX REGRESSION COEFFICIENTS vs MODEL FORMULATION
PRATT & WHITNEY JT9D-7A PILOT LOT DATA, IDLE TO TAKEOFF

(181 Observations)

MODEL	COEFFICIENT/STD ERROR				R^2
	CONSTANT	LNP3	T3	HAMB	
(1) LNNOX=f(T3,LNP3,HAMB)	-.2319	.0109	.004122	-19.73	.9771
	(.3289)	(.1075)	(.000340)	(3.16)	
(2) LNNOX=f(T3,HAMB)	-.1987	-	.004156	-19.94	.9771
	(.0362)		(.000048)	(2.37)	

CORRELATION COEFFICIENTS

	LNNOX	T3	LNP3	HAMB
LNNOX	1.00000	.98386	.97840	.06671
T3		1.00000	.98231	.16356
LNP3			1.00000	.03893
HAMB				1.00000

( ) = Coefficient Standard Error

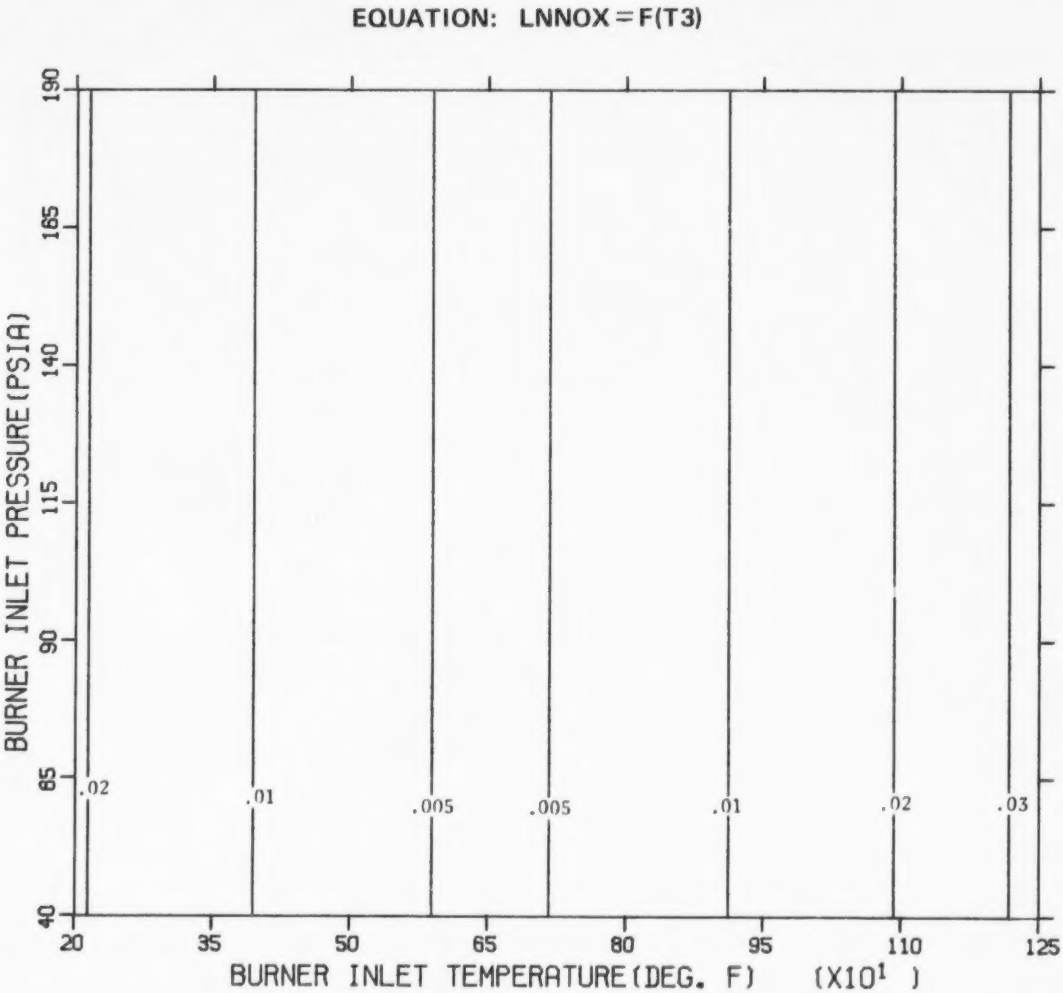

EQUATION: LNNOX = F(T3)

Figure C1 CFM56 VARIANCE MAP

TA,

EQUATION: LNNOX = F(T3, LNP3)

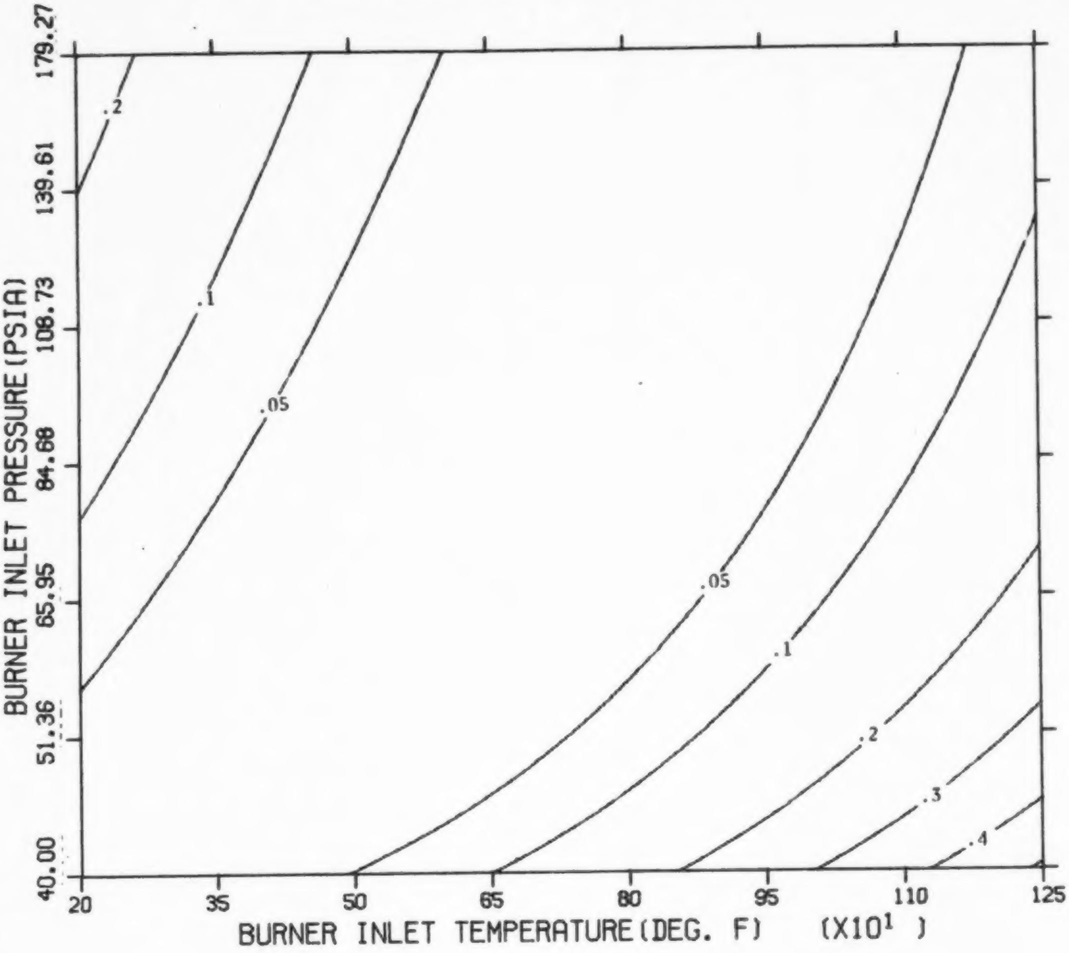

Figure C2 CFM56 VARIANCE MAP

APPENDIX D

COMBUSTOR RIG - FULL-SCALE ENGINE CORRELATION

This appendix summarizes investigations undertaken to analyze the correlation between combustor rig and full scale engine emissions. This analysis attempts to partially answer two interrelated questions:

1) Can emissions from combustor rigs operating at lower combustion inlet pressures than corresponding full scale engine be related to emissions from the full scale engine itself?

2) Is it reasonable to include correction factor coefficients developed using data from combustor rigs in the development of general full scale engine correction factors?

In order to investigate these questions, EPA-sponsored data on the T1 class ALF502 combustor rig and full scale engine were analyzed to determine the nature and extent of the rig-engine correlation. The ALF502 data was selected for this analysis since it represents the only data source for which sufficient ambient effects tests were performed on both the full scale engine and corresponding combustor rig.

The approach taken to assess the rig-engine correlation is suggested by several commonly used correlation methods summarized below which emphasize the role of combustor inlet pressure P3 (or its equivalent T3) on the emissions process.

SELECTED RIG-ENGINE CORRELATION TECHNIQUES

NASA

$$HC_{engine} = HC_{rig} \frac{P3_{rig}}{P3_{engine}}$$

$$CO_{engine} = CO_{rig} \left(\frac{P3_{rig}}{P3_{engine}}\right)^{N}$$

GE

$$NOX_{engine} = NOX_{rig} \left(\frac{P3_{rig}}{P3_{engine}}\right)^{-0.37}$$

$$SMOKE_{engine} = SMOKE_{rig} \left(\frac{P3_{rig}}{P3_{engine}}\right)^{-1.5}$$

In the analysis taken, individual equations of the form

$$LN(Pollutant) = f(1, LNP3)$$

were developed for HC, CO and NOX for both the engine and rig data. The natural logarithm of combustor inlet pressure LNP3 was selected for this analysis rather than combustor inlet temperature T3 so that direct comparisons with NASA and GE correlations could be made. Table D1 summarizes the results of these regressions. This regression analysis approach was used in the analysis since test data with the rig and engine operating under the same ambient conditions was not available.

The approach used to assess the degree of rig engine correlation is graphically illustrated in Figure D1 which presents the LNHC vs LNP3 rig and engine regression lines. The combustor rig and full scale engine can be correlated if the rig data operating at a combustor inlet pressure $P3_{rig}$ can be extrapolated to determine the emission levels of the full scale engine operating at $P3_{engine}$ where $P3_{engine} > P3_{rig}$. In mathematical terms, the ability to correlate rig and engine emissions can be established if both the slope (P3COEFF) and intercept (CONSTANT) of the rig and engine regression equations are equal. Under these conditions, the low combustor inlet pressure rig data can be treated as an extension of the full scale engine data. Since the slopes of the rig and engine equations are equal, the same emissions variation in response to changing ambient conditions can be expected even though the absolute emission levels may differ. Under the above circumstances, it is reasonable to include the rig correction factor coefficients in the development of a general correction factor scheme.

In order to assess the equality of rig and engine intercepts and slopes, Table D2 has been constructed. This table presents the 95% confidence bounds for the CONSTANT and P3COEF regression terms presented in Table D1. A comparison of the degree of overlap between the confidence bands suggests that a meaningful difference cannot be found between the rig and engine coefficients. For example, the confidence limits on the rig and engine CO pressure coefficients could be illustrated as follows:

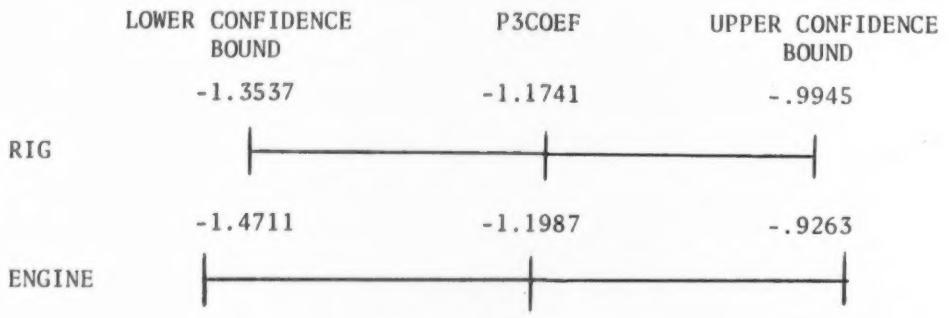

ALF502 CO PRESSURE COEFFICIENT CONFIDENCE LIMITS

As seen in this illustration, a considerable degree of overlap exists between the two CO coefficient confidence limits with the result that a meaningful difference between rig and engine does not exist. Similar conclusions can be drawn about the other confidence limits presented.

It should be noted that the confidence band analysis presented above is not a rigorous test for the equality of slopes and intercepts of two regression equations. Instead, it is presented as a satisfactory approximation relying to a great extent upon an engineering assessment of the practical significance of any small differences found in the model coefficients. A more rigorous analysis using the data from Table D1 and the method for comparing two linear bivariate regression lines presented in Appendix F was performed and also confirms the hypothesis that ALF502 rig and full scale engine emissions can be correlated.

To determine a suitable pressure correlating factor for HC, CO, and NOX, the weighted averages (based on sample size) of the rig and engine pressure coefficients were determined and are summarized below:

	P3COEF (Weighted Average)
HC	-2.36
CO	-1.18
NOX	0.76

ALF502 RIG/ENGINE WEIGHTED AVERAGE PRESSURE COEFFICIENTS

The method used to compute engine emissions from rig emissions is illustrated in Figure D1 for the representative case of HC.

$$LNHC_{eng} = LNHC_{rig} - 2.36\ (LNP3_{eng} - LNP3_{rig})$$

$$= LNHC_{rig} - 2.36\ LN\ \frac{P3_{eng}}{P3_{rig}}$$

Taking inverse logarithm

$$HC_{eng} = HC_{rig} * \left(\frac{P3_{eng}}{P3_{rig}} \right)^{-2.36}$$

or

$$HC_{eng} = HC_{rig} * \left(\frac{P3_{rig}}{P3_{eng}} \right)^{2.36}$$

The corresponding CO and NOX rig engine correlations are summarized below:

$$CO_{engine} = CO_{rig} \left(\frac{P3_{rig}}{P3_{engine}} \right)^{1.18}$$

$$NOX_{engine} = NOX_{rig} \left(\frac{P3_{rig}}{P3_{engine}} \right)^{-0.76}$$

CONCLUSIONS

Using the limited data available on the ALF502, the ability to correlate combustor rig and full scale engine emissions has been demonstrated. Of particular importance in this analysis has been the ability to demonstrate that the response to changes in ambient conditions (as seen in P3COEF) is of equal magnitude between the rig and full scale engine even though the absolute emission levels between rig and engine may differ.

TABLE D1

ALF502 RIG-ENGINE CORRELATION ANALYSIS

REGRESSION SUMMARY

LN(POLLUTANT) = CONSTANT + P3COEF*LNP3

		Rig	Engine
HC EI	Observations	66	21
	Constant	9.8189	10.7168
	Std Error	.6809	1.2174
	P3COEF	-2.2855	-2.5894
	Std Error	.1773	.3404
	Mean Square Error	.2271	.0199
	Variance (LNHC)	.8041	.0766
	R^2	.7218	.7528
CO EI	Observations	66	21
	Constant	7.8733	7.9157
	Std Error	.3448	.4869
	P3COEF	-1.1741	-1.1987
	Std Error	.0898	.1362
	Mean Square Error	.0582	.0032
	Variance (LNCO)	.2105	.0154
	R^2	.7276	.8031
NOX EI	Observations	66	28
	Constant	-1.5512	-1.8299
	Std Error	.1752	.0791
	P3COEF	0.7289	0.8196
	Std Error	.0456	.0210
	Mean Square Error	.0150	.0012
	Variance (LNNOX)	.0738	.0673
	R^2	.7994	.9832

TABLE D2

ALF502 RIG-ENGINE CORRELATION ANALYSIS
COEFFICIENT CONFIDENCE BOUND SUMMARY

$\alpha = 0.05$

		CONSTANT	P3COEF
HC	RIG	8.4571 to 11.1807	-2.6401 to -1.9309
EI	ENGINE	8.2820 to 13.1516	-3.2702 to -1.9086
CO	RIG	7.1837 to 8.5629	-1.3537 to -.9945
EI	ENGINE	6.9419 to 8.8895	-1.4711 to -.9263
NOX	RIG	-1.9016 to -1.2008	.6377 to .8201
EI	ENGINE	-1.9881 to -1.6717	.7776 to .8616

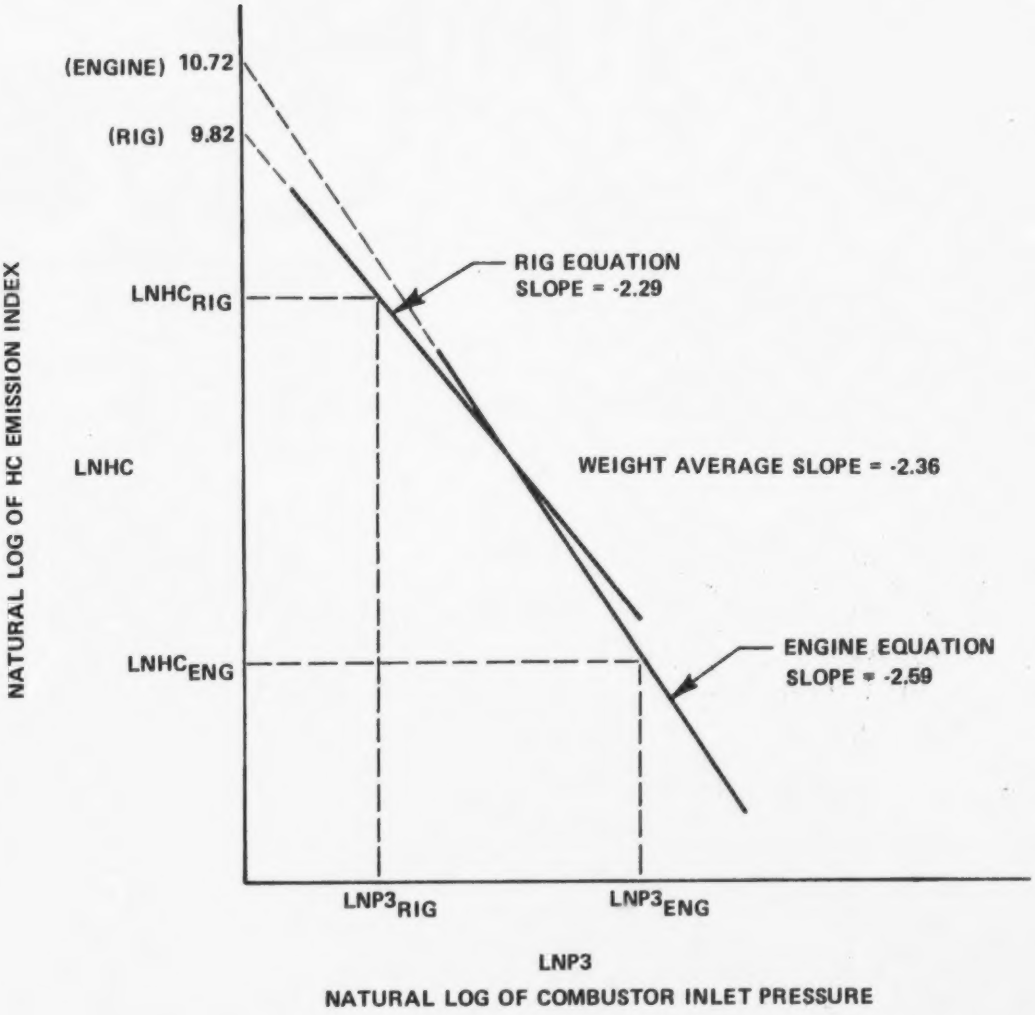

Figure D1 GRAPHICAL INTERPRETATION OF ALF502 RIG ENGINE CORRELATION

APPENDIX E

COMPARISON OF TWO LINEAR BIVARIATE REGRESSION LINES

Given two regressions:

$Y_1 = b_1 x_1 + a_1$ n_1 = number of points for Regression 1

$Y_2 = b_2 x_2 + a_2$ n_2 = number of points for Regression 2

Test the hypothesis that: $b_1 = b_2$

given that $(\sigma^2_{yx})_1$, $(\sigma^2_{yx})_2$ are unknown and unequal.

The test statistic t is given as:

$$t_{calc} = \frac{b_1 - b_2}{S_{D_b}}$$

and is compared to a t distribution with V_t D.F.

$$S^2_{D_b} = \frac{(S^2_{yx})_1}{S_{x_1}} + \frac{(S^2_{yx})_2}{S_{x_2}}$$

where

$$S_{x_1} = \mathrm{Var}(x_1) \cdot (n_1 - 1)$$

$$S_{x_2} = \mathrm{Var}(x_2) \cdot (n_2 - 1)$$

$(S^2_{yx})_1$ = estimate of $(\sigma^2_{yx})_1$ = Residual Mean Square 1

$(S^2_{yx})_2$ = estimate of $(\sigma^2_{yx})_2$ = Residual Mean Square 2

$$V_t = \frac{1}{K^2/V_1 + (1 - K)^2/V_2} \qquad V_1 = n_1 - 2$$

$$V_2 = n_2 - 2$$

$$K = \frac{(S^2_{yx})_1 \, S_{x_2}}{(S^2_{yx})_1 \, S_{x_2} + (S^2_{yx})_2 \, S_{x_1}}$$

$S^2_{D_b}$ is the pooled variance estimate of b_1, b_2 and the degrees of freedom are weighted by their respective variances.

DECISION RULE:

IF $t_{calc} < t_{V_t}$ Accept Hypothesis eg $b_1 = b_2$

IF $t_{calc} \geq t_{V_t}$ Reject Hypothesis eg $b_1 \neq b_2$

REFERENCES:

1. Documenta Geigy, Scientific Tables, ed. by K. Diem & C. Lenther, 7th edition, Geigy Pharmaceuticals, Division of CIBA-Geigy Corp., Ardsley, New York 10502.

2. Intro. Engineering Statistics, Guttman & Wilks.

APPENDIX F

SAMPLE EMISSION INDEX CORRECTION

This appendix illustrates the steps required to correct the emission indices for a particular engine. For the purposes of this illustration, the HC, CO, and NOX CFM56 combustor rig emission indices will be corrected using the coefficients developed specifically for this engine. The correction coefficients used in this example are:

HC: T3COEF = -0.023486
CO: T3COEF = -0.006443
NOX: T3COEF = 0.002503
HAMBCOEF -20.70

The reference engine conditions to which the emission levels were corrected are:

Reference Engine Conditions

Mode	% Rated	T3 (Deg. F)	P3(PSIA)
Idle	6	353	48.6
1.5 Idle	9	417	63.7
Approach	30	628	139.0
Climb	85	890	148.4
Takeoff	100	941	168.6

These reference conditions were obtained from the manufacturers' cycle deck for the rig operating under the following reference conditions:

Ambient Temperature = 59 DEG. F
Ambient Pressure = 29.31 IN HG
Ambient Humidity = 0.0075 lb H_2O/lb Air

It should be noted that the correction to "standard day" reference conditions is identical to the process outlined in this appendix except that values of

$T3_{ref}$ and $P3_{ref}$ corresponding to an ambient pressure of 29.92 IN HG and an ambient humidity of 0.00634 lb H_2O/lb Air are used.

The corrected emissions indices are generated on a mode-by-mode basis using the following expressions:

$$HC_{CORR} = HC_{MEAS} * e^{-.023486 * (T3_{Ref} - T3_{Meas})}$$

$$CO_{CORR} = CO_{MEAS} * e^{-.006443 * (T3_{Ref} - T3_{Meas})}$$

$$NOX_{CORR} = NOX_{MEAS} * e^{.002503 * (T3_{Ref} - T3_{Meas})} * e^{-20.7(HAMB_{Ref} - HAMB_{Meas})}$$

where $T3_{Ref}$ is different for each mode.

Tables F1 through F6 present plots of both the measured (uncorrected) and the corrected HC, CO and NOX CFM56 rig emission indices. The vertical lines in these figures correspond to the reference combustor inlet temperatures to which the data were corrected. Ideally, the corrected emissions data should be a horizontal line with a minimum vertical spread.

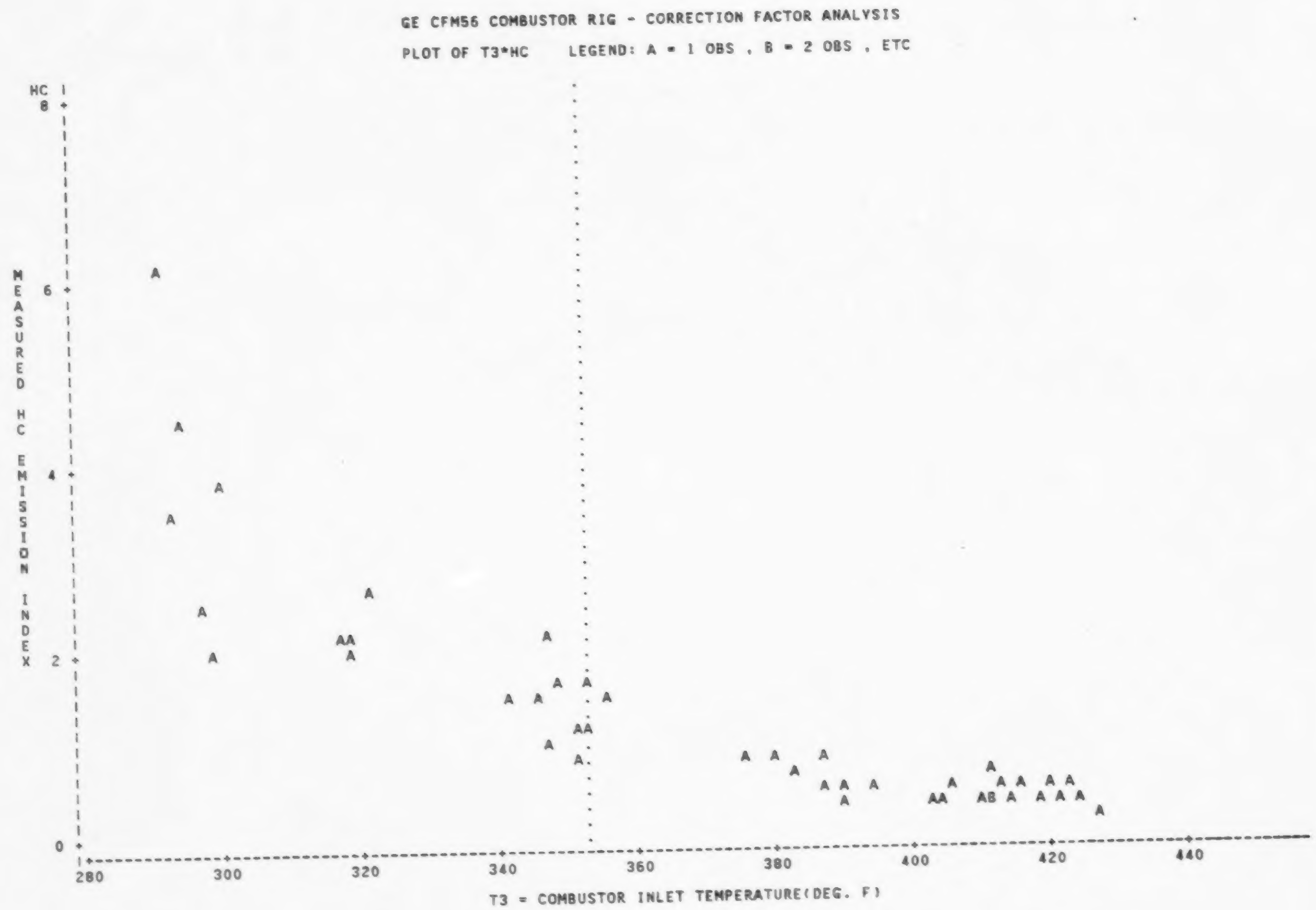

Figure F1 UNCORRECTED HC EMISSIONS INDEX versus COMBUSTOR INLET TEMPERATURE – CFM56 COMBUSTOR RIG, IDLE

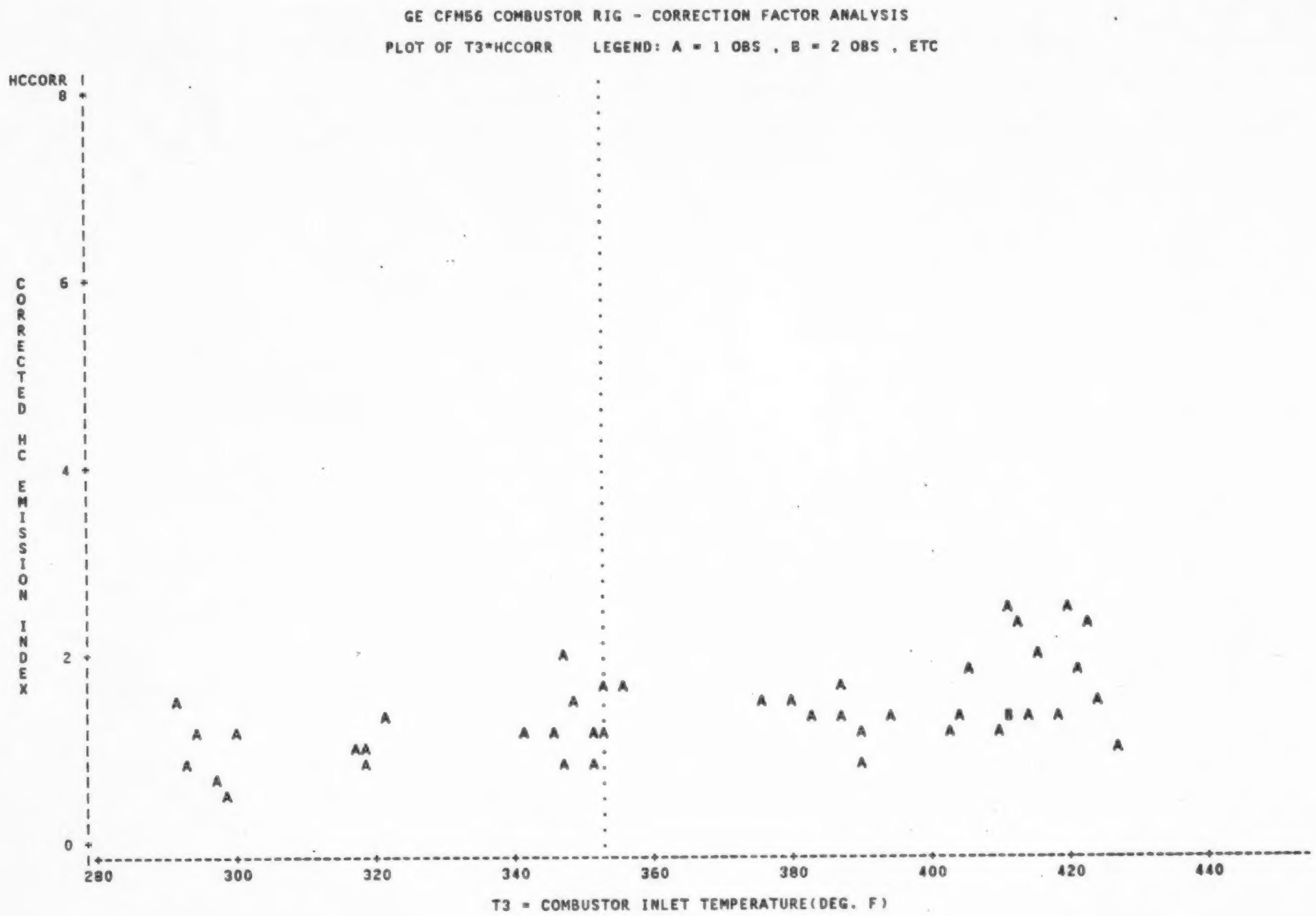

Figure F2 CORRECTED HC EMISSIONS INDEX versus COMBUSTOR INLET TEMPERATURE – CFM56 COMBUSTOR RIG, IDLE

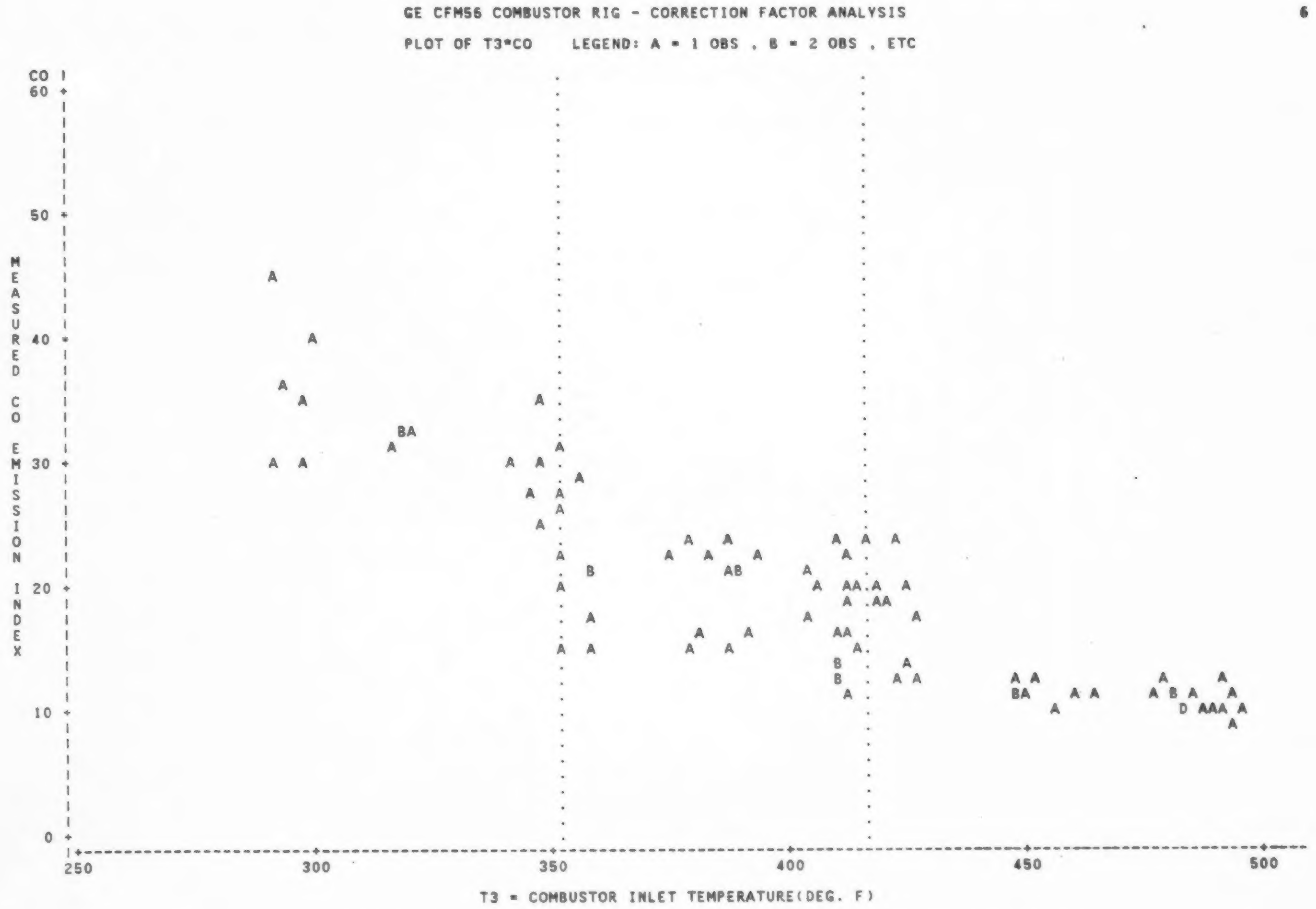

Figure F3 UNCORRECTED CO EMISSIONS INDEX versus COMBUSTOR INLET TEMPERATURE – CFM COMBUSTOR RIG, IDLE AND 1.5 IDLE

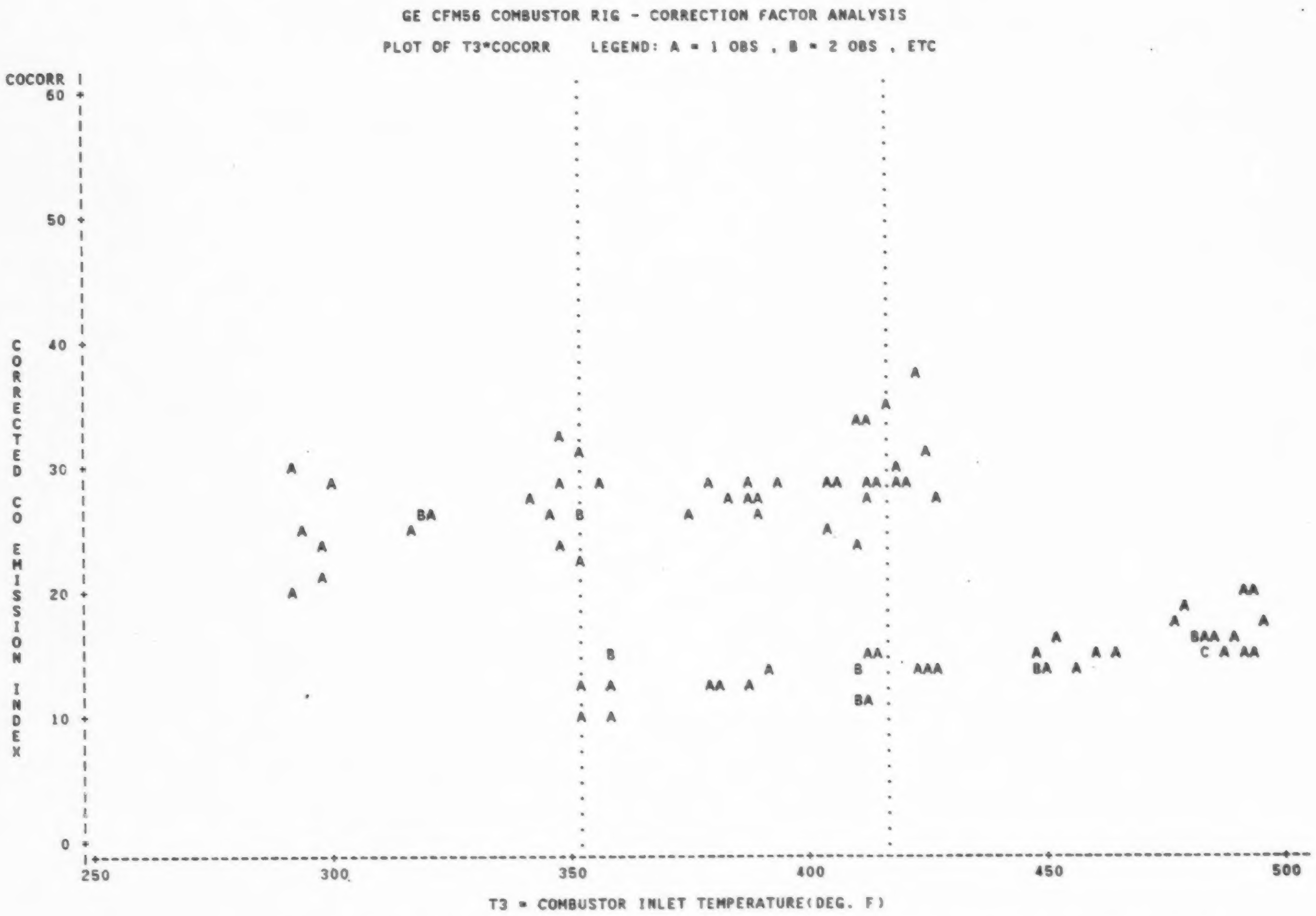

Figure F4 CORRECTED CO EMISSIONS INDEX versus COMBUSTOR INLET TEMPERATURE – CFM56 COMBUSTOR RIG, IDLE AND 1.5 IDLE

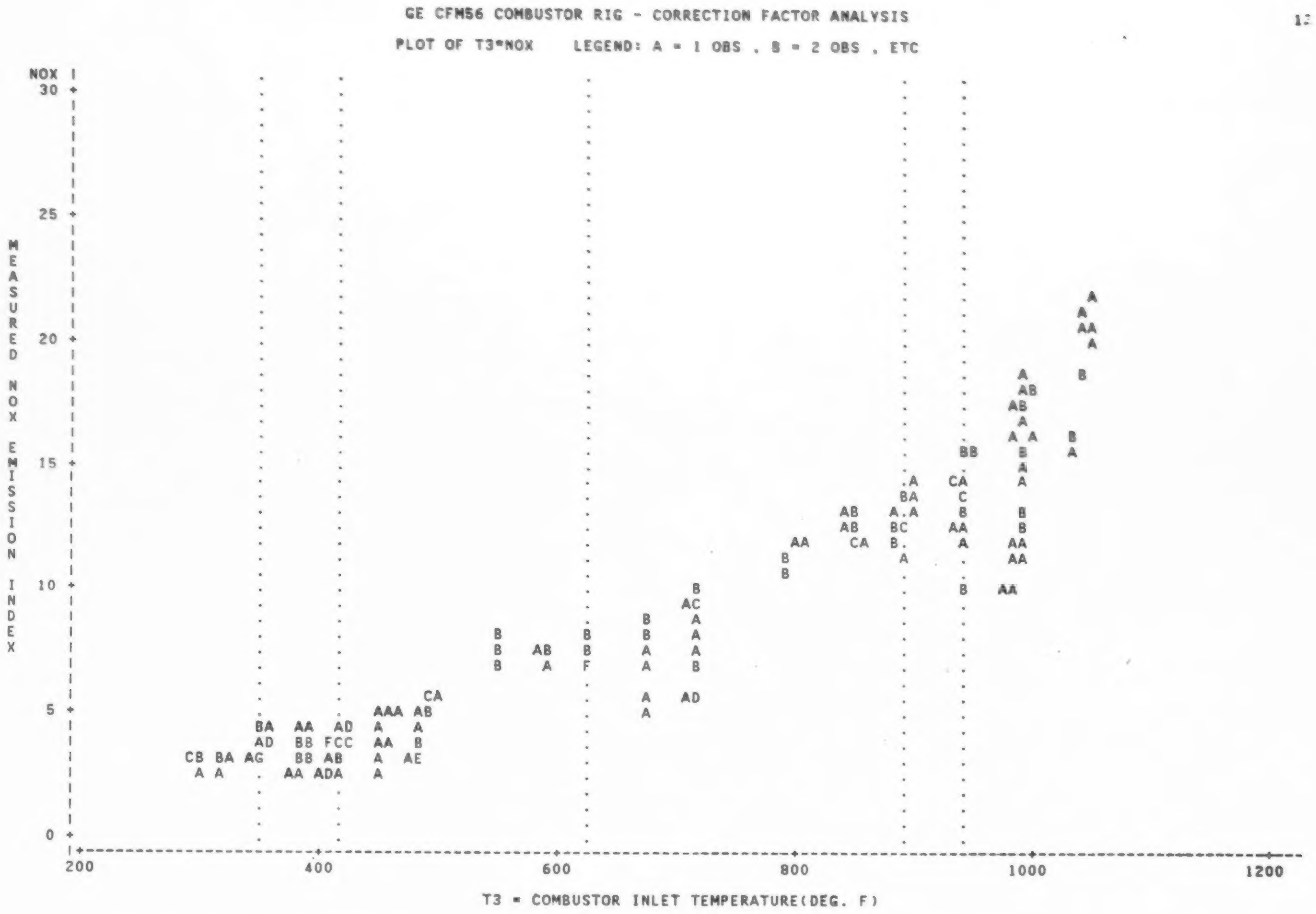

Figure F5 UNCORRECTED NOX EMISSIONS INDEX *versus* COMBUSTOR INLET TEMPERATURE – CFM56 COMBUSTOR RIG, IDLE TO TAKEOFF

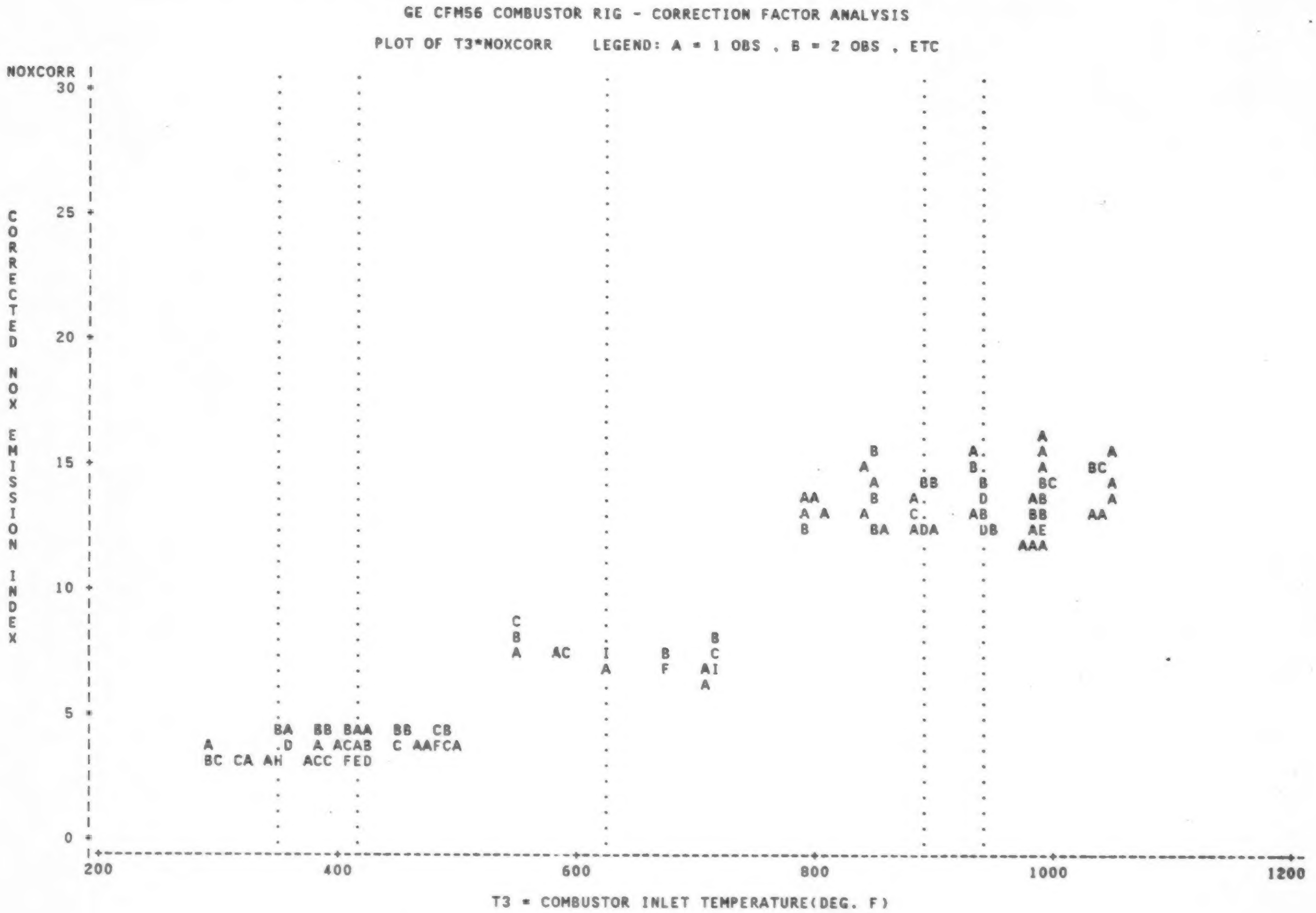

Figure F6 CORRECTED NOX EMISSIONS INDEX versus COMBUSTOR INLET TEMPERATURE – CFM56 COMBUSTOR RIG, IDLE TO TAKEOFF

APPENDIX G

COMPUTATION OF EPA EMISSION PARAMETERS (EPAP) FROM EMISSION INDEX AND SPECIFIC FUEL CONSUMPTION

The EPA Emission Parameter, or $EPAP_i$, for each gaseous emission component is computed from the Emission index (EI_{ij}) for each component and operating mode and from the specific fuel consumption for the corresponding mode after it has been corrected to standard conditions. Thrust specific fuel consumption (TSFC) is used in the case of a jet or fanjet engine, and brake specific fuel consumption in the case of a propjet engine (BSFC). The EPAP is, of course, a cumulative result obtained by summation over the complete EPA operating cycle of taxi/idle, takeoff, climbout, approach and taxi/idle.

EPAP is specified in units of pounds of pollutant per 1000 pounds of thrust-hr. EI is defined in units of pounds of pollutant per 1000 pounds of fuel burned. SFC is defined as fuel flow rate, pounds per hour per pound of thrust, or pounds of fuel per brake horsepower-hour. The commonality of terms among these parameters suggests that they are related and an expression for this is written by incorporating the time-in-mode of operation (TIM), as follows:

$$EPAP_i = \sum^{j} (EI_{ij}) \; (SFC_j) \; \left(\frac{TIM_j}{60}\right)$$

The subscript i indicates the specific pollutant and j denotes the prescribed mode of operation or power level.

SFC based upon measured values for actual fuel flow rate and thrust or power is corrected to SFC at standard conditions by the relation:

$$SFC_{corr.} = \frac{FF_{meas}/\gamma\sqrt{\Theta}}{Thrust_{meas}/\gamma} = \frac{SFC_{meas}}{\sqrt{\Theta}}$$

where $\Theta = \frac{\text{Ambient Temperature °R}}{519}$ and $\gamma = \frac{\text{Ambient Pressure PSIA}}{14.7}$

because the standard ambient temperature is 519 °R and standard pressure 14.7 psia.

Figures G1 and G2 illustrate a typical application of the above SFC correction formula for the case of the CFM56 combustor rig. In Figure G1 the measured fuel flow in lb/hr for each of five modes is plotted versus ambient pressure. As shown in this figure, uncorrected fuel flow rises significantly with increasing pressure. Figure G2 presents comparable data after the fuel flow has been corrected using the ambient temperature and pressure method outlined above. The corrected fuel flow as desired is independent of the ambient pressure. A similar plot versus ambient temperature also demonstrates the effectiveness of this correction method.

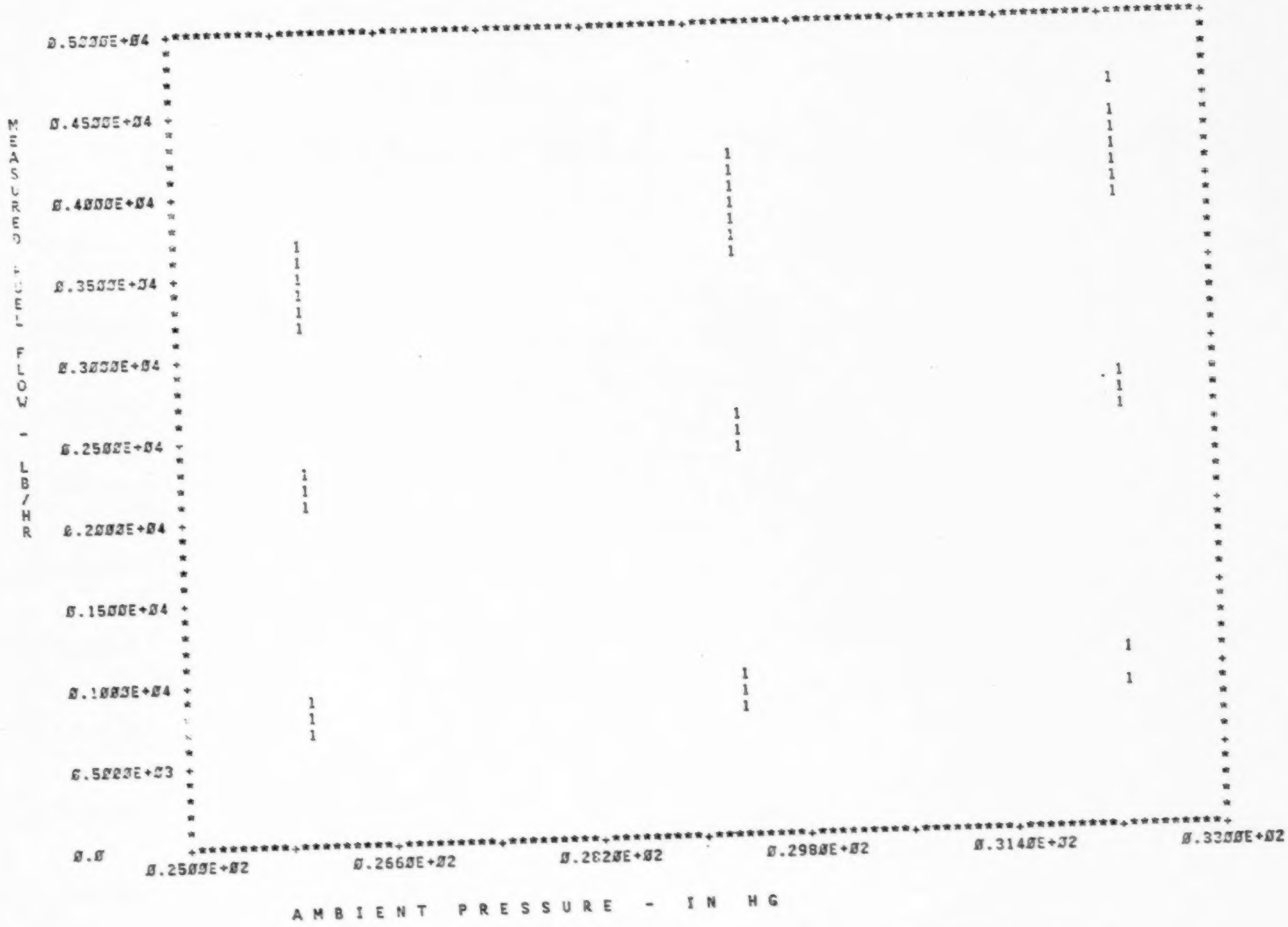

Figure G1 MEASURED FUEL FLOW VERSUS AMBIENT PRESSURE - CFM56 COMBUSTOR RIG, IDLE TO TAKEOFF

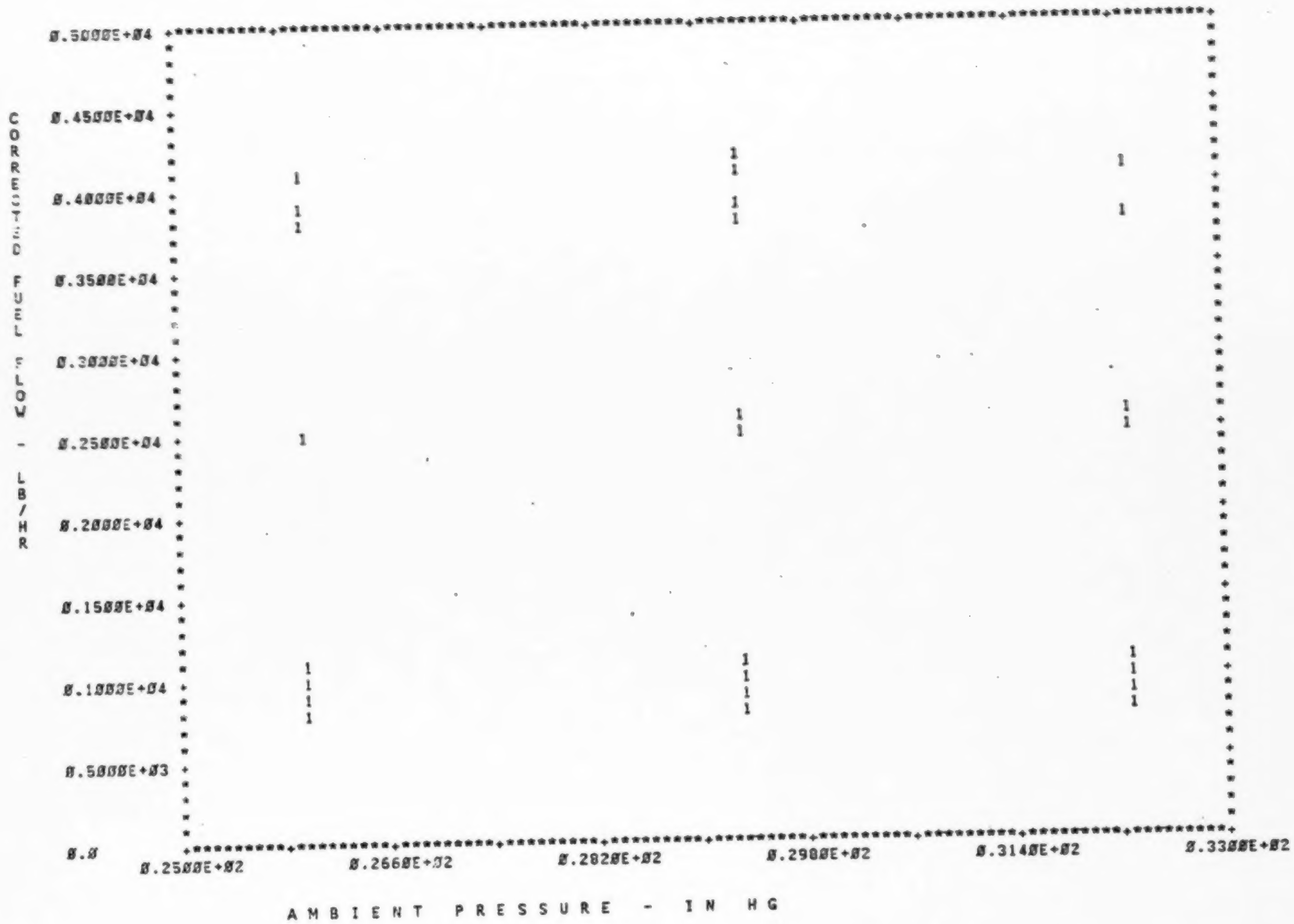

Figure G2 CORRECTED FUEL FLOW VERSUS AMBIENT PRESSURE - CFM56 COMBUSTOR RIG, IDLE TO TAKEOFF

ENVIRONMENTAL PROTECTION AGENCY
Technical Publications Branch
Office of Administration
Research Triangle Park, North Carolina 27711

OFFICIAL BUSINESS
AN EQUAL OPPORTUNITY EMPLOYER

POSTAGE AND FEES PAID
ENVIRONMENTAL PROTECTION AGENCY
EPA - 335

SPECIAL FOURTH-CLASS RATE
BOOK

U S MAIL

Return this sheet if you do NOT wish to receive this material ☐ or if change of address is needed ☐. (Indicate change, including ZIP code.)

PUBLICATION NO. EPA-460/3-77-019

B388
10